Intellectual Property and Publications Statements

I confirm that the work submitted is my own, except where work which has formed part of jointly authored publications has been included. My contribution and the other authors to this work has been explicitly indicated below. I confirm that appropriate credit has been given within the thesis where reference has been made to the work of others.

Within results Chapter 3, specifically section 3.2, results are taken from work on a joint first author publication with Dr Abdulla Watad, titled as the following:
Normal human enthesis harbours conventional CD4+ and CD8+ T cells with regulatory features and inducible IL-17A and TNF expression
Authors listed: Abdulla Watad, Hannah Rowe, Tobias Russell, Qiao Zhou, Lisa K Anderson, Almas Khan, Robert Dunsmuir, Peter Loughenbury, Vishal Borse, Abhay Rao, Peter A Millner, Nicola Luigi Bragazzi, Howard Amital, Richard Cuthbert, Miriam Wittmann, Kassem Sharif, Tony Kenna, Matthew A Brown, Darren Newton, Charlie Bridgewood, Dennis G McGonagle
Date of Publication: August 2020
Journal: Annals of the rheumatic diseases, Volume 79, Issue 8

I worked on all aspects of data acquisition and manuscript drafting within this paper however did receive support from both Dr Watad and Dr Bridgewood on when creating results relating to Figure 2 and Figure 3 within the paper, all other figures were created by myself.

Within results Chapter 3, specifically section 3.10, 3.11 and 3.12 respectively, results are taken from work on a joint first author publication with Dr Nicolas Rosine and Dr Surya Koturan, titled as the following:

Characterization of Blood Mucosal-Associated Invariant T Cells in Patients With Axial Spondyloarthritis and of Resident Mucosal-Associated Invariant T Cells From the Axial Entheses of Non-Axial Spondyloarthritis Control Patients

Authors listed: Nicolas Rosine, Hannah Rowe, Surya Koturan, Hanane Yahia-Cherbal, Claire Leloup, Abdulla Watad, Francis Berenbaum, Jeremie Sellam, Maxime Dougados, Vishukumar Aimanianda, Richard Cuthbert, Charlie Bridgewood, Darren Newton, Elisabetta Bianchi, Lars Rogge, Dennis McGonagle, Corinne Miceli-Richard

Date of Publication: November 2022

Journal: Arthritis and Rheumatology, Volume 74, Issue 11

I worked on all aspects of data acquisition and manuscript drafting within this paper, specifically relating to Figure 5 within the paper exclusively. I however did receive support from Dr Bridgewood on when creating results relating to Figure 5 within the paper, however the final submitted figure 5 was created by myself.

My work was supported by investigator-initiated nonclinical research funding from Novartis UK.

Ethics approval

The current research has been approved by the University of Leeds ethical approval committee.

Acknowledgements

I would first like to thank all the patients who agreed to participate in this study that made this work possible. I would like to thank my supervisors Dr Darren Newton, Dr Richard Cuthbert, Dr Miriam Wittmann, Dr Charlie Bridgewood and Professor Dennis McGonagle for their continued support during my studies. In particular Dr Darren Newton who really believed in me in times of uncertainty. I would also like to thank my friends and family and in particular my husband Diego and both my parents for their unrelenting support and kindness and belief in me through the highs and the lows of my time at university.

Abstract

Ankylosing Spondylitis (AS) is a seronegative chronic immune-mediated inflammatory arthritis which is part of the spondyloarthropathy (SpA) family of chronic joint diseases. AS mainly affects the spine and sacroiliac joints with enthesitis (inflammation at points where tendon, ligament, and joint capsules are inserted into bone) representing a key pathological lesion, furthermore, in severe AS cases this can culminate in complete fusion of the spine. It is believed that the pro-inflammatory cytokines including tumour necrosis factor α (TNFα) and Interleukin-17A (IL-17A) drive the inflammation at the enthesis, however currently there is limited data on which cells at the enthesis are producing IL-17A. Recent studies have shown that normal human spinal entheses harbour several innate immune cell populations including type 3 innate lymphoid cells (ILC3s), myeloid cells and also γδ T-cells. However, a description of adaptive immune T-cells at the enthesis has not been reported.

This project investigated whether spinal enthesis including peri-entheseal bone harboured resident CD4+ and CD8+ T-cells. Additionally, it evaluates the effects of blocking the production of pivotal SpA-related cytokines, TNFα and IL-17A in an “in vitro enthesitis model”. Also, it investigates T cell plasticity via gene expression of T helper IL-17 producing cells and regulatory T cells (Th17 and Treg respectively) markers following in vitro induction of entheseal inflammation.

Contents Page

Glossary

Full Form	Abbreviation
Ankylosing Spondylitis	AS
Antigen Presenting Cells	APCs
Aryl hydrocarbon receptor	AhR
Assessment of Spondyloarthritis international Society	ASAS
Axial Spondyloarthritis	AxSpA
C Reactive Protein	CRP
CD4+ T helper IL-17 cells	Th17
Cluster of Differentiation	CD
Complementarity Determining Region 3	CDR3
complementary DNA	cDNA
conventional Disease Modifying Anti Rheumatic Drug	csDMARD
Cyclooxygenase	COX
Cytotoxic Lymphocyte Antigen 4	CTLA4
Endoplasmic reticulum aminopeptidase 1	ERAP1
Endoplasmic reticulum aminopeptidase 2	ERAP2
Enteropathic Arthritis	EnA
Enzyme Linked Immunosorbent Assay	ELISA
Eomesodermin	EOMES
Forkhead Box P3	FOXP3
Gastrointestinal	GI
GATA binding protein 3	GATA-3
Genome-Wide Association Studies	GWAS

Homolog of Blimp-1 in T cells	Hobit
Human Leukocyte Antigen	HLA
Hypoxia-inducible factor 1α	HIF1α
Immunoglobulin A	IgA
Inflammatory Bowel Disease	IBD
Innate Lymphoid cell	ILC
Interferon regulatory factor 1	IRF1
Interferon regulatory factor 4	IRF4
Interferon γ	IFNγ
Interleukin	IL
Interleukin-22 Receptor	IL-22Rα
Interleukin-23 Receptor	IL-23R
Intestinal Epithelial Cells	IECs
JAK inhibitor	JAKi
Janus Kinase	JAK
Kruppel Like Factor 2	KLF2
Magnetic Resonance Imaging	MRI
Major Histocompatibility Complex	MHC
MHC-class Ib-related protein 1	MR1
Mucosal associated Invariant T-cell	MAIT
Natural Killer T-cell	NKT
Naturally occurring Treg	nTreg
Non-radiographic Axial Spondyloarthritis	nrAxSpA
Nuclear receptor retinoic acid receptor-related orphan receptor γt	RORγt
Nuclear Receptor subfamily 4 group A member 1	NR4A1
Peri-entheseal Bone	PEB

Peripheral blood mononuclear cells	PBMC’s
Peripherally induced Treg	iTreg
Phosphodiesterase 4	PDE4
Power Doppler Ultrasound	PDUS
Psoriatic arthritis	PsA
Quantitative real-time PCR	qRT-PCR
RAR Related Orphan Receptor C	RORC
Reactive Arthritis	ReA
Receptor Orphan Related protein A	RORA
Rheumatoid Arthritis	RA
Ribonucleic acid	RNA
Room Temperature	RT
Roswell Park Memorial Institute medium	RPMI
Runt-related transcription factor 1	Runx1
Runt-related transcription factor 3	Runx3
Secreted Immunoglobulin A	sIgA
Standard Error of the Mean	SEM
Single Nucleotide Polymorphism	SNP
Sphingosine-1-Phosphate Receptor 1	S1PR1
Spondyloarthropathy	SpA
T box expressed in T cells	T-bet
T cell receptor	TCR
T Central Memory	TCM
T Effector Memory	TEM
T Effector Memory CD45RA+	TEMRA
T Memory Stem Cells	TSCM

T regulatory cells	Tregs
Tissue Resident Memory	TRM
TNF receptor superfamily member 9	TNFRSF9
Transcription factor T-cell factor 1	TCF1
Transforming Growth Factor β	TGFβ
Tumour Necrosis Factor α	TNFα
Type 3 Innate Lymphoid Cells	ILC3
Tyrosine Kinase	TYK
Ulcerative Colitis	UC
Uniform Manifold Approximation and Projection	UMAP
Variable Diversity Joining	VDJ
Vascular Endothelial Growth Factor A	VEGFA
β2 Microglobulin	β2M

List of Patient Cohort

Patient I.D	Age (years)	Gender (M/F)	Use
HC13	26	M	qRT-PCR
HC18	40	M	qRT-PCR
HC19	25	F	qRT-PCR
Rc283	18	F	ELISA
Rc285	66	M	ELISA
Rc286	77	M	ELISA
Rc290	17	F	ELISA
Rc291	54	M	ELISA
Rc292	16	F	ELISA/ qRT-PCR
Rc293	13	F	ELISA/qRT-PCR
Rc295	30	F	ELISA
Rc296	55	M	ELISA/qRT-PCR
Rc297	66	F	ELISA/qRT-PCR
Rc299	19	F	ELISA/qRT-PCR
Rc302	15	M	ELISA/qRT-PCR
Rc303	84	M	ELISA/qRT-PCR
Rc304	15	F	CD45RA CD69 memory staining
Rc305	77	F	CD45RA CD69 memory staining
Rc306	15	F	CD45RA CD69 memory staining
Rc307	47	F	CD45RA CD69 memory staining
RC323	59	M	CD45RA CD69 memory staining
RC396	15	F	CD4 CD8 Flow Cytometry
Rc399	79	F	CD4 CD8 Flow Cytometry

Rc400	16	F	CD4 CD8 Flow Cytometry
Rc415	20	F	CD4 CD8 Flow Cytometry
Rc419	76	F	CD4 CD8 Flow Cytometry
Rc456	15	M	CD4 CD8 Flow Cytometry
Rc461	70	F	CD4 CD8 Flow Cytometry
Rc462	57	F	CD4 CD8 Flow Cytometry
Rc472	74	M	CD4 CD8 Flow Cytometry
Rc473	82	M	CD4 CD8 Flow Cytometry
HC371	40	M	Flow cytometry Cell Viability testing
HC372	26	M	Flow cytometry Cell Viability testing
HC373	32	F	Flow cytometry Cell Viability testing
Rc161	26	M	Bulk RNA-seq
Rc163	23	M	Bulk RNA-seq
Rc193	54	F	Bulk RNA-seq
Rc195	18	F	Bulk RNA-seq
Rc547	54	F	Single Cell RNA-Seq
Rc548	62	M	Single Cell RNA-Seq
Rc562	40	F	Single Cell RNA-Seq
RC563	65	F	Single Cell RNA-Seq
Rc558	16	F	MAIT Flow Cytometry
Rc559	58	F	MAIT Flow Cytometry
Rc564	17	F	MAIT Flow Cytometry

List of Buffers

FACS Buffer	500mL PBS, 0.1% Bovine Serum Albumin, 0.01% Sodium Azide, 200μL of 2mM Na EDTA
FACS Blocking Buffer	10% mouse serum and 1% human IgG in FACS buffer
MACS Buffer	47.5 mL MACS rinsing solution with 2.5 mL Bovine Serum Albumin
ELISA Wash Buffer	PBS with 0.05% Tween-20 pH 7.4

List of qRT-PCR primers

Gene of Interest (Primer)	Assay_ID
HPRT1 (Housekeeping)	Hs99999909_m1
IL-6	Hs00174131_m1
IL-10	Hs00961622_m1
FOXP3	Hs01085834_m1
TGFβ1	Hs00998133_m1
IL-17A	Hs00174383_m1
STAT3	Hs00374280_m1
STAT5A	Hs00234181_m1
JAK2	Hs01078136_m1
RORA	Hs00536545_m1
RORC	Hs01076122_m1
AhR	Hs00169233_m1
IL-22	Hs01574152_g1
TNFα	Hs99999043_m1

List of Gene of Interest used in Bulk RNA Seq

Gene name	Enterez Gene ID
CD103 (ITGAE)	3682
ITGA1 (CD49a)	3672
S1PR1 (Sphingosine-1-Phosphate Receptor 1)	1901
HPRT (Hypoxanthine Phosphoribosyltransferase 1)	3251
GADPH(Glyceraldehyde-3-Phosphate Dehydrogenase)	2597
CD101	9398
PDCD1 (Programmed Cell Death 1)	5133
CXCR6	10663
TGFB1 (Transforming Growth Factor β)	7040
CD69	969
CD4	920
CD8a	925
CD3e	916
B-actin	60
ABCB1 (ATP Binding Cassette Subfamily B Member 1)	5243
AhR (Aryl hydrocarbon receptor)	196
Bax (BCL2 Associated X, Apoptosis Regulator)	581
Bcl2 (BCL2 Apoptosis Regulator)	596
Blimp-1 (B lymphocyte-induced maturation protein 1)	639
CARD3 (Receptor Interacting Serine/Threonine Kinase 2)	8767
CCR6	1235
CD161	3820
CD226	10666
CD28	940
CD40L	959
CD49b (ITGA2)	3673
C-Maf	4094

CTLA4 (Cytotoxic Lymphocyte Antigen 4)	1493
CXCR3	2833
CXCR4	7852
EOMES (Eomesodermin)	8320
ERAP-1 (Endoplasmic reticulum aminopeptidase 1)	51752
ERAP-2 (Endoplasmic reticulum aminopeptidase 2)	64167
FOXP3 (Forkhead box 3)	50943
HIF1α (Hypoxia-inducible factor 1α)	3091
HLA-B (Major Histocompatibility Complex, Class I, B)	3106
IFNA1 (Interferon Alpha 1)	3439
IFNB1 (Interferon Beta 1)	3456
IFNγ (Interferon Gamma)	3458
IL-10	3586
IL-12RB1 (p40)	3594
IL-17A	3605
IL-17F	112744
IL-17RA	23765
IL-17RC	84818
IL-18	3606
IL-18R1	8809
IL-2	3558
IL-22	50616
IL-23A (p19)	51561
IL-23R	149233
IL-6	3569
IL-7	3574
IL-7R (CD127)	3575
IRF3 (interferon regulatory factor 3)	3661
IRF4 (interferon regulatory factor 4)	3662
JAK2 (Janus Kinase 2)	3717
LAG3 (Lymphocyte Activating 3, CD223)	3902
MKI67 (marker of Ki67)	4288
MR1 (MHC-class Ib-related protein 1, CD154)	3140
PIAS1 (Protein Inhibitor of Activated STAT1)	8554

PIAS2 (Protein Inhibitor of Activated STAT2)	9063
PIAS3 (Protein Inhibitor of Activated STAT3)	10401
PIAS4 (Protein Inhibitor of Activated STAT4)	51588
PLZF (Promyelocytic leukemia zinc finger protein)	7704
RORA (RAR Related Orphan Receptor A)	6095
RORC (RAR Related Orphan Receptor C)	6097
RUNX3 (RUNX Family Transcription Factor 3)	864
SOCS1 (Suppressor of cytokine signalling 1)	8651
SOCS2 (Suppressor of cytokine signalling 2)	8835
SOCS3 (Suppressor of cytokine signalling 3)	9021
STAT3 (signal transducer and activator of transcription 3)	6774
STAT5A (signal transducer and activator of transcription 5A)	6776
TBX21 (T-Bet)	30009
TYK2 (Tyrosine Kinase 2)	7297
ZNF683 (Hobit)	257101
α4β1 (VLA-4)	3676
Furin (Furin, Paired Basic Amino Acid Cleaving Enzyme)	5045
CD45R	5788
CD38	952
HLA-DRA (Major Histocompatibility Complex, Class II, DR Alpha)	3122
CCR7	1236
CD57	27087
CD27	939

List of Figures

Chapter 1

Introduction

1.1 Spondyloarthropathies

The spondyloarthropathies (SpA) are a family of chronic joint diseases including Ankylosing Spondylitis (AS), Psoriatic Arthritis (PsA), Reactive Arthritis (ReA) and Enteropathic Arthritis (EnA). In addition, patients with Inflammatory Bowel Disease (IBD) have an increased risk of developing SpA. Using the Assessment of Spondyloarthritis international Society (ASAS) classification criteria, seronegative SpA can be distinguished from other forms of arthritis due to the development of chronic inflammation in both axial and peripheral joints, new bone formation that is centred on enthesis that are ligament and tendon anchorage points. Collectively the SpA group of conditions are associated with extra-articular manifestations including psoriasis, uveitis, IBD, Crohn's disease and ulcerative colitis (UC).

Axial spondyloarthritis (AxSpA) is a classification of seronegative spondyloarthropathies characterised by radiographic damage and ankylosis of the sacroiliac joint. This classification includes ankylosing spondylitis (AS), which is associated with radiographic findings, as well as non-radiographic axial spondyloarthritis (nrAxSpA), which does not exhibit radiographic changes but may show signs of inflammation in the sacroiliac joint via magnetic resonance imaging (MRI) or power Doppler ultrasound (PDUS) (1). Where the AxSpA and nrAxSpA morbidities are associated with excessive tissue repair responses ultimately culminating with new bone formation. This is distinct from rheumatoid arthritis (RA) responses where inflammation leads to both bone and cartilage destruction (2). Target tissues in AxSpA include the skin, gut and aortic root aside from the skeleton, these sites become biomechanically or chemically stressed and are linked with damage and repair responses. In AxSpA common symptoms associated with disease pathogenesis are inflammation, bone and cartilage loss, and subsequent remodelling with new bone formation taking place in the enthesis, axial skeleton, and peripheral joints. AxSpA patients also often present with extra-articular manifestations, including inflammatory bowel lesions, psoriasis, and uveitis, emphasising AxSpA as a debilitating disease frequently associated with chronic pain and a reduced quality of life as a result.

The global prevalence of AS ranges from ~9 to 30 per 10,000 in the general population, with the caveat of a wide range of variance dependent on the country (3) when looking at epidemiological AS studies. Where AS prevalence has a wide scale ranging from 6.5 per 100,000 in Japan to 540 per 100,000 in Turkey (4). Whereas nrAxSpA was seen to be more frequent in females with lower C reactive protein (CRP) levels accompanied by less structural damage. The progression of non-radiographic to radiographic SpA is ~10-20% within the first year increasing to <20% over two to six years, however, progression is dependent on baseline CRP/positive MRI (5).

One of the key markers associated with AS susceptibility is the presence of the major histocompatibility complex 1 (MHC-I) allele, human leukocyte antigen B27 (HLA-B27). However, even though HLA-B27 is present in ~90% of AS patients, this only confers ~20-25% of the genetic risk (6). Furthermore, AS only develops in a small fraction of the HLA-B27+ individuals, thus highlighting the contribution of other factors associated with increased AS susceptibility (7), these include polymorphisms in endoplasmic reticulum aminopeptidase 1 and endoplasmic reticulum aminopeptidase 2 (ERAP1/ ERAP2), which trims antigenic peptides residues for MHC-I binding (8) and bacterial dysbiosis in locations remote to the affected joint, which is a classic feature of the SpA's where ~70% of people suffering from AS see inflammation in the gut mucosa where in ~5-10% of these patients this eventually progresses into Inflammatory bowel disease (IBD) (9). Whilst AS is strongly associated with MHC class I, namely HLA-B27, AS also shows MHC class II associations. In the absence of autoantibodies, and given the IL-23R pathway Single Nucleotide Polymorphisms (SNPs) it is credible that Th17 cells may play a role in AS disease pathogenesis.

Several genetic variants associated with increased AS susceptibility have been identified including several polymorphisms within the IL-23/IL-17 signalling pathway including Interleukin 23 receptor (IL23R), IL12B, IL6R, Janus Kinase 2 (JAK2) and Tyrosine kinase 2 (TYK2) (10) (11). The Genome-Wide Association Studies (GWAS) data incriminating lymphocytes in axial SpA is supported by basic immunology principles where both innate and conventional αβ T-cells found at the normal human enthesis have inducible key SpA-associated cytokines, IL-

17A and TNFα (12). Where CD4+ and CD8+ T-cells were reported to constitute a lymphocyte lineage derived from precursors that moved into entheseal tissue during an active phase of an immune response and remained within that tissue (12). Furthermore, both the IL-17A and TNF pathways have been targeted in humans providing support for the pivotal role of these pathways in AS pathogenesis.

1.2 Signalling Pathways

Previous literature has identified several immune cell types that are associated with pro-inflammatory cytokine production of IL-17, IL-22, IL-23 and TNF that are involved in tissue repair responses (13). The finding that IL-17 and cyclooxygenase (COX) pathway inhibition is effective in AS but not RA highlights the importance of these pathways in relation to SpA pathogenesis (14). Evidence from studies shows that individuals with AS have elevated prostaglandin levels, generated by the COX-2 enzyme, in their synovial fluid during inflammation (15), as COX-2 is an inducible enzyme that is mainly found at sites of inflammation.

The discovery of the IL-17/IL-23 pathway in 2005 unveiled new therapeutic targets for AxSpA and psoriatic arthritis (PsA) (16). IL-23 is essential in the pathogenesis of many inflammatory conditions such as psoriasis, UC and Crohn’s disease to name a few, where it stimulates a cell population that exhibits a unique inflammatory gene signature, including IL-17A, IL-17F, IL-6, CCL20, and IL23R. This specific gene expression, coupled with the activation of the JAK2/STAT3 signalling pathway, facilitated the identification of a new subset of IL-17-producing T-cells known as Th17 cells (17). Polymorphisms in the IL-23 signalling pathway, including Interleukin-23 Receptor (IL23R), IL-12β, JAK2, and TYK2, have all been linked with increased AS susceptibility showing its importance in IL-17A production (18). IL-23 is essential for the terminal differentiation of Th17 cells and the differentiation, survival and expansion of a specific subset of γδ T-cells that are known to produce IL-17 (19). γδ T-cells are a non-MHC specific T-cell type that can be divided into three subsets based on their ability to produce either IL-17 (γδT17), IFN-γ (γδT1) or both IL-4 and IFN-γ (γδNKT), respectively (20). IL-23R signalling enhances Th17 development in the presence of IL-23. It is immunomodulatory which is mediated by downstream IL-17 and IL-22. IL-22 is associated with intestinal epithelial repair and has a protective role at the gut barrier but can also be pro-inflammatory where its function is dependent on the cell type that produced the IL-22 and the surrounding cytokine milieu. Furthermore, osteoproliferation seen in SpA is mediated by IL-22 (21). The IL-22 receptor (IL-22Rα) is not expressed in immune cells which creates a uni-directional signalling pathway meaning only certain populations of immune cells including T-cells, γδ T-cells and Natural Killer T-cell (NKT) cells can express IL-22. The murine model study conducted by Sherlock *et al.* in 2012, demonstrated that spondyloarthritis is independent of Th17 cells which is consistent with the key role of the resident IL-23R+ entheseal cell population in mediating disease (22). However, whether this finding also translates to human studies has yet to be fully elucidated.

IL-23 is a heterodimer composed of one IL12p40 and one IL23p19 subunit, modulation of the IL-23/IL-17 pathway through biologics targeting IL-12/23, IL-23, IL-17A or IL-17RA has provided validation of its critical role in human autoimmune disease but crucially only in some SpA family member diseases and not RA (23), however it is not yet fully understood how these pathways are altered and why some biologics work in certain diseases but not in others. For example, Phosphodiesterase 4 (PDE4) inhibitors which target the IL-12/IL-23 pathway are effective in SpA but not RA. The genetic associations of variants of the IL-17/IL-23 pathway had been demonstrated in the axial form of the disease (AS) (24) surprisingly, clinical trials targeting IL-23, either via IL23p19 (Risankizumab) or IL-12p40 (Ustekinumab), failed in the axial forms of the disease (AS and RA respectively) (25) (26), while their use in the peripheral forms (PsA) was effective (27) (28). These results suggest distinct pathophysiology between the different forms of the disease and underline our incomplete understanding of the mechanisms of action of these molecules during the course of the disease. One of the hypotheses put forward to explain this discordant effect of IL-23 targeting on axial and peripheral forms of SpA is that other IL-17-producing cells may be independent of IL-23 (29), (30), (31). Assuming this, therapeutic strategies targeting IL-23 would not be effective in preventing the secretion of the effector cytokine (IL-17) and would be ineffective in treating the axial form, AS, in which these cells would be involved.

1.3 T-cells

The most common lymphocytes found at the normal enthesis were CD4+ T-cells, where it is well documented that CD4+ T-cells aid in CD8+ T-cell activation and survival during infection and immunisation via upregulation of IL2R and dendritic cell interactions (32). Over the past three decades, the number of recognised T helper cell lineages has increased highlighting the diversity of T cell fates, each with distinct functional properties in mediating adaptive immunity and autoimmune diseases (33). The first subpopulations discovered in 1986 are the Th1 and Th2 cells, where Th1 cells participate in intracellular bacterial clearance, whereas Th2 cells increase the humoral response, typically against helminths via IL-4, IL-5, and IL-13 mediated inflammation. Protection against bacterial and fungal infection is mediated by Th17 cells (34). In healthy individuals' inflammation is regulated via the CD4+ T regulatory cells (Tregs) which limits the availability for the CD28 costimulatory binding, which is required for complete T-cell activation. Whilst CD4+ T-helper subsets are important in pathogen clearance; their dysregulation can cause excessive inflammation and subsequent tissue damage. Because Th cells are so central to adaptive immunity, elucidating differences in patterns of “Th” immunology is important for therapeutic development in chronic inflammatory non-infectious diseases.

1.4 Gut Microbiome

Increased microbiota diversity (or richness) and resilience (i.e., the ability to recover from perturbations) are generally associated with enhanced health, where a shift from the steady state, known as dysbiosis, is associated with disease pathogenesis in obesity, IBD and AS to name a few (35). The interdependent relationship between the immune system and the microbiota is highlighted by studies showing that a loss of microbial diversity correlates with inflammation and immune cell activation creating a feedback mechanism for further dysbiosis (36). In healthy subjects the innate immune system rarely impacts the microbiota equilibrium, however, in cases of chronic inflammation this can alter the microbiota due to recruitment of antigen-presenting cells (APCs) and subsequent pro-inflammatory cytokine production. The *Klebsiella spp*. which usually resides in the oral mucosa can colonise the gut and elicit increased IFNγ expression via a Th1 response (37), where the colonisation occurs during microbiota dysbiosis culminating in severe gut inflammation. The microbiota is integral in controlling the Th17/Treg balance, where members of the *Citrobacter rodentium* can induce intestinal Th17 cells (38) in mice, and *Clostridium spp.* can induce Treg cells (39) in humans. This is important as it is well documented that both IL-17A and IL-6, provide a protective role in intestinal barrier function (40), where IL-17A is crucial for the maintenance of tight junctions where damage can result in a ‘leaky gut’.

Th17 cells can arise in the gut via IL-23-dependent and independent mechanisms (41), these cells subsequently circulate to the joints where they release IL-17 causing subsequent inflammation. The gastrointestinal (GI) tract has evolutionarily adapted to the ‘physiological hypoxia’ observed at a steady state, where Intestinal epithelial cells (IECs) permit the appropriate function of the epithelium which allows for mucosal barrier functionality (42). For most immune cells to adapt to the hypoxic environment, hypoxia-inducible factor 1α (HIF-1α) activation is utilised. Previous work has shown that HIF-1α induced activation increases proliferation and differentiation in Th17 cells whilst impairing Treg cell differentiation via FOXP3 protein degradation (43), moreover, *in vitro* and *in vivo* Th17 differentiation is deficient in T-cells lacking HIF-1α. Furthermore, when T-cells are in conditions favouring Th17 differentiation (IL-6, Transforming growth factor beta (TGFβ)) there is a positive regulation of STAT3-dependent HIF-1α (44).

Immunoglobulin A (IgA) plays an important role in both preventing host colonisation and pathogen invasion at the mucosal barrier of the intestines. Furthermore, IgA can modulate intestinal commensal colonisation and subsequent symbiosis in *B. fragilis* (45). This is important to note as secreted IgA (sIgA) can be produced in a T-cell-dependent manner (46), where studies have seen dysbiosis in the gut microbiome caused by IgA deficiency (47) highlighting its importance in maintaining gut homeostasis with regards to adaptive immunity.

Hypothesis

The primary hypothesis of this study was to ascertain whether T-cells are present in the normal human enthesis and if they are capable of producing IL-17A. Additionally, it aimed to verify the presence of Cytotoxic CD8+ T cells within entheseal tissue and their potential to produce IL-17A.

Aims

This research aimed to address several objectives, the primary one being to ascertain whether T-cells are present in the human enthesis. Additionally, I sought to characterise the immune status of T-cells both at the enthesis and in matched peripheral blood. Alongside this to complete an evaluation of potential novel drug targets for AS patients, focusing on conventional disease modifying antirheumatic drugs (csDMARD’s), JAK inhibitors (JAKi), retinoic acid receptor-related orphan receptor γt (RORγti) and phosphodiesterase 4 inhibitors (PDE4i’s). In this work, a CD4+ entheseal-derived T-cell population capable of producing IL-17A and TNF could be a clear therapeutic target to alleviate excessive inflammatory responses associated with AS pathogenesis. Furthermore, to confirm findings at the transcript level in functional studies. The final objective is to compare IL-17 production in an IL-23 dependent and independent manner within the identified T-cell subsets.

Chapter 2

Materials and Methods

2.1 Ethical Approval

This study was conducted in accordance with the ethical guidelines and principles of the 1964 Helsinki declaration and its subsequent amendments. The study protocol was approved by the North West-Greater Manchester West Research Ethics Committee (REC: 16/NM/0797). For the CD4/CD8 T-cell analysis, human interspinous process and matched peripheral blood were obtained from 25 patients (patients completed an Understanding Osteogenesis in Health, Development and Disease Consent form) (mean age of 42.4±27, median age of 39, and female to male ratio of 3:2) who underwent elective spinal surgery for either decompression or scoliosis correction. For the MAIT cell analysis human interspinous process and matched peripheral blood were obtained from 5 non-axSpA patients (with informed written consent) (mean age of 42.6±12, median age of 47, and female to male ratio of 4:1) who underwent elective spinal surgery.

2.2 Sample processing

Entheseal samples were separated into entheseal soft tissue (EST) and peri-entheseal bone (PEB) whereby both were enzymatically digested. Entheseal samples were collected from patients and transported in sterile saline where processing took place immediately or after overnight storage at 4°c. The entheseal sample was broken into <5mm^2 fragments using a scalpel and bone forceps, this is where EST and PEB were separated, following this the weight of each was recorded. The sample (EST and PEB) was then washed several times with RPMI media to isolate cells and passed through a 0.22μm sterile filter unit (Millipore express); any material that could not pass through the filter was discarded; the sample was then centrifuged at *700g* for 10 minutes. These cells were re-suspended in complete RPMI (Roswell Park Memorial Institute medium containing 10% heat-inactivated fetal bovine serum, 50 U/ml penicillin, 50 μg/ml streptomycin) and counted using a haemocytometer with trypan blue as a viability stain. Peripheral venous blood (5mL) was collected from patients and stored aseptically in sterile EDTA vacutainers and processing took place immediately or after overnight storage at 4°c.

For both cell preparations, entheseal-derived and blood-derived cells, density gradient separation (Lymphoprep) was conducted in order to obtain peripheral blood mononuclear cells (PBMCs) and entheseal mononuclear cells (EMCs), respectively.

2.3 $CD4^+$/$CD8^+$ Magnetic Separation

Following the isolation of EMCs from digested entheseal samples and PBMCs from processed blood, CD4+ and CD8+ T cells were isolated using biotinylated anti-CD4 or CD8 (both from Miltenyi Biotech). Cells were isolated using magnetic separation (Miltenyi Biotech LS columns), according to the manufacturer's instructions. Following cell counting, both PBMC and PEB samples were re-suspended in FACS blocking buffer (100 µL / 1x 10^6 cells) with 2µL CD4+ - Biotin Human Ab (clone: M-T466 Miltenyi Biotech) per 100 µL FACS blocking buffer for a 15-minute incubation at RT. Following this, volumes were made to 5mL using ice-cold MACS Buffer and centrifuged for 5 minutes at *500g*. The supernatant was removed and the pellet was re-suspended in a 1:5 dilution of Anti Biotin Microbeads (Miltenyi Biotech) for 15 minutes at 2-8°C.

During this incubation step LD columns (Miltenyi Biotech) were prepared, these are used for the depletion of unwanted cells and placed inside a magnet for negative selection, where even weakly labelled cells are efficiently retained within the column. Following incubation, volumes were made up to 5mL using ice-cold MACS Buffer and centrifuged for 5 minutes at *500g* at room temperature (RT), following this the supernatant was removed and the pellet re-suspended in 500µL MACS buffer. The sample was then passed through the LD column, this was subsequently followed by 3 mL MACS Buffer which was allowed to drip through, these cells were collected and kept on ice for later use.

Next, the column was removed from the magnet and placed into a 50 mL falcon tube and 3 mL MACS buffer was added, using the plunger, cells were collected at the bottom of the falcon tube. The isolated cells were taken and repeated the process, from the LD column preparation stage, with a new LD column and plunging the cells through as previous, classifying these cells as $CD4^+$ isolated cells.

We then repeated the whole bead separation process, with the cells kept on ice, adding 2 µL anti CD8- biotin Human Ab (clone: REA734 Miltenyi Biotech) per 100 µL FACS blocking buffer, isolating $CD8^+$ cells. Following the isolation of both cell types, the cells were counted on a haemocytometer and stained for viability using trypan blue.

2.4 Cell Culture

Following cell isolation, CD4+ and CD8+ T cells were plated out in a 96-well plate (minimum of 5×10^4 cells/well) in RPMI (GIBCO) containing 10% fetal calf serum and 1% penicillin/streptomycin. For inhibition studies, cells were incubated with the following compounds for 1 hour in standard culture conditions (5%CO2, 37°C): RORγt inhibitor 10 µM (Pfizer), Methotrexate, 5 mg/mL (Cayman Chemical), Rolipram (a PDE4 inhibitor) 10 µM (Cayman Chemical), Tofacitinib 1µM (Pfizer) or dimethyl sulfoxide (DMSO) control (0.1%). All drugs were diluted to maintain a final concentration of 0.1% DMSO. Cells were stimulated using anti-CD3/CD28 (GIBCO) for 48 hours. To test the potential of compounds to affect cell viability, flow cytometry was used to assess CD45+, CD3+, CD4/CD8+ and live dead viability by Zombie Aqua (BV405, Biolegend).

2.5 Enzyme Linked Immunosorbent Assay

Following 48 hours of stimulation, cells were removed by centrifugation and supernatant was stored at −80°C. Concentrations of TNF and IL-17A were measured using sandwich ELISAs from eBioscience/Thermo Fisher (Waltham, Massachusetts, USA). ELISAs were carried out according to the manufacturer’s protocol. The absorbance readings were produced using the Ascent software (Version 2.6, Thermo Fisher) measuring at 450 nm and 540 nm. In order to remove optical inconsistences caused by plate variation, the 540 nm reading was subtracted from the 450 nm readings. Following this, pg/mL and pg/cell were calculated.

2.6 Intracellular Flow Cytometry

Entheseal mononuclear cells, 5 $x10^6$, were plated out and stimulated with anti-CD3/CD28 as before in the presence of Golgi plug (BD) for 3 hours. The cells were fixed using Intraprep kit (Beckman Coulter) and stained intracellularly with IL-17A and TNF and assessed via flow cytometry. In order to collect the appropriate data a flow cytometry gating system was used, whereby cells were filtered based on lymphocyte gating, doublet exclusion, live/ dead staining followed by CD3+ CD45+ filtering ultimately culminating in CD4+ and CD8+ T-cell sub-populations.

2.7 MAIT Cell Protein expression analysis

Stimulated cells from PEB EMCs were intracellularly stained for IL-18 and analysed using flow cytometry gating system, as described in section 2.1.6. Following 24hr LPS stimulation (100ng/mL) IL-18 protein was analysed in the supernatant using Legendplex inflammation panel (BioLegend) using the Cytoflex LX flow cytometer (BD) according to the manufacturer's instructions.

2.8 RNA extraction

Ribonucleic acid (RNA) purification was completed following the Norgen Total RNA purification kit (Norgen Biotek Corporation) protocol. Following this, RNA concentration (ng/µL) and quality was checked using the Nano drop (ND 1000). Purified RNA was stored at -80°c for subsequent complementary DNA (cDNA) synthesis.

2.9 cDNA synthesis

Following RNA purification cDNA synthesis was performed following the High capacity cDNA Reverse transcription kit protocol (Applied Biosystems) as per the manufacturer’s instructions. The reaction volumes were set to 20µL and subsequently loaded into a thermal cycler (Veriti 96 well thermal cycler, Applied Biosystems), samples were then stored at -20°c.

2.10 Quantitative real-time PCR

T-cells were sorted using an Influx (BD) cell sorter directly into RNA extraction buffer, supplied as a component of the PicoPure RNA isolation kit (Thermo Fisher). cDNA was synthesised with a reverse transcription kit then underwent preamplification (18 cycles) using a pre-amp master mix (Fluidigm) with a solution containing all primer sets. All primers were purchased from Applied Biosystems. Transcript analysis was performed by qPCR using the Biomark HD gene expression system (Fluidigm); values displayed are log $10^{\Delta Ct}$ relative to the HPRT1 housekeeping gene.

qRT-PCR was completed using the TaqMan Gene expression assay as per the manufacturer's instructions (Applied Biosystems). Samples, no template control (NTC) and positive controls (pooled cDNA) were loaded onto either a MicroAmp Optical 96-Well Reaction Plate (Applied Biosystems) or a MicroAmp Optical 384-Well Reaction Plate (Applied Biosystems) and run on either the Quantstudio 5 or Quantstudio 7 instrument, respectively (both from Applied Biosystems) using the Quantstudio Design and Analysis software (V. 1.4, Thermo Scientific), the Comparative Threshold (Ct) value was subsequently normalised using the HPRT1 housekeeping gene and unstimulated control for $2^{-\Delta\Delta Ct}$. All primers were purchased from Applied Biosystems.

2.11 Bulk RNA-Seq

Bulk RNAseq was performed on CD3+CD45+CD4+ or CD8+ T-cell subsets isolated from entheseal digests n=4 for both PEB and EST. RNA was then purified using the PicoPure RNA isolation kit (Thermo Fisher), RIN (RNA Integrity Number) scores and concentration in ng/μL were determined by Tape Station prior to RNAseq analysis. Following this, MiXCR (V.3) was used to extract clonal TCR rearrangements. CDR3 (complementary determining region 3) amino acid sequences were used to interrogate the TCR3 database (https://tcr3d.ibbr.umd.edu/) in order to assess epitope specificities based on model-based scoring matrices (PAM-30).

CD4 and CD8 T-cells from both the bone and soft tissue were flow sorted and transcripts were sequenced on a NovoSeq using an Illumina TruSeq stranded Total RNA kit. Reads were aligned to hg38 using HISAT2 and counts were generated using Feature Counts, both accessed through the Galaxy platform. The generated CSV files from the BAM files gave Entrez Gene I.D numbers, this allowed for gene identification from both lanes using Entrez which is the NCBI's (National Center for Biotechnology Information) molecular biology database system for gene-specific information. All results were subsequently normalised with the GADPH housekeeping gene to create normalised expression values.

2.12 Single Cell RNA-Seq

Entheseal samples were enzymatically digested and stored in complete RPMI media at 2-8°C ready for transportation to complete single cell RNA-Seq analysis (n=4, 3 Female, 1 Male). The sequence data was run through Cellranger (v6, with transcriptome reference "refdata-gex-GRCh38-2020-A") and pre-processing pipelines (https://github.com/COMBATOxford/cellhub-devel, access available on request) to generate a single matrix ("all.cells.matrix") with the count data for all of the cells (no qc filtering applied). There is an accompanying cell metadata file ("all.cells.metadata.tsv.gz") that provides a mapping between cell barcodes and samples. It also contains pre-computed QC statistics and scrublet doublet scores for each cell as well as the experimental metadata. These files were subsequently used for downstream analysis with Seurat.

To provide an initial overview to help guide downstream analysis a first-pass analysis of the full dataset (bone and enthesis together) was performed using alignment and analysis pipelines with "default" settings. For this analysis, no QC filters were applied (cell quality was not assessed) and parameters were selected without inspection of the diagnostic plots (30 PCAs, 2000 variable genes being used). Further downstream filtering was completed using Juypter Notebook, an open-source interactive computational environment. I implemented a simple filtering strategy in order to clean the data, this included the removal of cells that have less than 200 genes, the removal of genes that are detected in less than 3 cells, the removal of cells that had too many mitochondrial genes expressed and the removal of cells that had <20,000 in total counts respectively. Harmony was used to align the data (by sample id), and the subsequent Uniform Manifold Approximation and Projections (UMAPs) created are using resolution 1.0 respectively.

2.13 Statistical Analysis

Analysis was performed using GraphPad Prism software (GraphPad Software, La Jolla, California, USA) and statistical analysis was performed in SPSS (IBM SPSS Statistics V.25, USA). Error bars represent the SE of the mean (SEM); refer to the Results section for specific tests used per experimental procedure.

Chapter 3

CD4+ and CD8+ T-cells at the Enthesis

Results

3.1 CD4+ and CD8+ T-cells are present in the human enthesis

3.2 Transcriptional and flow cytometric profiling of entheseal CD4+ and CD8+ T-cells compared with peripheral blood supports TRM status

3.3 Inducible IL-17A and TNF in entheseal CD4+ and CD8+ T-cells

3.4 Analysis of regulatory markers in entheseal and blood-derived T-cells

3.5 RORγti, MTX, Tofacitinib and PDE4i impact on enthesis CD4+ and CD8+ T-cell cytokine production

3.1 CD4+ and CD8+ T-cells are present in the human enthesis

To begin studies within the enthesis I wanted to determine whether there were T-cells present and their exact locations. To investigate entheseal T-cell topography, anti-CD3 immunofluorescence was utilised where tonsil tissue was used as a positive control. T-cells at the enthesis were sparse and often located in small clusters as seen in Figure 1.1.

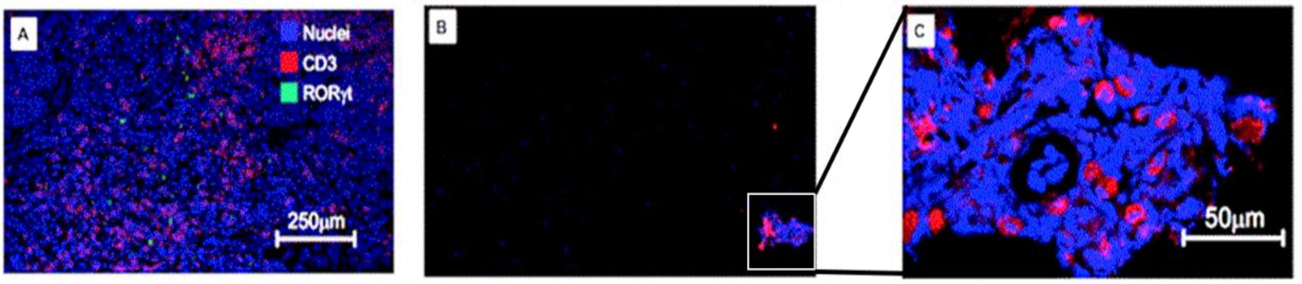

Figure 1.0: Anti-CD3 Immunofluorescence microscopy at the enthesis

Figure 1.1 displays immunofluorescence in entheseal T-cells. Anti-CD3 immunofluorescence staining showing T-cells in the tonsil as a positive control (A), in the enthesis at lower power (B) and at higher power (C) where a small region of CD3 positivity in (B) is magnified, where nuclei are blue, CD3 is red and RORγt is green.

For immunofluorescence microscopy in Figure 1.1, frozen sections of healthy entheseal soft tissue (EST) were incubated with an Alexa Fluor 647 labelled antibody against CD3 (clone UCHT1, BD Biosciences) and counterstained with 4′,6-Diamidine-2′-phenylindole dihydrochloride (DAPI).

Following enzymatic digestion of the peri-entheseal bone (PEB) spinal samples, flow cytometry was used to identify CD4+ and CD8+ T-cells from the enthesis, where distinct populations of both CD4+ and CD8+ T-cells were identified at the enthesis as seen in Figure 1.2. This suggests the importance of T-cells with regards to the inflammatory response present at the enthesis, which is under constant mechanical stress. This inflammatory response to mechanical stress is not only seen in SpA at the enthesis, but is also applicable to other tissues in association with cancer pathogenesis respectively when an immune response is triggered (48).

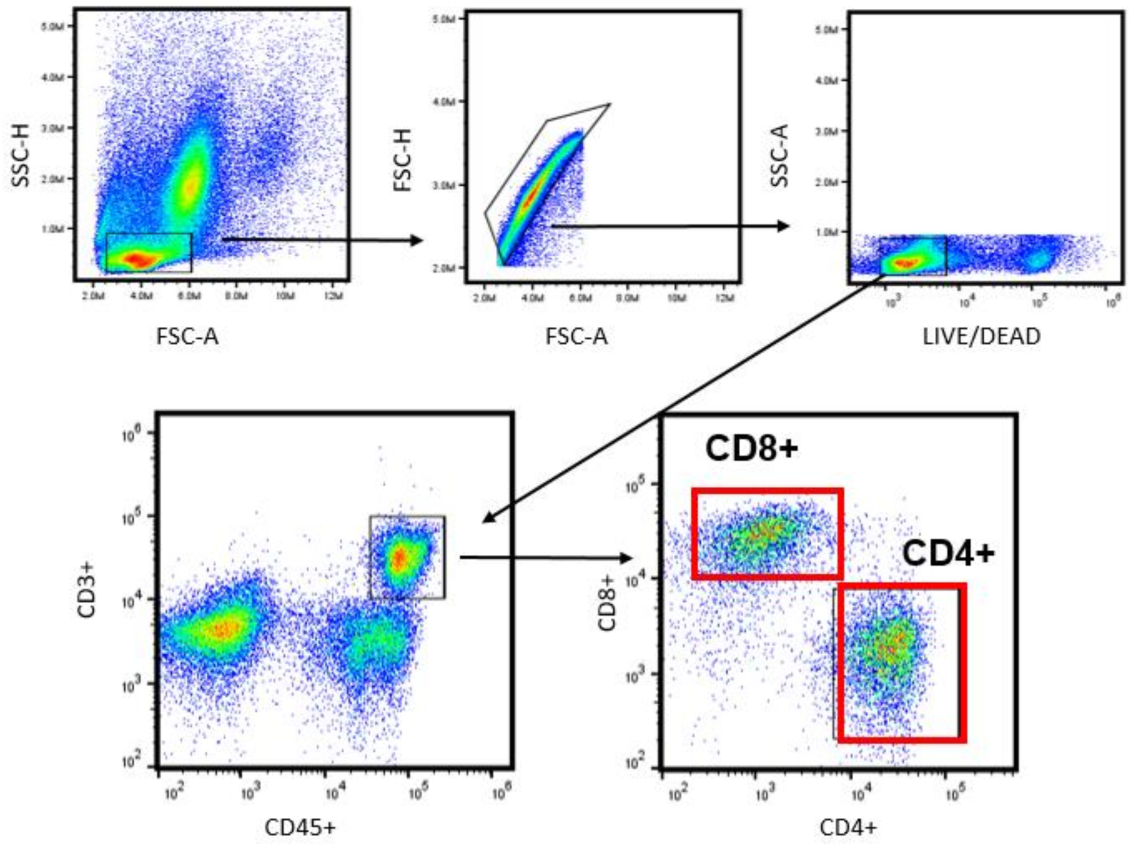

Figure 1.2: Flow Cytometry identifying CD4+ and CD8+ T-cells at the enthesis

Phenotypic identification of CD4+ and CD8+ T-cells by FACS following digestion of human enthesis. Following doublet exclusions seen in panel 2 and live/dead staining, seen in panel 3, cells were gated on CD45+ (all white cell count) and CD3+ (all T-cells) as shown in panel 4; this gate was then further subdivided into CD4+ and CD8+ T-cells as seen in panel 5. In Figure 1.2 the percentage of CD4+ T-cells was higher in peripheral blood when compared to enthesis (56.6% (43.61-66.2) and 32.7% (7.44-51.7), respectively) (p=0.0013). However, there was no significant difference in CD8+ T-cells percentages between peripheral blood and enthesis (31.1% (25.1-39.5) and 32.1% (19.4-46.1), respectively) (p=0.875).

3.2 Transcriptional and flow cytometric profiling of entheseal CD4+ and CD8+ T-cells compared with peripheral blood supports TRM status

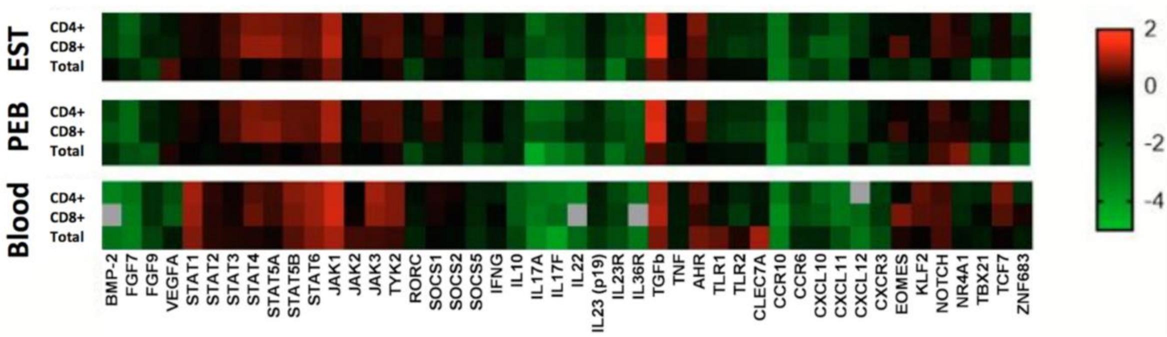

Figure 1.3: Transcriptional profiling of entheseal T-cells

CD4+ and CD8+ T-cells were sorted from entheseal soft tissue, Peri-entheseal Bone and Peripheral Blood, (EST, PEB, and Blood respectively) following digestion.

Basal expression of cytokines, chemokines, growth factors, signalling molecules, and tissue residency markers were assessed. Colour coding refers to differentially expressed genes where values less than −1 indicate lower expression and values greater than 1 indicate higher expression, those with

grey boxes indicate no values; values displayed are log 10ΔCt relative to the HPRT housekeeping gene, where the HPRT gene has been widely used as a endogenous control in molecular studies (49). (n=16 samples)

In order to investigate the T-cell biology of the enthesis, I assessed transcriptional profiling, as this was a more efficient way to look at key T-cell markers and associated transcription factors when compared to flow cytometry. For the data in Figure 1.3, all sample data was non-parametric, and therefore I used the Kruskal-Wallis test with Dunn's *post-hoc* testing to determine whether there was statistical significance. Blood-derived and entheseal-derived (from PEB and EST) T-cell transcripts (CD4+ and CD8+ T-cells) indicate tissue-resident T-cells, as illustrated in Figure 1.3, as entheseal T-cells express higher *AhR* and *NR4A1* transcripts, with the former having statistical significance in both T-cell subtypes (CD4+ and CD8+), where CD4+ PEB vs blood gave p=0.044 and CD4+ Blood vs EST p=0.004, with no significant difference between PEB and EST. Where Aryl hydrocarbon receptor (AhR) has been shown to promote TRM status in CD8+ T-cells, and NR4A1 expression has been shown to be is increased in a TRM phenotype (50) (51).

CD8+ T-cells also showed statistical significance with regards to AhR Expression, where PEB vs blood gave p=0.028 and blood vs EST p=0.006, similarly to CD4+ T-cells there was no statistical significance when comparing PEB and EST. The highest statistical significance, with regards to NR4A1 expression, was seen in the CD8+ T-cell subset, where PEB vs blood gave p=0.036 and blood vs EST gave p=0.013. The only significant difference for NR4A1 in CD4+ T-cells was that between blood and EST p=0.005, in the same way as the AhR expression neither CD4+ or CD8+ subsets showed any significance between PEB and EST. Where the results showed elevated expression levels of NR4A1 in EST, supporting TRM phenotype in tissue.

Additionally, blood-derived T-cells expressed elevated levels of Kruppel Like Factor 2 (KLF2) and T box expressed in T cells (T-Bet) transcripts that indicate circulating T-cells. Where studies have shown KLF2 to be downregulated in TRM cells, whereas circulating T-effector cells express high levels of T-bet (52) (53). Whereby blood-derived CD4+ T-cells showed statistical significance, with regards to KLF2 transcript when compared to PEB (p=0.04) and EST (p=0.006) in Dunn’s post-hoc testing. Blood-derived CD8+ T-cells also showed significance but only when compared to EST (p=0.004). T-Bet did not show any statistically significant differences in either CD4+ or CD8+ T-cells following Dunn’s *post-hoc* testing, which begs the question of whether T-Bet has a role in Th1 polarisation.

A comparison with peripheral blood revealed that entheseal CD4+ and CD8+ T-cells expressed higher levels of Vascular endothelial growth factor A (VEGFA), TGFβ1, and IL-10, which are molecules associated with tissue repair and homeostasis. These findings are important as they identify entheseal tissue-resident T-cells with tissue repair and homeostatic capacities, rather than pro-inflammatory capacities.

VEGFA transcripts showed statistical significance in CD4+ T-cells when comparing PEB vs Blood (p=0.01) and Blood vs EST (p=0.006) with Dunn’s *post-*

hoc testing. The results with regards to CD8+ T-cells were similar, with significance between PEB vs blood and Blood vs EST (p=0.001 and p=0.017 respectively). TGFβ1 transcripts also showed significance with CD4+ T-cells in PEB vs Blood and Blood vs EST (p=0.007 and p=0.003 respectively). Again similarly to VEGFA CD8+ T-cells show significance between PEB vs blood and Blood vs EST (p=0.049 and p=0.000 respectively). IL-10 saw the same patterns of significant differences as the previous transcripts mentioned, VEFGA and TGFβ1, where CD4+ T-cells had significance in PEB vs Blood and Blood vs EST (p=0.007 and p=0.006 respectively). The same was seen in CD8+ T-cells in PEB vs Blood and Blood vs EST (p=0.022 and p=0.009 respectively).

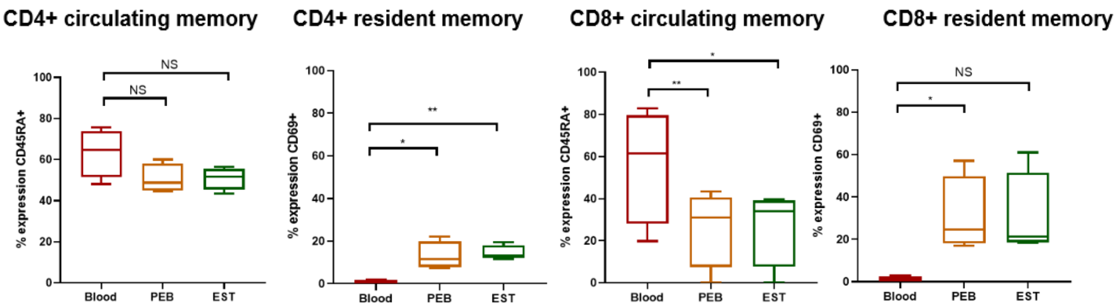

Figure 1.4: Flow cytometric profiling of entheseal T-cells

Flow cytometry was used to assess the percentage of circulating memory T-cells (CD69- CD45RA+) and resident memory T-cells (CD69+ CD45RA-) in both CD4 + and CD8+ T-cells in PEB, EST, and PB paired t-tests, (n=4) 4 Female, Mean Age 38.5. *p<0.05; **p<0.01; ***p<0.001; NS not significant. EST, entheseal soft tissue; PEB, perientheseal bone.

Next, I wanted to assess both the entheseal and blood-derived T-cell phenotype further via cytometric profiling. Subsequently, I found entheseal-derived CD4+ and CD8+ T-cells showed significantly higher CD69 expression, supporting a tissue-resident memory (TRM) phenotype as opposed to CD45RA+ cells which are more indicative of naïve cell types. In contrast, a greater percentage of blood-derived T-cells had CD45RA expression, a marker classically used to identify naïve/ early memory T-cells, compared to entheseal-derived T-cells, which further corroborates the story of tissue residency in entheseal T-cells.

Figure 1.4 displays the number of CD4+ resident-memory T-cells (CD69+) that show statistical significance between both Blood and PEB and Blood and EST following paired T-tests, p=0.0355 and p=0.0053 respectively. In CD8+ circulating-memory (CD45RA+) significance is seen between Blood vs PEB and EST vs Blood, p=0.0088 and p=0.0136 respectively. CD8+ resident-memory T-cells show statistical significance when comparing Blood and PEB p=0.0394, with the comparison between EST and blood being close albeit outside of the range for statistical significance (p=0.0558).

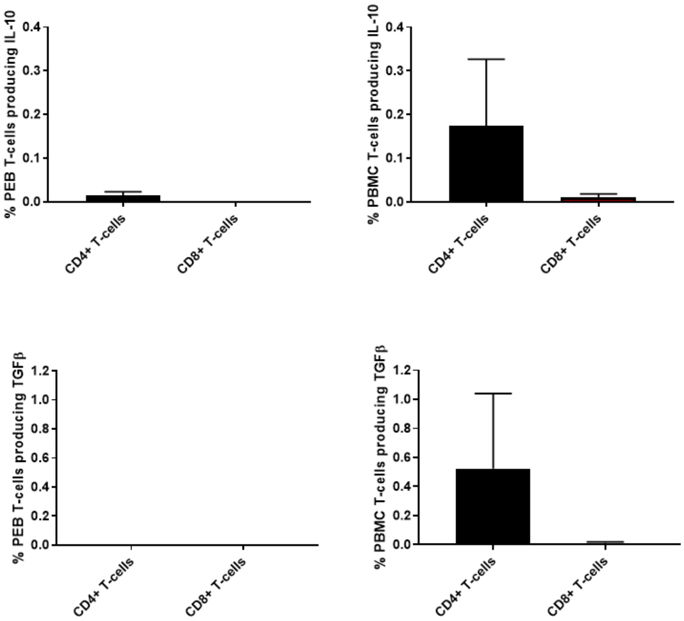

Figure 1.5: Basal IL-10 and TGFβ1 production by entheseal resident and PBMC CD4+ and CD8+ T-cells

Following digestion, basal levels of intracellular IL-10 and TGFβ1 were measured via flow cytometry (n=6 Mean Age 66.16, 3 Female, 3 Male) Mean±SEM. Viable lymphocytes in PBMC average =72097.5 cells and viable lymphocytes in PEB average=27436.6 cells PEB, perientheseal bone, PBMC peripheral blood mononucleated cells. Where the top left indicates IL-10 levels in PEB, the bottom left indicates TGFβ levels in PEB, the top right indicates IL-10 levels in PBMC and the bottom right indicates TGFβ levels in PBMC respectively.

Following the staining, 0.014% and 0% of CD4+ basal PEB T-cells expressed IL-10 and TGFβ1 respectively (Figure 1.5). In CD8+ PEB T-cells, neither IL-10 nor

TGFβ1 was expressed basally (Figure 1.5). In PBMC populations, 0.17% and 0.52% of CD4+ unstimulated PEB T-cells expressed IL-10 and TGFβ1 respectively. In CD8+ PBMC populations, there is 0.01% basal expression for both IL-10 and TGFβ1 respectively. This confirms low-level basal expression of IL-10 and TGFβ1 in peripheral blood subpopulations, as both IL-10 and TGFβ1 have immunomodulatory capabilities this may suggest a more anti-inflammatory population within the periphery.

3.3 Inducible IL-17A and TNF in entheseal CD4+ and CD8+ T-cells

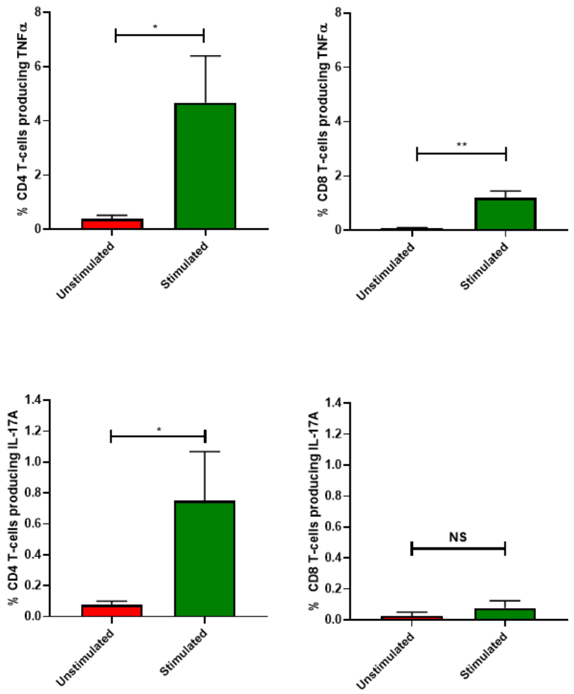

Figure 1.6: Inducible TNFα and IL-17A production by entheseal resident CD4+ and CD8+ T-cells

Intracellular IL-17A and TNF induction in entheseal CD4+ and CD8+ T-cells. Following digestion of human entheseal samples (PEB), cells were stimulated with anti-CD3/CD28 in the presence of Golgi plug for 3 hours. (n=4) Where the top left graph shows TNFα produced by CD4+ PEB cells, the bottom left graph shows IL-17A produced by CD4+ PEB cells, the top right graph shows TNFα produced by CD8+ PEB cells, the bottom right graph shows IL-17A produced by CD8+ PEB cells respectively. Unpaired T-tests *$p<0.05$; **$p<0.01$.

Following anti-CD3/CD28 stimulation, in order to simulate an *in-vivo* inflammatory response, a significantly greater proportion of entheseal-derived CD4+ T-cells showed increased IL-17A and TNF production compared to unstimulated controls. Furthermore, there was a significant increase in the proportion of CD8+

entheseal-derived T-cells upregulating TNF production, where p=0.0020 following unpaired T-tests, and although IL-17A production did in fact increase following stimulation this was not statistically significant. Statistical significance is seen in both CD4+ populations with IL-17A having slightly more significance than TNF production, p=0.0392 and p=0.0473 respectively.

3.4 Analysis of regulatory markers in entheseal and blood-derived T-cells

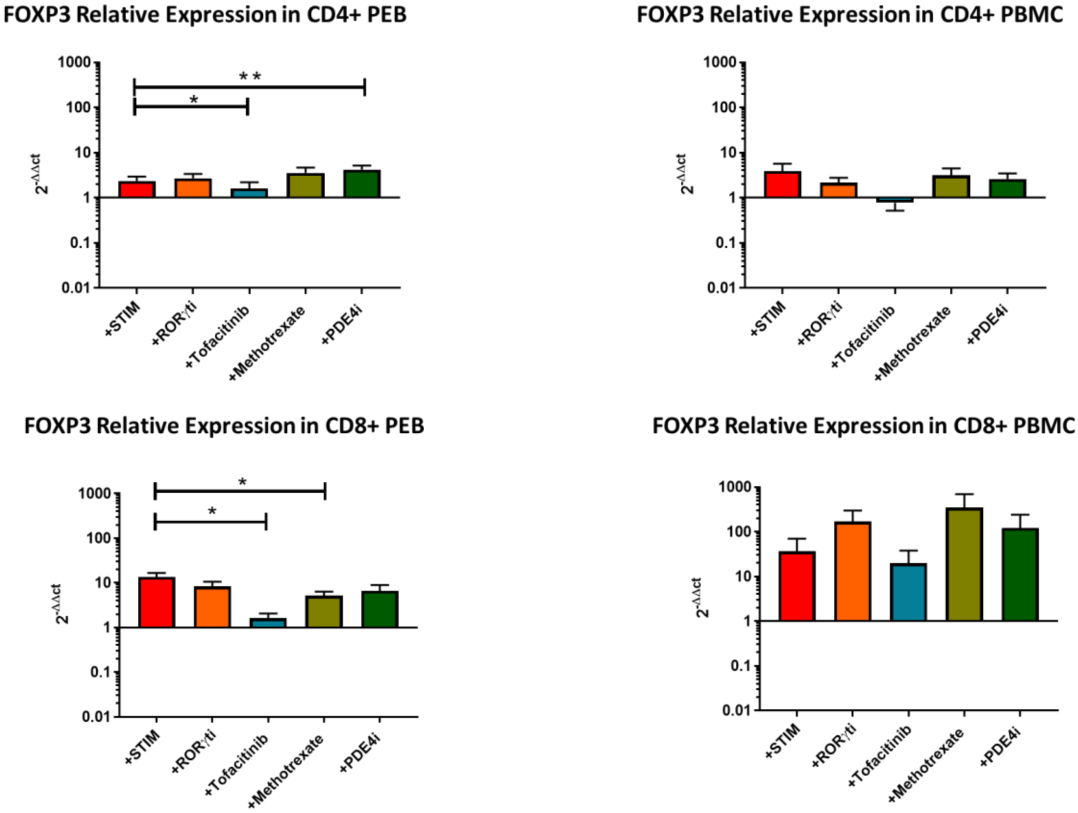

Figure 1.7: FOXP3 transcript in CD4+ and CD8+ T-cells

CD4+ and CD8+ T-cells were isolated from PEB or matched peripheral blood and stimulated with anti-CD3/CD28 for 48 hours with and without therapeutic agents indicated. qRT-PCR was used to determine the expression of FOXP3. $2^{-\Delta\Delta Ct}$ was used to measure relative expression fold change with HPRT as the housekeeping gene. (n=8) *Post-hoc* Mann-Whitney testing *p<0.05; **p<0.01

Since entheseal T-cells expressed high levels of TGFβ1 transcript in contrast to pro-inflammatory cytokine transcripts, I sought to determine whether they were regulatory in nature. Despite having a population of CD4+ CD25+ FOXP3+ Tregs readily detectable in blood, the same was not evident in the enthesis, where Tregs are essential for maintaining the balance of Th17 cells and inhibiting exaggerated T effector cell responses, so this data may suggest that the pro-inflammatory balance is heavily favoured within the enthesis. For further investigation, I evaluated a series of clinically relevant compounds' effects on Treg products, FoxP3 and TGFβ1. Anti-CD3/CD28 was used once more to stimulate isolated T-cells with and without RORγti, tofacitinib, methotrexate, and PDE4i. In CD4+ entheseal T-cells, only the PDE4i and tofacitinib showed statistically significant differences with regards *FoxP3* expression, (Figure 1.7) where p=0.036 and p=0.008 respectively when compared to the stimulated control. The therapeutic agents did not significantly affect *TGFβ1* expression (Figure 1.8), except in CD4+ entheseal T-cells, where tofacitinib-treated cells and PDE4i-treated cells expressed more TGFβ1, following post-hoc Mann Whitney testing, p=0.041 and p=0.035 respectively when compared to the stimulated control. A significant reduction in *FoxP3* expression was observed in entheseal CD8+ T-cells treated with tofacitinib and methotrexate, where p=0.021 and p=0.043 respectively when compared to the stimulated control.

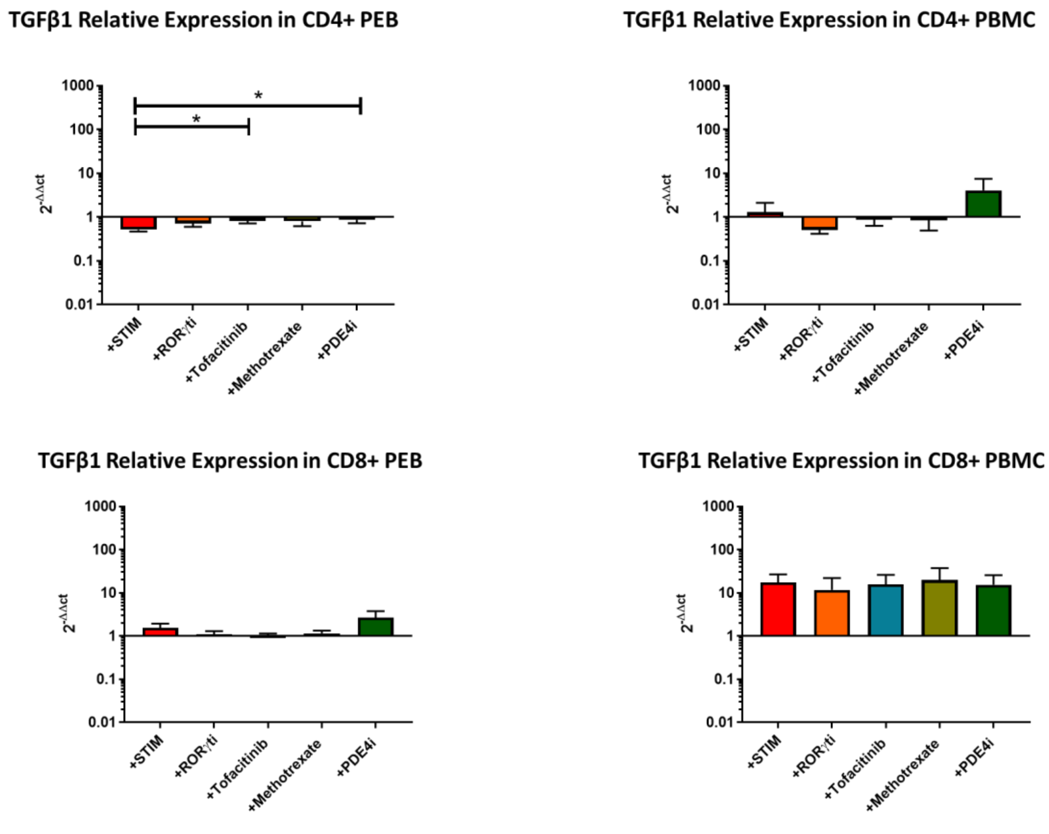

Figure 1.8: TGFβ1 transcript in CD4+ and CD8+ T-cells

CD4+ and CD8+ T-cells were isolated from PEB or matched peripheral blood and stimulated with anti-CD3/CD28 for 48 hours with and without therapeutic agents indicated. qRT-PCR was used to determine the expression of TGFβ1. 2-ΔΔCt was used to measure relative expression fold change with HPRT as the housekeeping gene. $n=8$ Post-hoc Mann-Whitney testing *$p<0.05$; **$p<0.01$

3.5 RORγti, MTX, Tofacitinib and PDE4i impact on enthesis CD4+ and CD8+ T-cell cytokine production

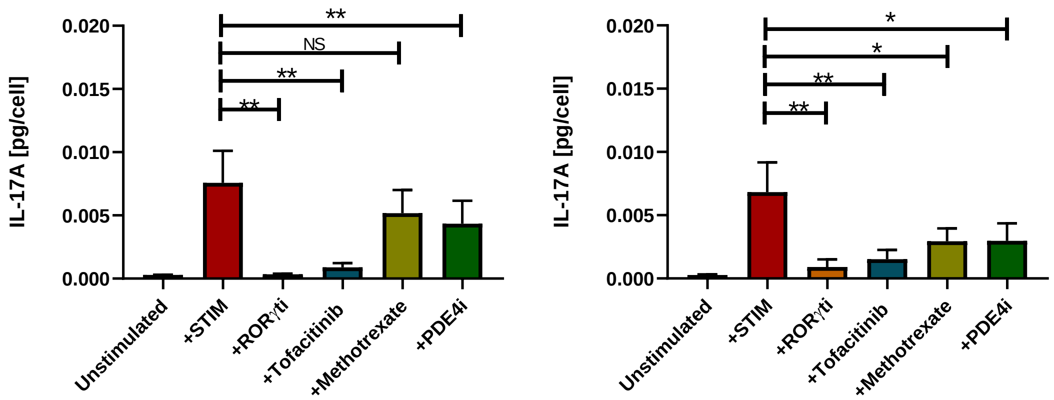

Figure 1.9: IL-17A protein secretion by entheseal-derived CD4+ T-cells with and without therapeutic agents measured via ELISA

IL-17A protein secretion was measured by ELISA (Figure 1.9) Following digestion of human entheseal samples (PEB) on the leftmost panel and matched blood cells (PBMC) on the right panel, these were stimulated with anti-CD3/CD28 in the presence of Golgi plug for 3 hours (n=8) Paired T-test, *p<0.05; **p<0.01.

I compared matched entheseal and blood-derived T-cells to clinically relevant drugs, even those not generally known to be effective for enthesitis, such as methotrexate which is a well-known csDMARD widely used to treat RA and PsA. Additionally, I included specific drugs that might be effective, such as PDE4i, tofacitinib, and RORγti. The latter was included as RORγt is well-known as the master transcription factor for Th17 cells, and as a driver of IL-17A, IL-17F, and IL-22 production in both innate and adaptive immune cells. Therapeutic agents were tested for their ability to suppress TNF and IL-17A secretion. CD4+ and CD8+ T-cells were isolated from the enthesis and matched blood, following magnetic separation and lymphoprep techniques and were subsequently stimulated with anti-CD3/CD28, where TNF and IL-17A were measured by ELISA. CD4+ T-cells robustly secreted IL-17A and TNF in both entheseal and peripheral blood samples respectively, with an average of 0.011 pg/cell and 0.0108 pg/cell of IL-17A respectively (Figure 1.9) and 0.0806 pg/cell and 0.115 pg/cells of TNFα, respectively (Figure 1.10). Whereas CD8+ only secreted TNF with a mean of 0.0066 pg/cell and 0.047 pg/cells of TNFα, respectively (Figure 1.11, IL-17A was undetectable, data not shown), with this information further supports the notion that the IL-17A producing CD4+ are in fact Th17 cells. The fact that CD4+ T-cells produce higher levels of proinflammatory IL17A is in keeping with the classical concept that these cells are "helpers" and drive pivotal cytokine expression including TNF and IL-17A (Th1 and Th17 respectively).

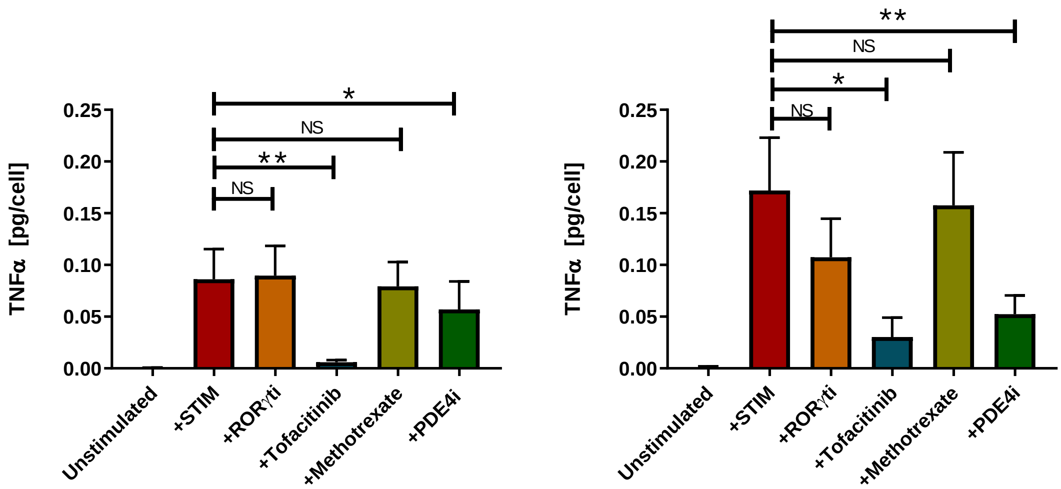

Figure 1.10: TNF protein secretion by entheseal-derived CD4+ T-cells with and without therapeutic agents measured via ELISA

TNF protein secretion was measured by ELISA (Figure 1.10) Following digestion of human entheseal samples (PEB) on the leftmost panel and matched blood (PBMC) on the right panel, cells were stimulated with anti-CD3/CD28 in the presence of Golgi plug for 3 hours (n=8) Paired T-test, *p<0.05; **p<0.01.

The therapeutic agents, PDE4i, Tofacitinib, and RORγti, all significantly reduced IL-17A secretion from both enthesis-derived and blood-derived CD4+ T-cells following paired T-tests (Figure 1.9) (With regards to PEB, stimulated vs PDE4i p=0.0089, stimulated vs tofacitinib p=0.0074 and stimulated vs RORγti p=0.0073) whereas MTX failed to significantly decrease IL-17A secretion in CD4+ entheseal-derived T-cells; however, MTX did attenuate IL-17A secretion in the same population in matched blood (Stimulated vs Methotrexate p=0.0474). Furthermore, in the CD4+ blood population, I also saw a significant reduction in IL-17A production following the application of the therapeutic agents respectively (stimulated vs RORγti p=0.0063, stimulated vs tofacitinib p=0.0057, stimulated vs PDE4i p=0.0192).

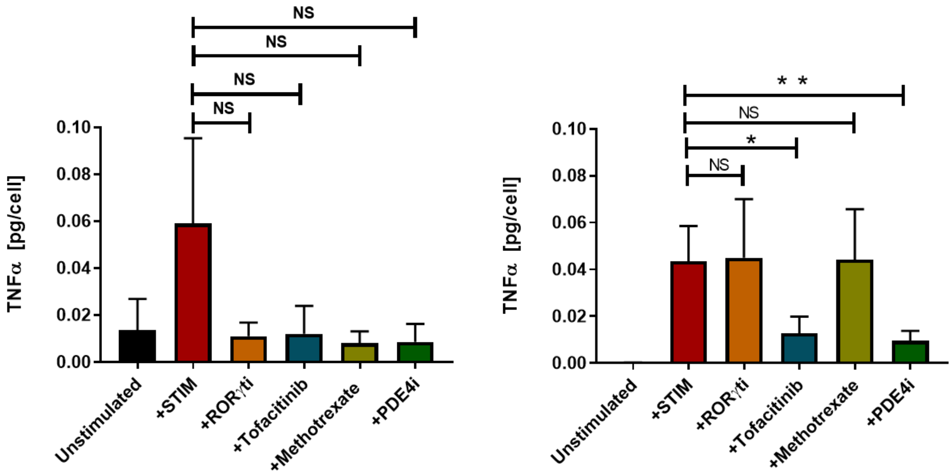

Figure 1.11: TNF protein secretion by entheseal-derived CD8+ T-cells with and without therapeutic agents measured via ELISA

TNF protein secretion was measured by ELISA (Figure 1.11) Following digestion of human entheseal samples (PEB) on the leftmost panel and matched blood (PBMC) on the right panel, cells were stimulated with anti-CD3/CD28 in the presence of Golgi plug for 3 hours (n=8) Paired T-test, *p<0.05; **p<0.01.

TNF derived from both entheseal and blood-derived CD4+ T-cells was significantly attenuated by PDE4i and Tofacitinib following paired t-tests (Figure 1.10) (stimulated vs tofacitinib p= 0.0083, stimulated vs PDE4i p=0.0398 and stimulated vs tofacitinib p=0.0147, stimulated vs PDE4i p=0.0065 respectively), but not RORγti or MTX. The same was true for CD8+ T-cell-derived TNF (Figure 1.11), specifically blood-derived CD8+ T-cells, which was reduced by Tofacitinib and PDE4i (stimulated vs tofacitinib p=0.0117, stimulated vs PDE4i p= 0.0053), but not by RORγti or MTX, whereas CD8+ T-cells from PEB did not show any statistical significance.

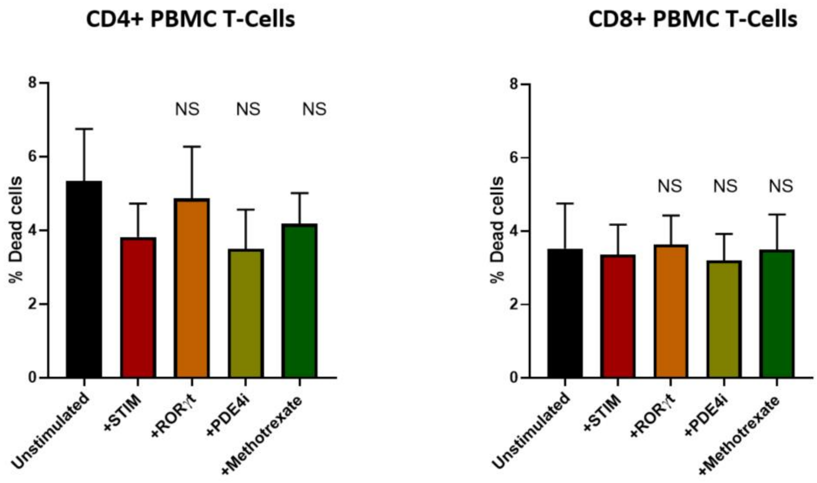

Figure 1.12: Cell Viability testing for therapeutic agents

To test the potential of therapeutic agents on their effects on cell viability, flow cytometry was used to assess CD45+, CD3+, CD4/CD8+ and live dead viability by zombie aqua staining. RORγt inhibitor 10 μM (Pfzier), Rolipram (a PDE4 inhibitor) 10 μM (Cayman Chemical), and methotrexate (MTX, 5 mg/mL (Cayman Chemical) n=5, NS Not Significant.

The propensity for compounds to attenuate cytokine secretion may be in part due to increased cell death, for this reason, cell viability was tested for all four agents and none showed significant effects on either CD4+ or CD8+ T-cell viability (Figure 1.12). Then, I assessed any potential difference in drug inhibition between the entheseal and blood-derived T-cells. CD4+ IL-17A inhibition by RORγti showed no significant difference between enthesis and blood. For both T-cell subsets, there were no significant differences between inhibition of TNF or IL-17A by PDE4i between the enthesis and blood. In general, the results from peripheral blood T-cells with drug inhibition were similar to those from the enthesis.

Chapter 3

Bulk and Single Cell RNA Seq

Results

3.6 Galaxy workflow for Bulk RNA-Seq

3.7 Assessment of entheseal bone and soft tissue CD4+ and CD8+ T-cell repertoire

3.8 Bulk RNA Seq

3.9 Single Cell RNA Seq data using Juypter notebook

3.6 Galaxy workflow for Bulk RNA-Seq

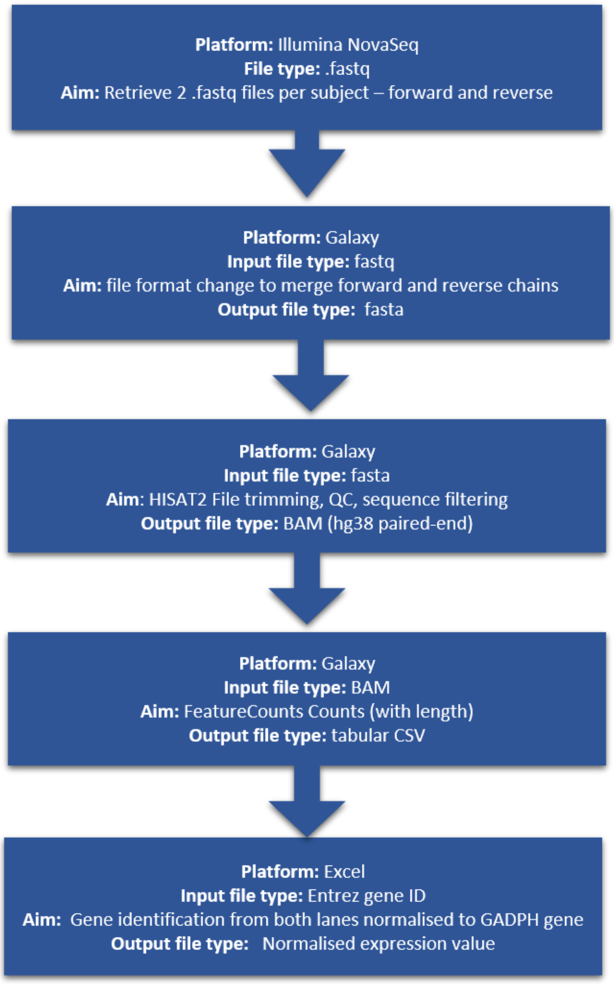

Figure 1.13: Brief overview of the stages required to process the RNA-Seq data obtained from the NovaSeq sequencing platform

The first stage retrieves fastq files from the Illumina sequencing platform. The second stage requires the transfer of these fastq files to the Galaxy open access database for the following actions: (I) file trimming, (II) QC, (III) filtering (IV) fastq to fasta file conversion, and (V) fasta file modifications. The fourth stage follows the creation of a BAM file to obtain FeatureCounts from the data. This is subsequently modified into a tabular CSV file with Entrez Gene I.D. used to determine gene usage and relative expression to the GADPH housekeeping gene.

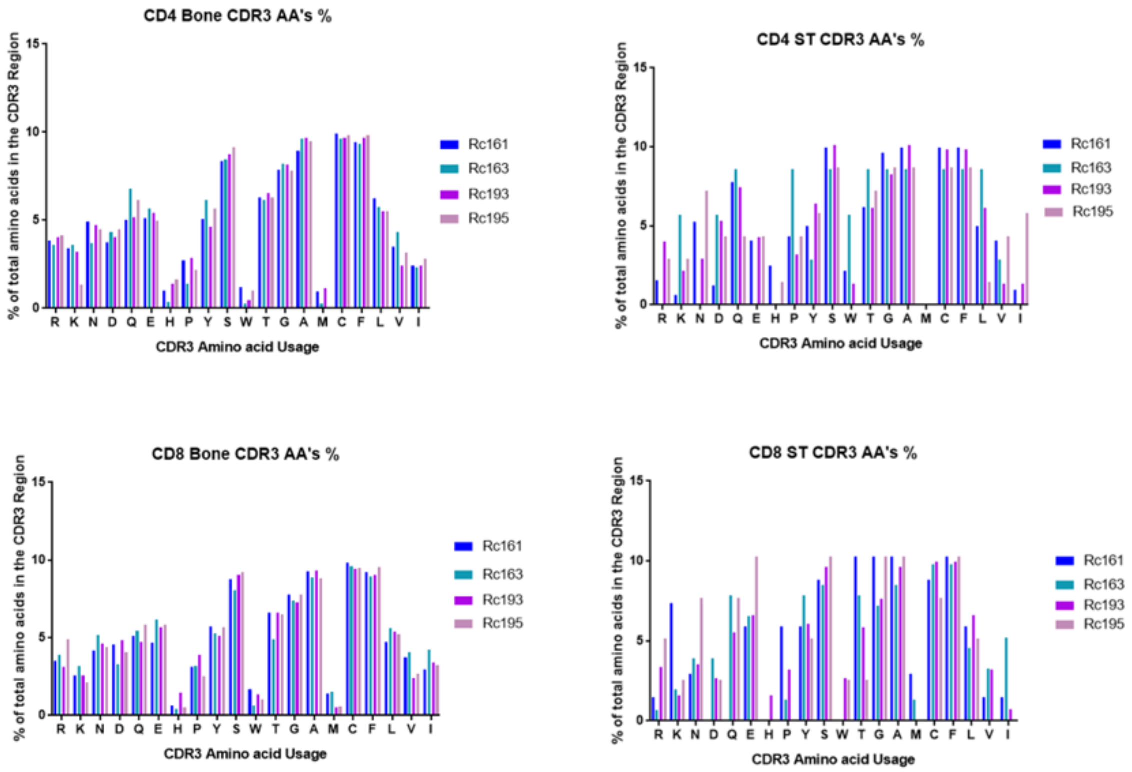

Figure 1.14: CDR3 Amino acid usage in bulk RNA-Seq patients

The percentage of amino acid usage in the CDR3 region in bulk RNA-Seq patients (n=4), ordered from hydrophilic (negative) to hydrophobic (positive) with (R) Arginine being the most negative and (I) Isoleucine being the most positive respectively.

The amino acid usage of the CDR3 region in PEB and soft tissue can be seen in Figure 1.14, where PEB favours more positive amino acids such as Alanine (A), Cysteine (C), and Phenylalanine (F), whereas soft tissue has a greater diversity across both positive and negative amino acids. One similarity in all tissue types irrespective of surface expression is the absence of Methionine (M) usage.

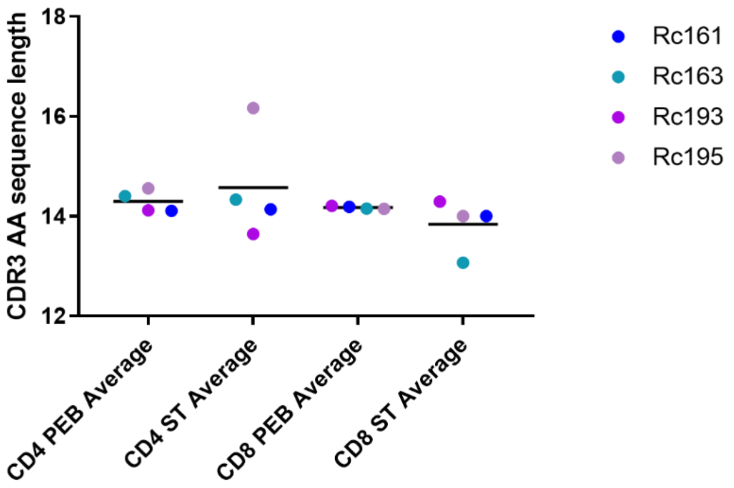

Figure 1.15: CDR3 Amino acid length in bulk RNA-Seq patients

The mean length of CDR3 Amino acids from bulk RNA Seq patients (n=4) ranging from 13.07 to 16.17 Amino acids.

As we can see in Figure 1.15 there is little difference between the mean length in both CD4+ and CD8+ PEB respectively, however, there are some distinct differences in length in soft tissue with the youngest patient in the cohort having the highest average CDR3 length in CD4+ soft tissue (16.17), whereas the second youngest patient had the lowest average in CD8+ soft tissue (13.07).

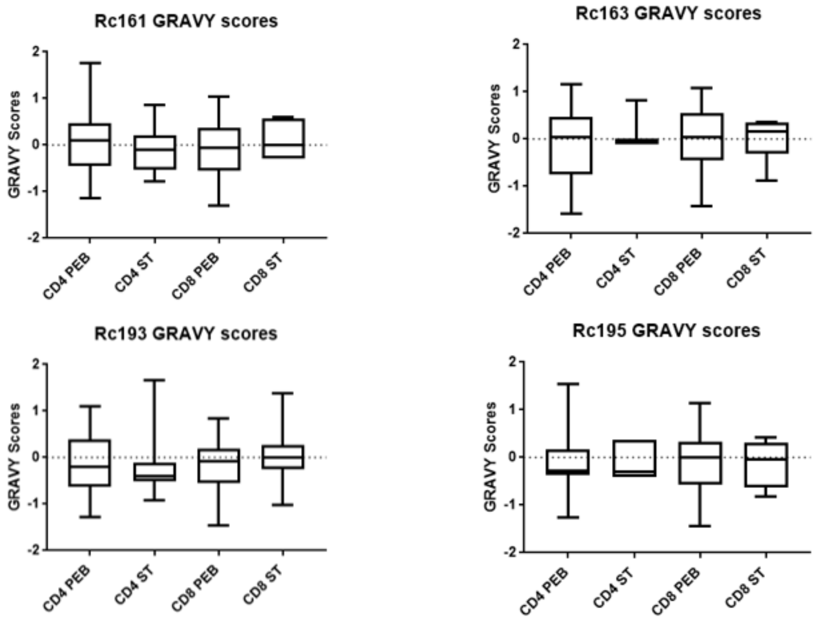

Figure 1.16: GRAVY scores in bulk RNA Seq patients

The Grand average of hydrophobicity score, (GRAVY score) for a protein or a peptide is calculated by adding the hydropathy values of each amino acid residues and dividing by the number of residues in the sequence or length of the sequence (54). An increasing positive score indicates a greater degree of hydrophobicity. Only 5 Amino acids contribute to the overall charge of a protein, where Arginine and Lysine are positively charged (+1 or Basic), histidine which is mildly basic +0.5 whereas Aspartic acid and glutamic acid are negatively charged (-1 or Acidic) where basic regions are often associated with DNA binding sites. When looking at the patient cohort GRAVY scores, as seen in Figure 1.16, while there are no clear correlations in GRAVY scores between the tissue sites or surface markers (PEB vs ST, CD4 vs CD8), the CD4+ T-cell subsets tend to be more basic.

3.7 Assessment of entheseal bone and soft tissue CD4+ and CD8+ T-cell repertoire

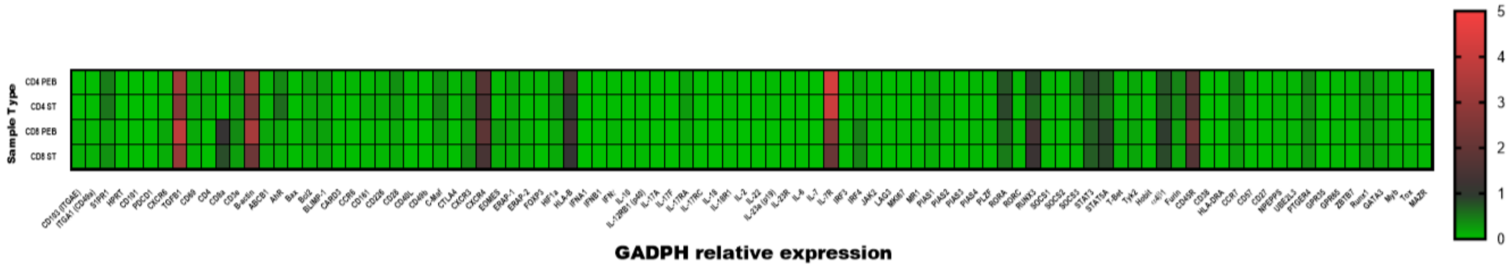

Figure 1.17: Transcriptional profiling of entheseal T-cells following Bulk RNA-Seq

CD4+ and CD8+ T-cells were sorted from Novaseq RNA-Seq data. Basal expression of cytokines, chemokines, growth factors, signalling molecules, tissue residency markers was assessed. Colour coding refers to differentially expressed genes where values less than 1 indicate low expression and values greater than 1 indicate higher expression, values displayed are relative to the GADPH housekeeping gene. (n=4 sample) ST, soft tissue; PEB, perientheseal bone.

Bulk RNAseq analysis of the CD4+ and CD8+ T cells (n=6 in total) was undertaken for tissue residency markers including CD69, CD103, CD49a, and S1PR1 following normalisation with the GADPH housekeeping gene (Figure 1.17). As confirmed by flow cytometry CD69 transcript was substantially higher in enthesis compared with blood but the other transcripts were comparable between enthesis and blood. However, in four entheseal samples, CD103 and CD49a transcripts were 3.8-fold and 4.6-fold higher in entheseal CD8+ T cells, respectively, compared with CD4+ entheseal T cells with S1PR1 transcripts correspondingly reduced. From other studies, it appears that expression of CD69 leads to the inactivation and internalisation of S1PR1 which supports the concept of these cells showing tissue residency.

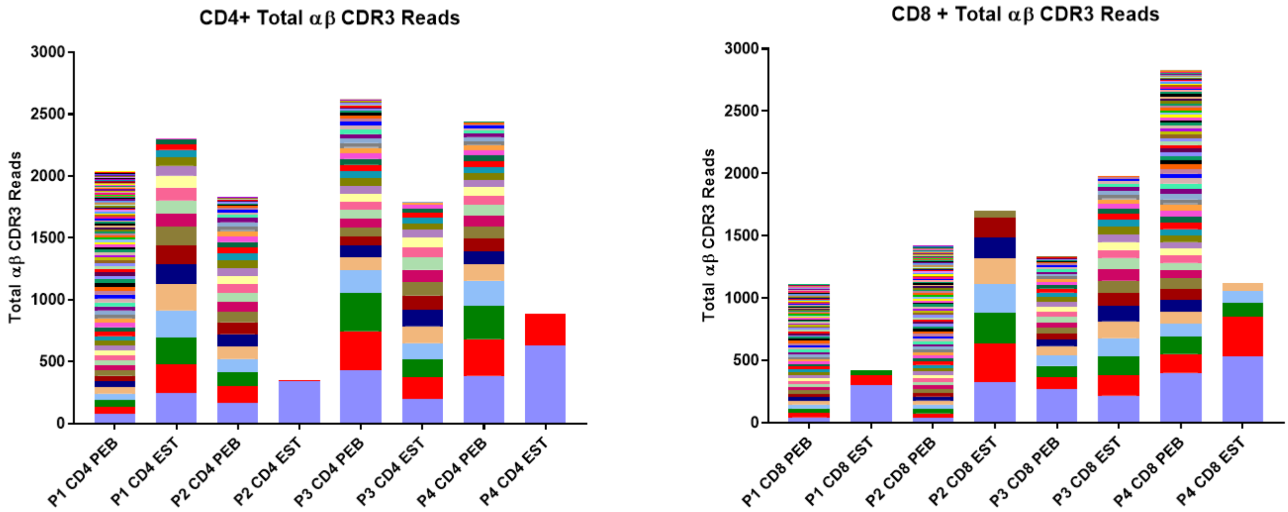

Figure 1.18: Total CDR3 Reads in CD4+ and CD8+ T-cells

Assessment of the T-cell repertoire in peri-entheseal bone (PEB) and entheseal soft tissue (EST) within the CD4+ and CD8+ T-cell subpopulations. Following MiXCR outputs, RNAseq data were used to determine potential clonality within the T-cell subpopulations, from both PEB and EST in both CD4+ and CD8+ T-cell populations where each individual clone is represented by a different colour. n=4 (2 female, 2 male); mean age=30.2 years. Where P1 relates to the first patient, P2 relates to the second patient, P3 relates to the third patient and P4 relates to the fourth patient.

Following Bulk RNASeq the analysis of the TCRs highlighted the noticeable reduction in clonal diversity in EST compared to matched PEB, as seen in Figure 1.18, where there was evidence to suggest that PEB subpopulations are more diverse than their EST counterparts. Furthermore, I identified greater numbers of sorted cells in PEB compared with EST, where CD4+ populations contained (17353±6147 cells and 1419±988 cells, respectively), the same trend is also seen in CD8+ populations (20524±5545 cells and 1384±1076 cells, respectively). Next, I assessed T-cell clones for potential viral reactivity, which is determined by looking at epitope specificities from the TCR3 database (https://tcr3d.ibbr.umd.edu/); out of the 13 potentially reactive clonal sequences, the most common viral targets were Cytomegalovirus (CMV) in eight sequences and influenza A virus (IAV) in two sequences.

3.8 Bulk RNA Seq

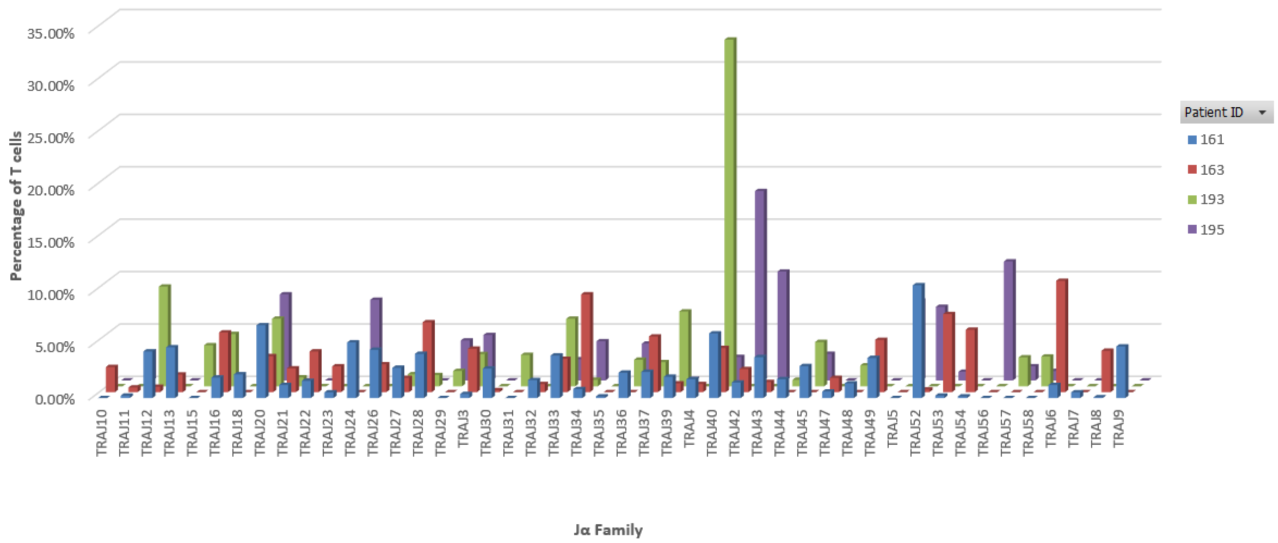

Figure 1.19: TRAJ40 highest clade in CD4⁺ CD8⁺ PEB

Following RNA seq, the Joining α Family (Jα) percentage in T cells was calculated for $CD4^+$ and $CD8^+$ T cells in bone, with the clades shown having the highest Hit score, with Rc193 having the highest individual hit (33.00%) in TRAJ40. n=4 2 Male, 2 Female (Mean age=30.2)

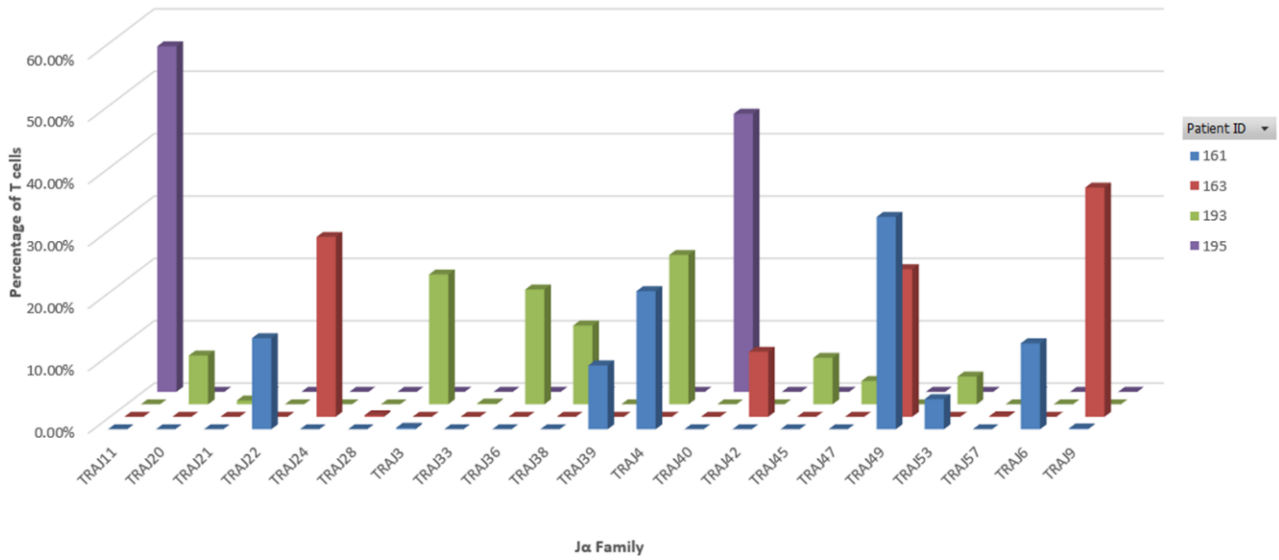

Figure 1.20: TRAJ49 highest clade in $CD4^+$ $CD8^+$ Soft Tissue

Following RNA seq, the Joining α Family (Jα) percentage in T cells was calculated for CD4+ and CD8+ T cells in soft tissue, with the clades shown having the highest Hit score, with Rc195 having the highest individual hit (55.40%) in TRAJ11. n=4 2 Male, 2 Female (Mean age=30.2)

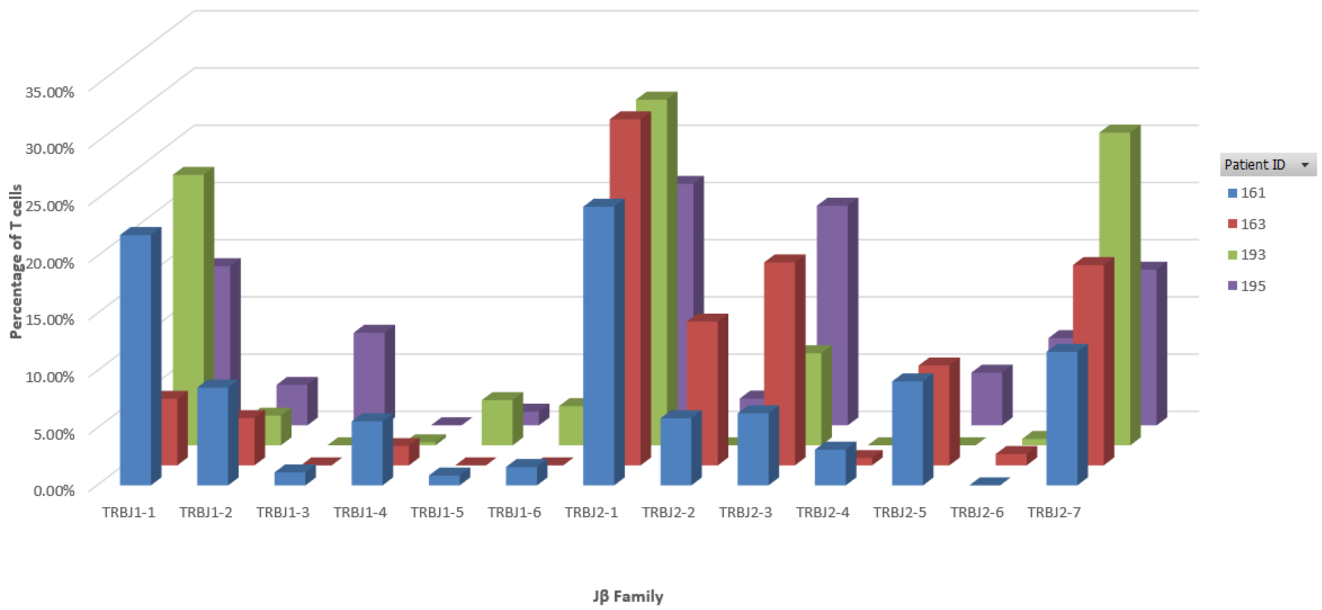

Figure 1.21: TRBJ2-1 highest clade in CD4+ CD8+ PEB

Following RNA seq, the Joining β Family (Jβ) percentage in T cells was calculated for CD4+ and CD8+ T cells in bone, with the clades shown having the highest Hit score, with Rc193 having the highest individual hit (30.20%) in TRBJ2-1. n=4 2 Male, 2 Female (Mean age=30.2)

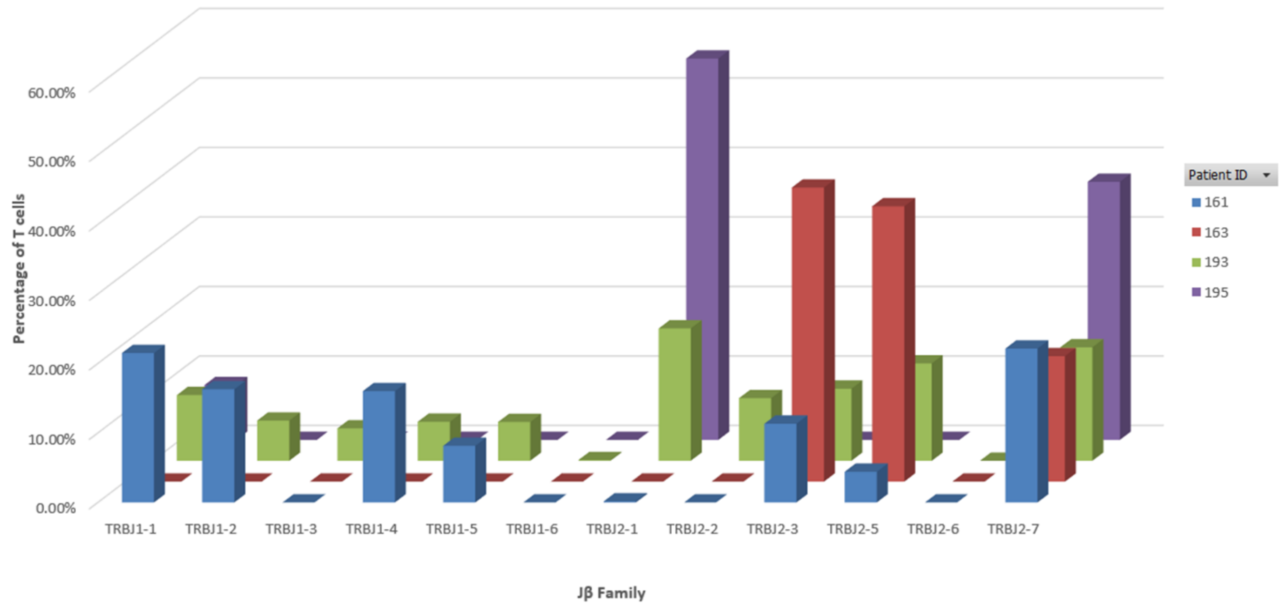

Figure 1.22: TRBJ2-1 highest clade in CD4+ CD8+ Soft Tissue

Following RNA seq, the Joining β Family (Jβ) percentage in T cells was calculated for CD4⁺ and CD8⁺ T cells in soft tissue, with the clades shown having the highest Hit score with Rc195 having the highest individual hit (54.90%) in TRBJ2-1. n=4 2 Male, 2 Female (Mean age=30.2)

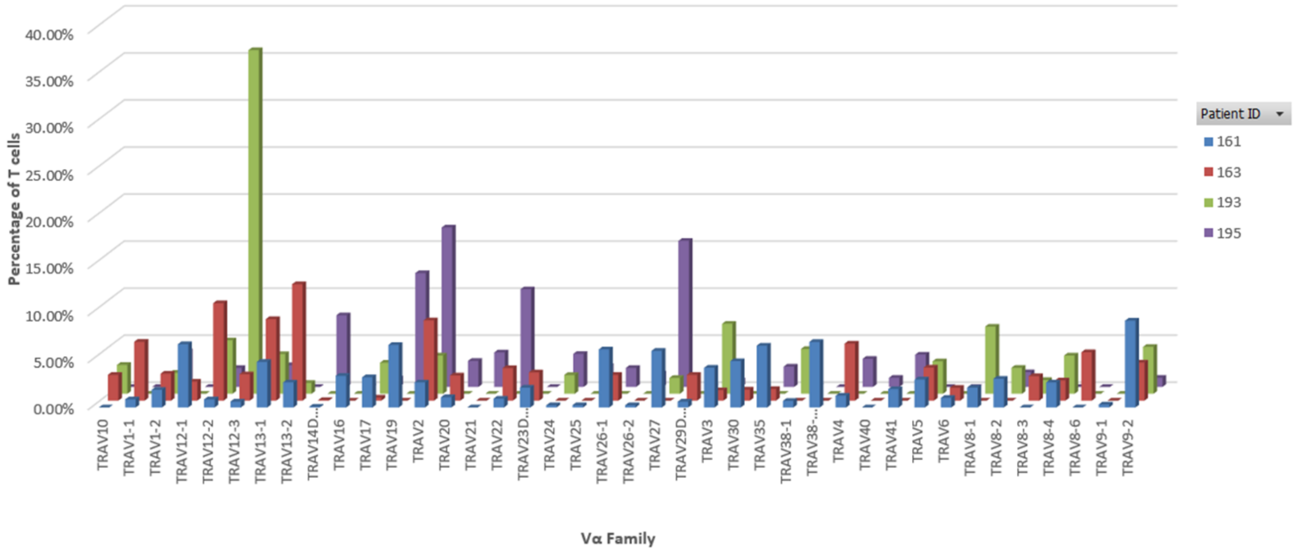

Figure 1.23: TRAV12-3 highest clade in CD4⁺ CD8⁺ PEB

Following RNA seq, the Variable α Family (Vα) percentage in T cells was calculated for CD4⁺ and CD8⁺ T cells in bone, with the clades shown having the highest Hit score, with Rc193 having the highest individual hit (36.50%) in TRAV12-3. n=4 2 Male, 2 Female (Mean age=30.2)

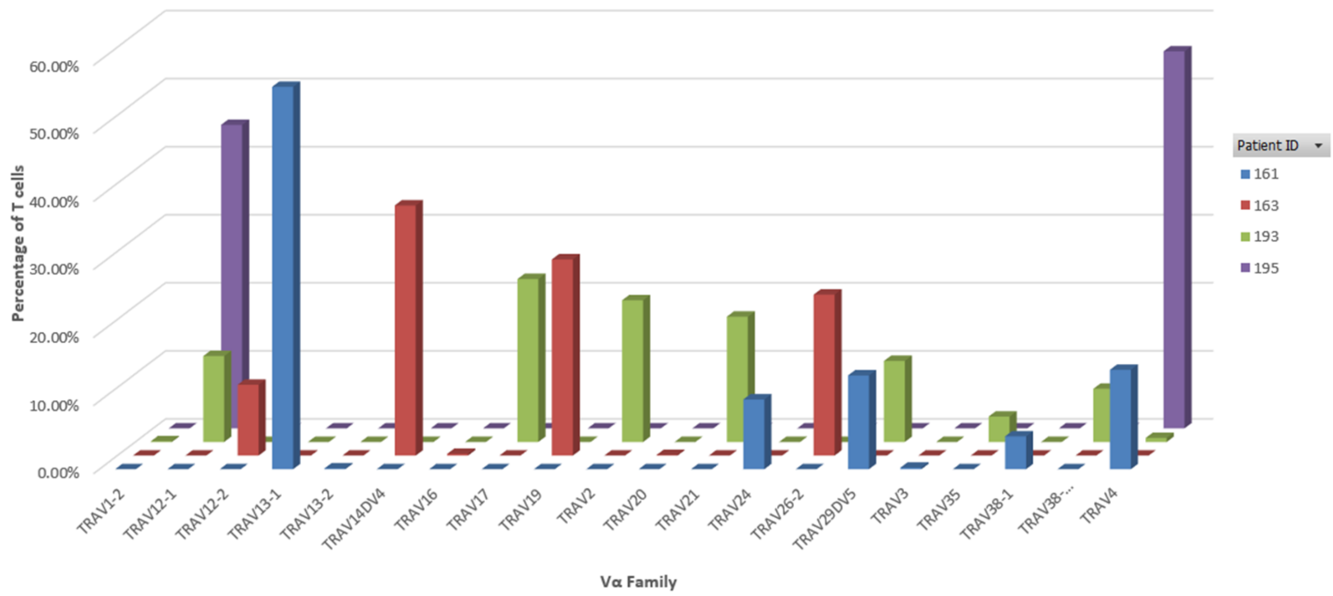

Figure 1.24: TRAV4 highest clade in CD4⁺ CD8⁺ Soft Tissue

Following RNA seq, the Variable α Family (Vα) percentage in T cells was calculated for CD4⁺ and CD8⁺ T cells in soft tissue, with the clades shown having the highest Hit score, with Rc195 having the highest individual hit (56.18%) in TRAV4. n=4 2 Male, 2 Female (Mean age=30.2)

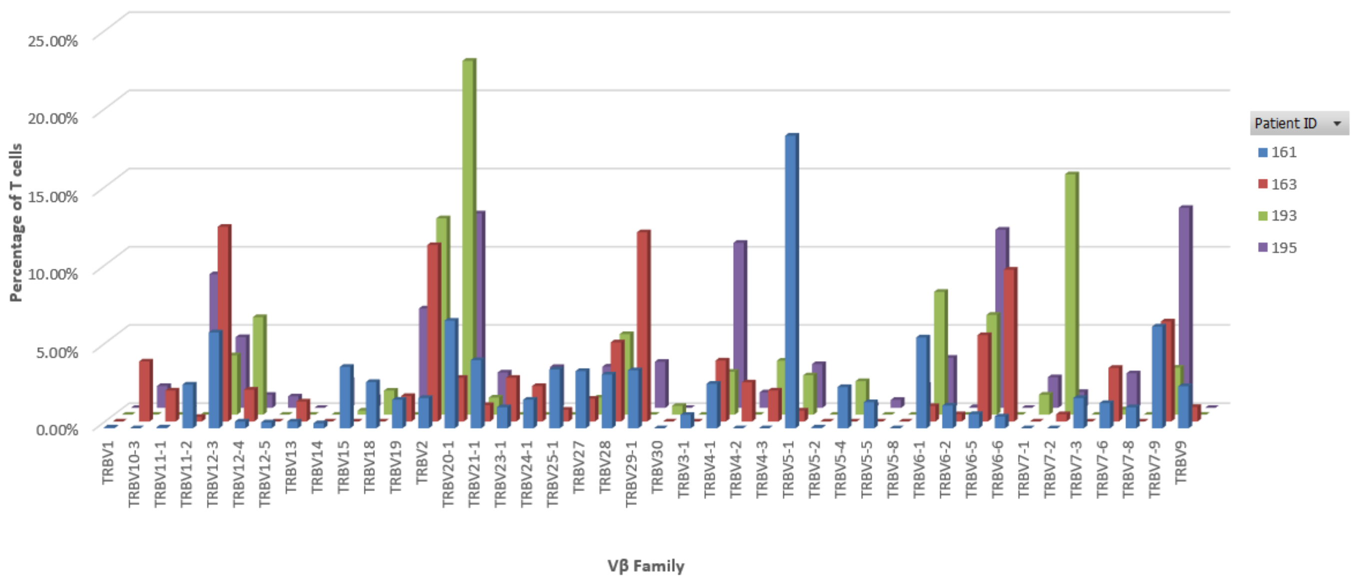

Figure 1.25: TRBV20-1 highest clade in CD4⁺ CD8⁺ PEB

Following RNA seq, the Variable β Family (Vβ) percentage in T cells was calculated for CD4⁺ and CD8⁺ T cells in bone, with the clades shown having the highest Hit score, with Rc193 having the highest individual hit (22.60%) in TRBV20-1. n=4 2 Male, 2 Female (Mean age=30.2)

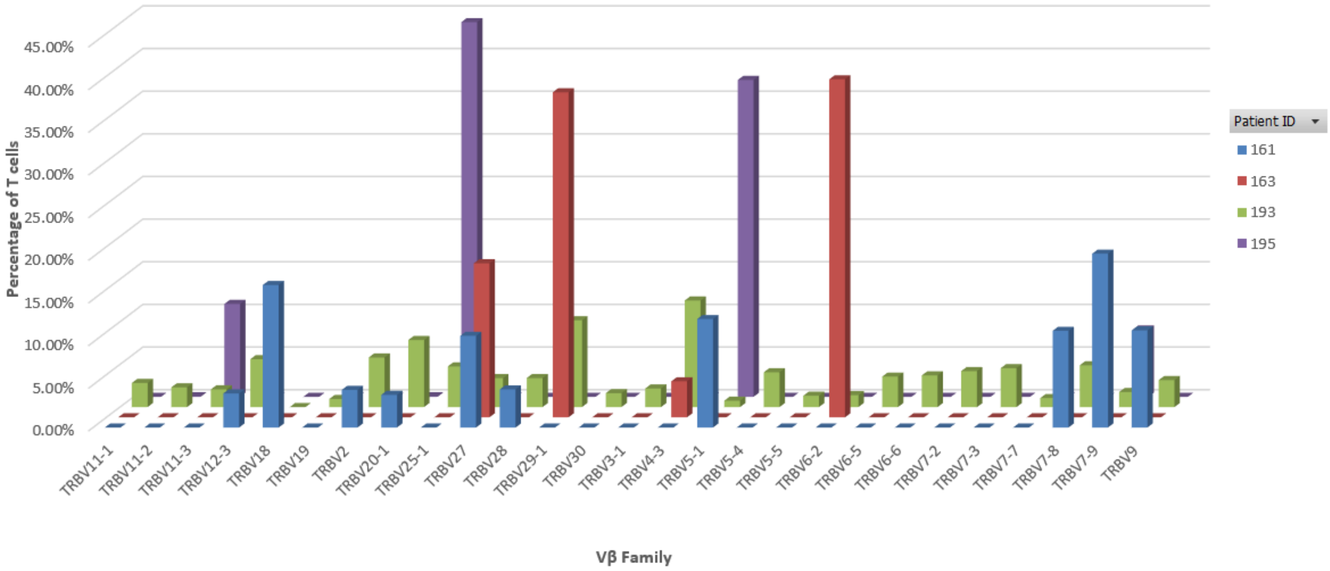

Figure 1.26: TRBV5-1 highest clade in CD4⁺ CD8⁺ Soft Tissue

Following RNA seq, the Variable β Family (Vβ) percentage in T cells was calculated for CD4⁺ and CD8⁺ T cells in soft tissue, with the clades shown having the highest Hit score, with Rc195 having the highest individual hit (43.90%) in TRBV25-1. n=4 2 Male, 2 Female (Mean age=30.2)

Following the extraction of sequences using MiXCR, the initial analysis of TCRs highlighted the reduced diversity in soft tissue compared to PEB dervied T-cells, (Figure 1.19, Figure 1.20, Figure 1.21, Figure 1.22, Figure 1.23, Figure 1.24, Figure 1.25 and Figure 1.26 respectively) this may be due to the haematopoietic marrow that PEB contains. The results also emphasise patient variability due to the variation with regard to clade association across all samples. The highest individual hits in patient Rc193 in Vα and Jα in PEB (Figure 1.23 and Figure 1.19 respectively) suggests a potentially clonal population caused by either response to a previous viral infection or tissue repair, however, this may also be caused by a reduced immune repertoire as the patient in question is >50 years old.

3.9 Single Cell RNA Seq data using Juypter notebook

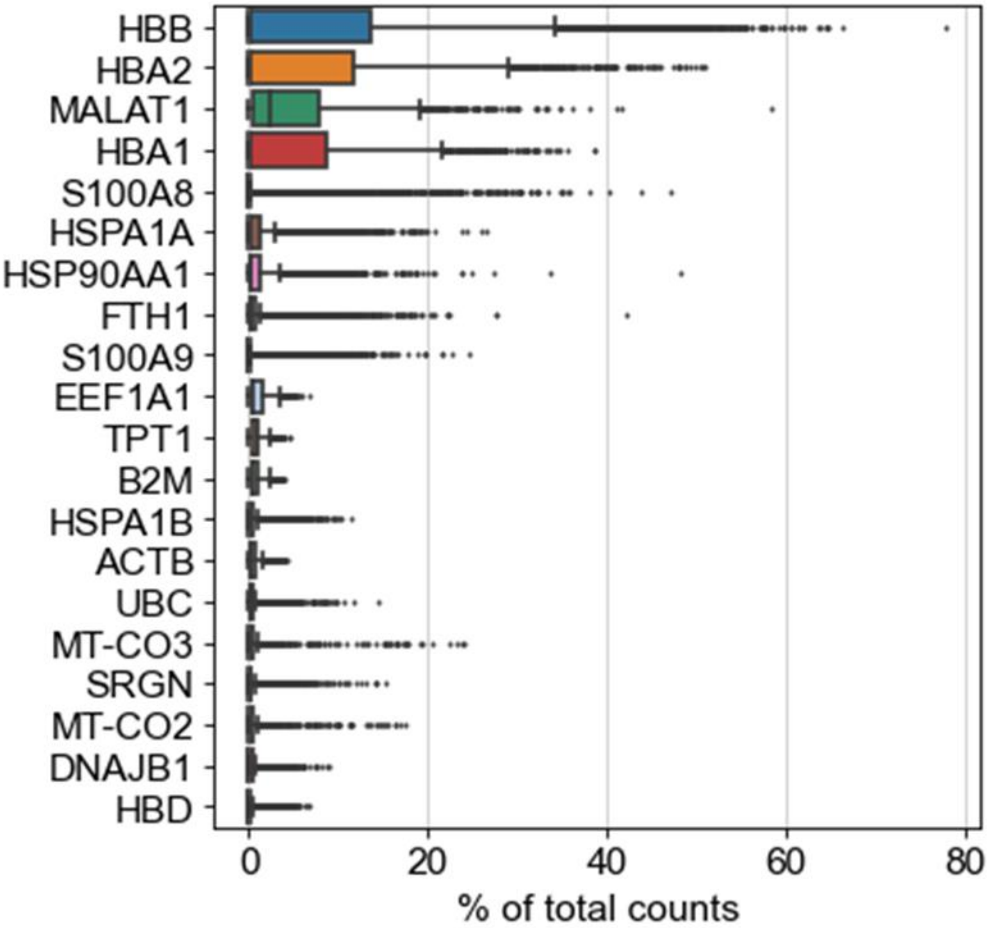

Figure 1.27: Top 20 genes with the highest percentage of total counts in Rc547

Utilising Juypter notebooks for the Single cell RNA-Seq data we are able to view the genetic information of each sample at a more in-depth level than Bulk RNA-Seq, in Figure 1.27 we can see the top 20 genes with the highest percentage of total counts in Rc547 data following the removal of both the ribosomal protein genes, which are the small 40S and the large 60S ribosomal subunits and, as such, are designated RPS or RPL respectively. However, after completing some simple filtering, in order to have a truer representation of the genetic signature, seen in Figure 1.28, i.e the removal of cells that have less than 200 genes and the removal of genes that are detected in less than 3 cells we can see a clearer picture of those top 20 genes, including a mix of haemoglobin subunits and heat shock proteins.

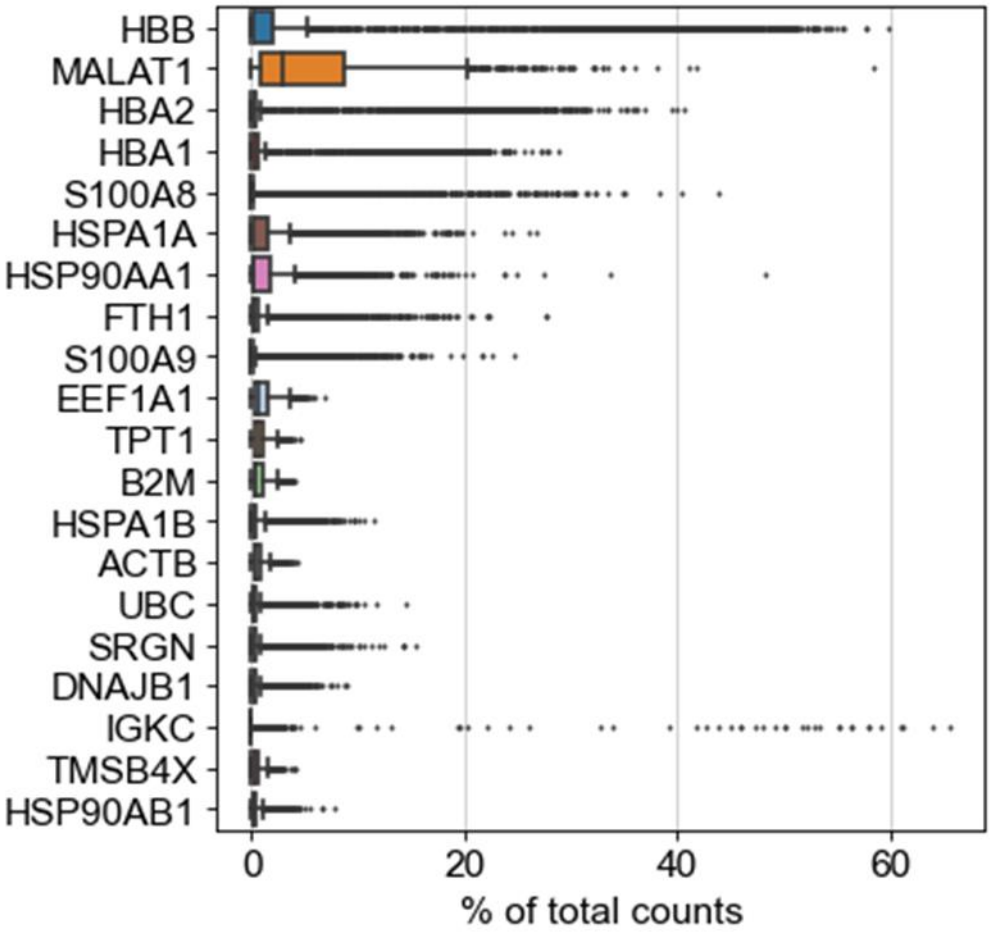

Figure 1.28: Top 20 genes with the highest percentage of total counts in Rc547 following data filtering

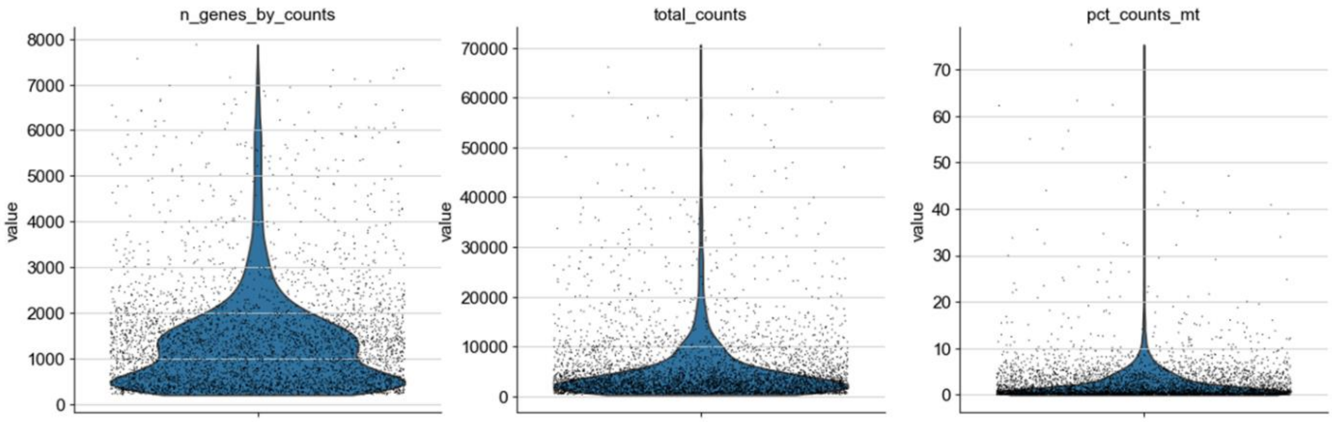

Figure 1.29: Violin plots for Rc547 Single Cell RNA-Seq raw data

In Figure 1.29 we can see the unfiltered Rc547 data (including the RPL and RPS gene removal) which shows the number of genes expressed in the count matrix, the total counts per cell, and the percentage of counts in mitochondrial genes going from left to right respectively. Similarly to Figure 1.27 without any filtering applied to ‘clean’ the data this does not show a true representation of the data.

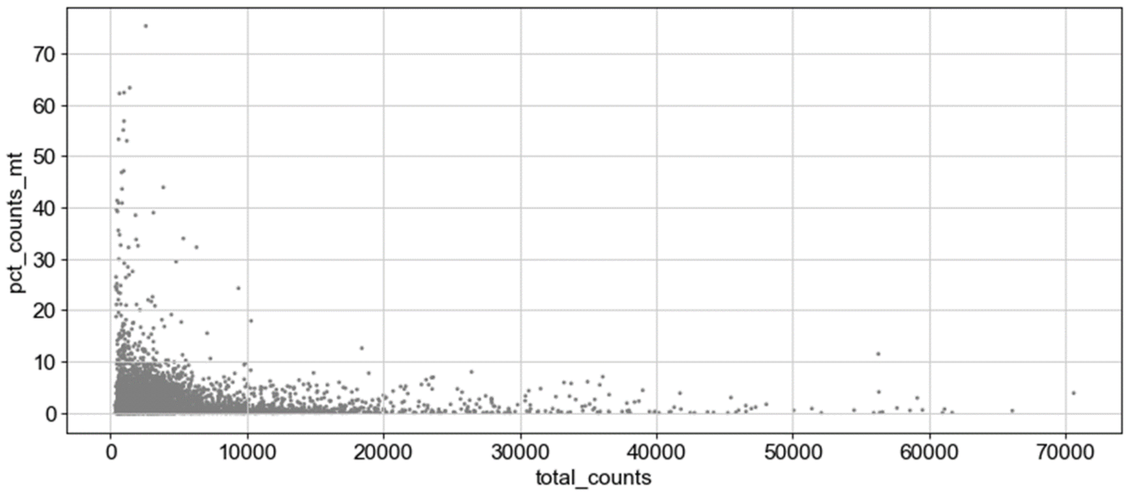

Figure 1.30: Percentage counts in mitochondrial genes by count depth in Rc547 Single Cell RNA-Seq data

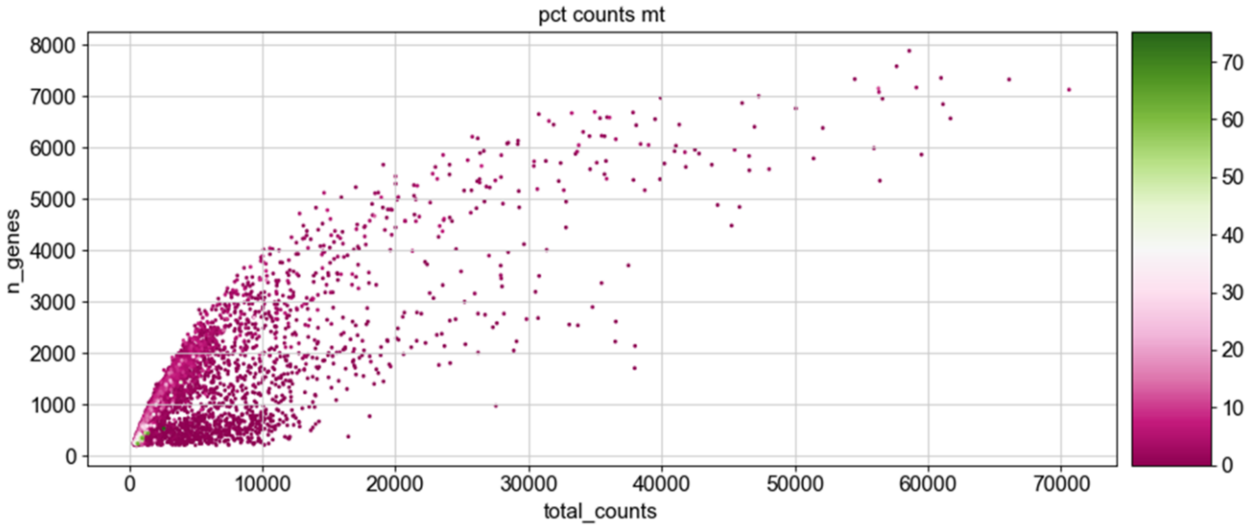

Figure 1.31: Number of genes by count depth and percentage counts in mitochondrial genes in Rc547 Single Cell RNA-Seq data

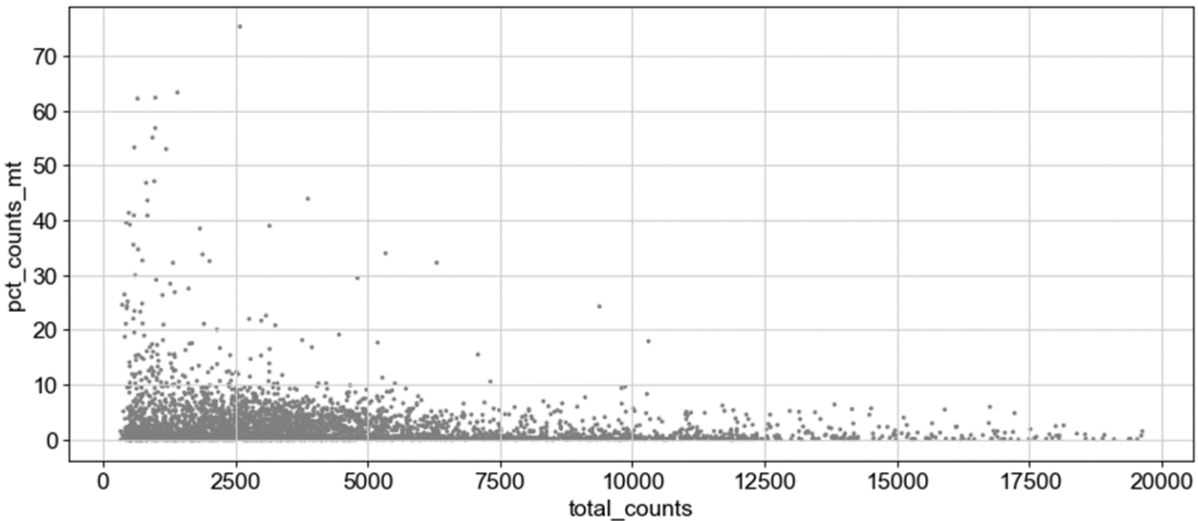

Figure 1.32: Percentage counts in mitochondrial genes by count depth in Rc547 Single Cell RNA-Seq data post-filtering

In Figure 1.32 and Figure 1.33, I decided to filter the data in order to see a clearer representation of the RNA-Seq data, in order to remove cells that have too many mitochondrial genes expressed or too many total counts I sliced the Annotated data (AnnData) to show only cells that have <4000 genes expressed, and <20,000 in total counts.

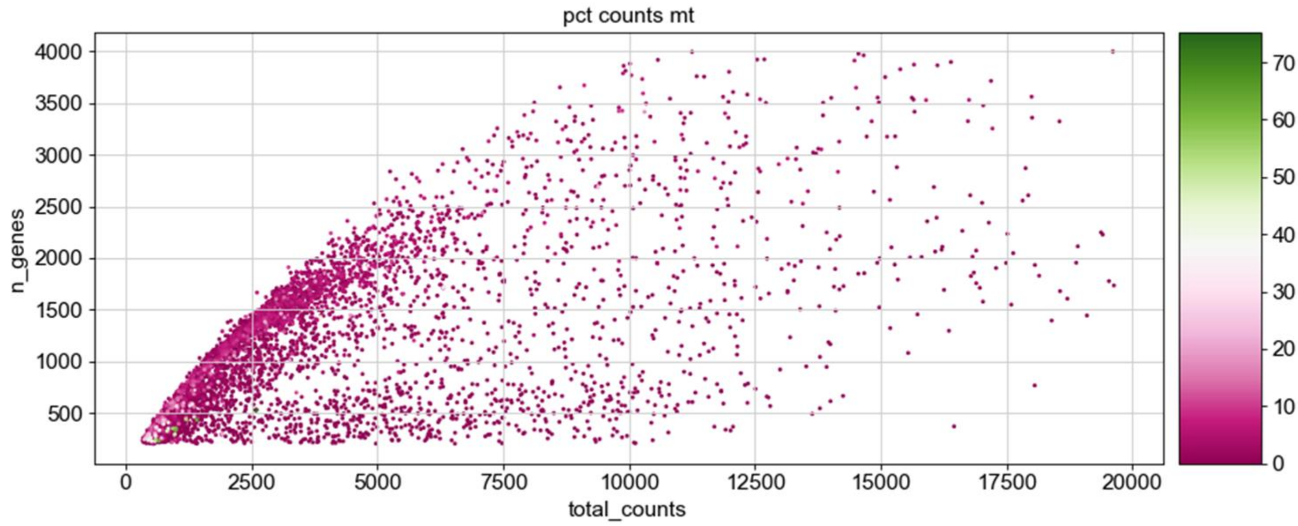

Figure 1.33: Number of genes by count depth and percentage counts in mitochondrial genes in Rc547 Single Cell RNA-Seq data post-filtering

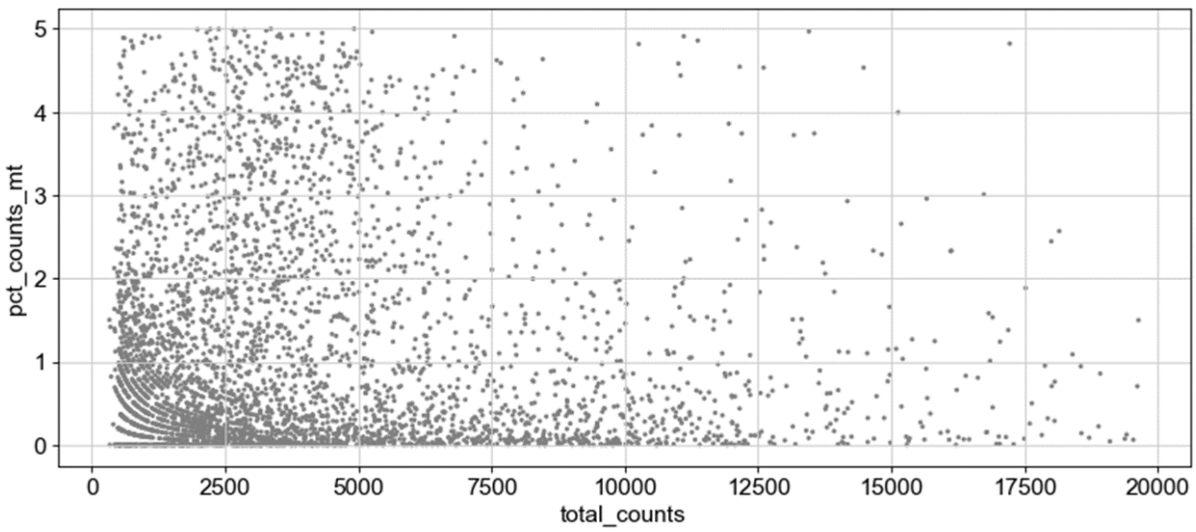

Figure 1.34: Percentage counts in mitochondrial genes by count depth in Rc547 Single Cell RNA-Seq data post-filtering

In Figure 1.34 we can see the ‘cleanest’ plots, whereby we only look at cell data of cells with a percentage count of mitochondrial genes that is <5% following the filtering process completed for Figure 1.32 and Figure 1.33. The data from Figure

1.34 allows us to visualise the RNA-Seq data without the inclusion of ribosomal and mitochondrial genetic information that would otherwise disrupt the 'true' genetic data of the RNA-Seq sample in order to ascertain definitive cell populations seen in UMAP graphs in Figure 1.37.

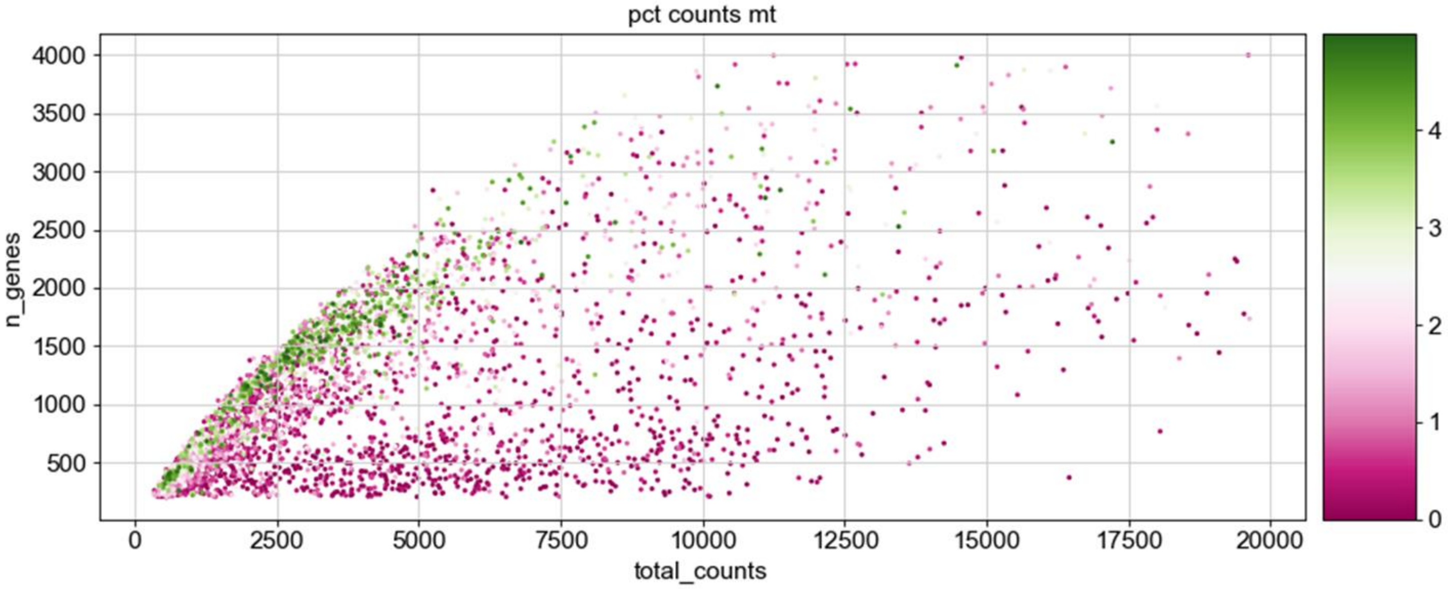

Figure 1.35: Number of genes by count depth and <5 percentage counts in mitochondrial genes in Rc547 Single Cell RNA-Seq data post-filtering

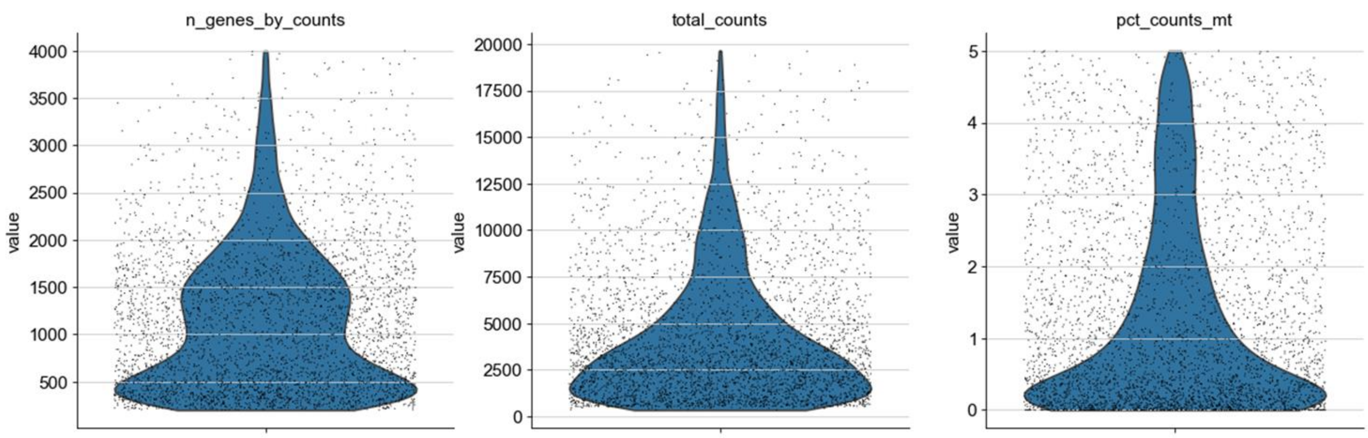

Figure 1.36: Violin plots for Rc547 Single Cell RNA-Seq data post-filtering

In Figure 1.36 following several filtering processes in order to ‘clean’ the data we can see the same Violin plots as seen in Figure 1.29 which shows the number of genes expressed in the count matrix, the total counts per cell and the percentage of counts in mitochondrial genes going from left to right respectively, however in Figure 1.36 this shows a truer representation of the cell data that is relevant to cell-type populations rather than outliers and excessive mitochondrial genetic data.

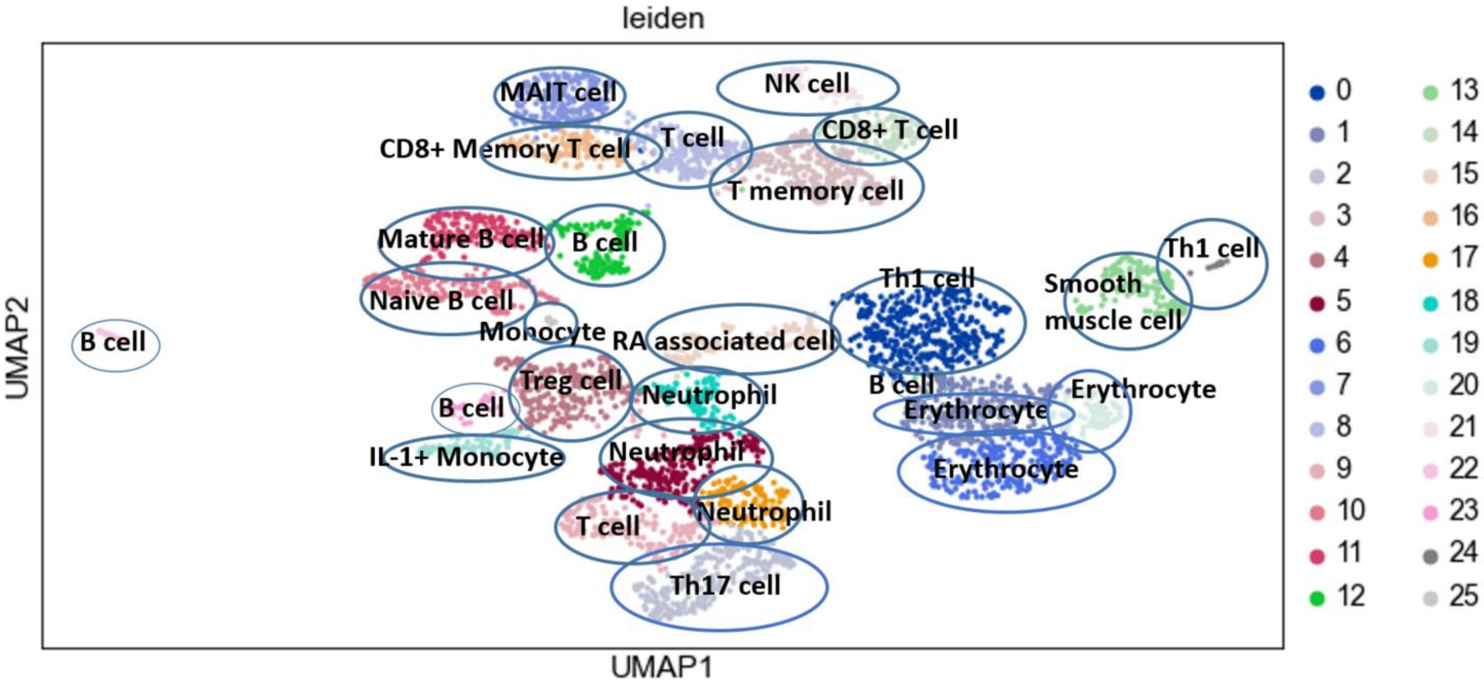

Figure 1.37: UMAP for Rc547 Single Cell RNA-Seq data post-filtering

In Figure 1.37 following data filtering previously stated I created a Uniform Manifold Approximation and Projection (UMAP) at the 1.0 resolution showing 25 Leiden clusters whereby each is represented by a distinctive colour to indicate a different cell population with a unique genetic signature. Whereby a distinctive clustering of erythrocyte cell populations is seen as well as neutrophil and B cell populations.

Chapter 3
Mucosal Associated Invariant T (MAIT) cells at the enthesis

Results

3.10 MAIT cells are present in the human enthesis

3.11 Basal IL-18 expression in entheseal-derived MAIT cells

3.12 Transcriptional profiling of entheseal MAIT cells compared to peripheral blood-derived MAIT cells

3.10 MAIT cells are present in the human enthesis

Considering that the hallmark of axial SpA pathogenesis is entheseal inflammation, I investigated and found the presence of MAIT cells within human axial enthesis (Figure 1.38). Within both EST and PEB, MAIT cells mainly expressed the CD69 resident memory marker compared to MAIT cells from the peripheral blood which were mainly CD45RA+ corresponding to a naïve/circulating phenotype (Figure 1.38).

3.11 Basal IL-18 expression in entheseal-derived MAIT cells

Basal levels of expression of IL-18 were demonstrated in MAIT cells isolated from the normal human enthesis, (Figure 1.42), following appropriate flow cytometry gating (Figure 1.40), which arguably supports the importance of IL-18 in MAIT cell modulation.

3.12 Transcriptional profiling of entheseal MAIT cells compared to peripheral blood-derived MAIT cells

The comparison of blood and entheseal-derived (from both PEB and EST) MAIT cell transcripts (Vα7.2+ CD161+) identified EST MAIT cells with a phenotype compromising of higher *AhR, JAK1*, *STAT4,* and *TGFβ1* transcript expression (Figure 1.39). Furthermore, transcripts indicative of circulating T-cells, such as *KLF2* and *T-bet* showed higher transcript expression in blood MAITs (Figure 1.39). Entheseal MAIT cells also showed higher expression of growth factors and molecules associated with tissue repair and homeostasis, such as *VEGFA* and *IL-10* when compared to matched peripheral blood (Figure 1.39).

In comparison to blood-derived MAITs, entheseal-derived MAITs showed higher *CXCR3* and *CCR6* expression which could suggest that entheseal-derived MAITs are better equipped to mediate pro-inflammatory signals and tissue migration. Where significance between PB and PEB MAITs is only seen in CCR6, following an independent samples T-test p=0.038.

Following suitable flow cytometric gating strategies, as seen in Figure 1.40, and previous studies showing blood-derived MAIT cells producing IL-17 (55), I next investigated if entheseal MAITs had the ability to produce this cytokine. Following PMA/ionomycin stimulation, MAITs showed elevated expression of TNFα and IL-17A through intracellular flow (Figure 1.41). Overall, 3.5% of MAITs had inducible IL-17A and 11.7% inducible TNF (n=2). Given that IL-18 was reported to enhance IL-17 production alongside IL-12, I also investigated and confirmed that IL-18 was present in the human enthesis at basal levels (Figure 3.5).

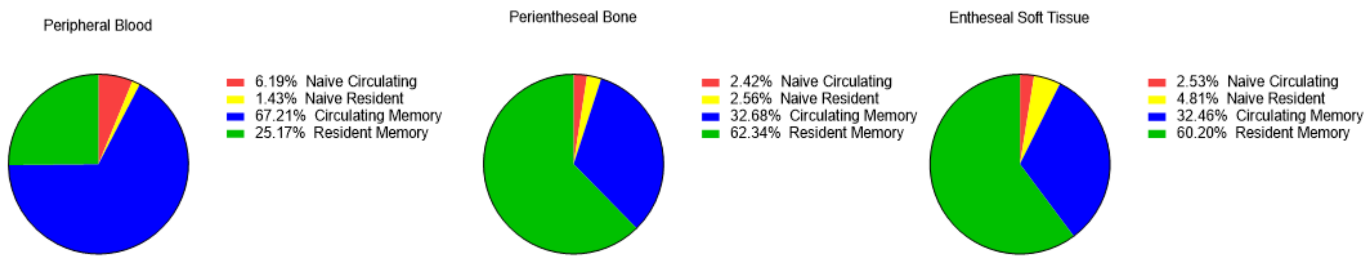

Figure 1.38: Percentage of MAIT cells from PB, PEB, and EST

Figure 1.38 shows MAIT cells that were sorted from Peripheral Blood (PB) Peri-entheseal Bone (PEB) and Entheseal Soft Tissue (EST), defined by their expression of Vα7.2 TCR and CD161. Cells expressing tissue-resident (R)/memory (M) markers were identified by CD69+ and naïve (N)/circulating (C) cells by CD45RA+. Results displayed as mean from n=5

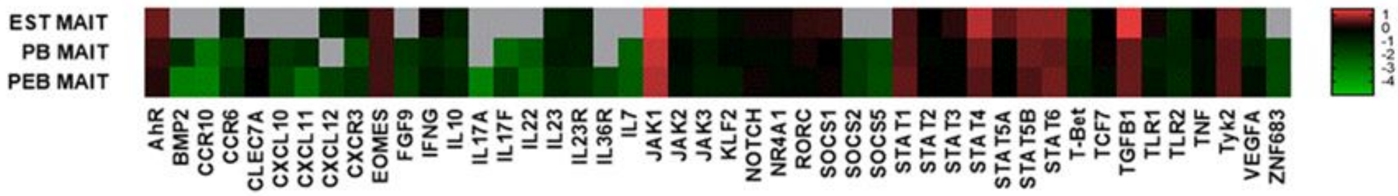

Figure 1.39: Transcriptional profiling of MAIT cells from EST, PB and PEB

Basal expression of cytokines, chemokines, growth factors, signalling molecules, tissue residency markers was assessed. Colour coding refers to differentially expressed genes where values less than −1 indicate low expression and values greater than 1 indicate higher expression, those with grey boxes indicate no values, and values displayed are log 10ΔCt relative to HPRT (n=7).

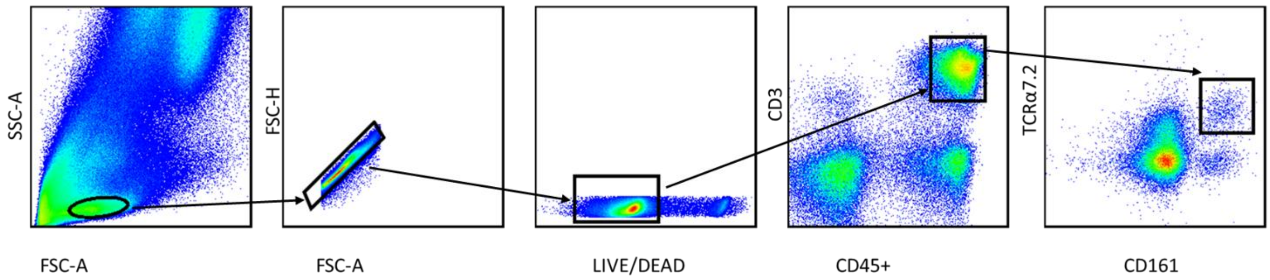

Figure 1.40: Flow cytometry gating strategy for phenotypic identification of MAIT cells in entheseal tissues and peripheral blood cells

Doublet excluded EMCs (PEB and EST) or PBMCs were stained with zombie aqua (live/dead discrimination, Biolegend), anti-CD45 (to exclude non-leucocytes), and anti-CD3 (T-cell inclusion). MAIT cells were identified by CD161+ and Vα7.2 TCR+ staining. PEB EMCs were plated out at a minimum of $4x10^6$/mL in RPMI (containing 10% FCS, 1% penicillin/streptomycin) and stimulated with PMA (50 ng/ml) and Ionomycin (1 µg/ml) for 3 hours in the presence of Golgi Plug (BD).

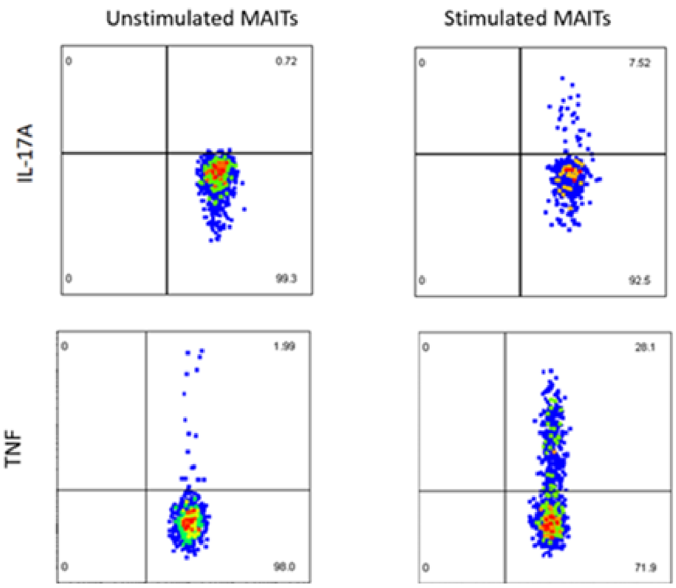

Figure 1.41: Pro-inflammatory cytokine induction in entheseal-derived MAITs

Figure 1.41 shows intracellular TNF and IL-17 cytokine expression with and without stimulation with PMA (50 ng/ml) and Ionomycin (1 µg/ml) for 3 hours in the presence of Golgi Plug (BD) in PEB-derived MAIT cells (n=2).

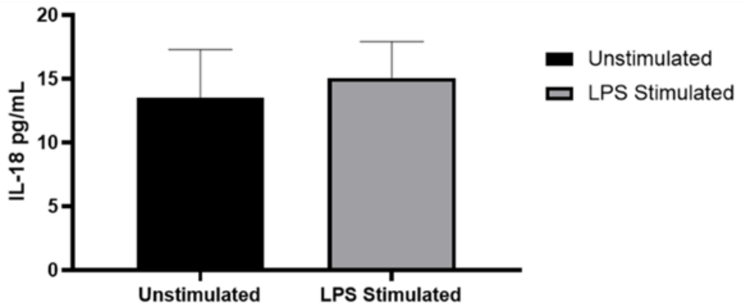

Figure 1.42: Basal production of IL-18 in MAIT cells from entheseal tissue

Protein expression of IL-18 (pg/mL) in unstimulated and LPS stimulated (100ng/mL) EMCs from PEB Mean ±SEM (n=6). PEB EMCs were plated out at 5x10^6/mL in RPMI (containing 10% FCS, 1% penicillin/streptomycin) and stimulated with LPS (100ng/mL) for 24 hours

Chapter 4
Discussion

4.1 CD4 CD8 T-Cells

This project confirms the presence of CD4+ and CD8+ T-cells at the normal human enthesis, which are present in both perientheseal bone and spinal soft tissue. In health, these T-cells exhibited regulatory features including elevated TGFβ1 transcripts, while showing low levels of pro-inflammatory cytokine transcripts and protein production. Unlike the matched blood samples, a clear FoxP3 regulatory T-cell population was not identifiable at the healthy enthesis, however, T-cell stimulation in the presence of PDE4 inhibition was capable of FoxP3 transcript upregulation. I also confirmed that these entheseal T-cells have the capability to secrete pivotal disease-relevant cytokines such as TNF and IL-17A following CD3/CD28 stimulation, without the use of other exogenous cytokines such as IL-23. This is significant as IL-23 is an upstream activating cytokine of IL-17 therefore theoretically blocking IL-23 should be effective in AxSpA, furthermore, within the synonymous Sherlock *et al.* mouse model study (22), they showed that blocking IL-23 led to a notable reduction in IL-17A production. However, it appears results from animal studies did not translate into human clinical trials in AS, as studies have yielded minimal efficacy thus far (56,57). The results indicated that CD4+ T-cells derived from the enthesis secreted both TNF and IL-17A upon stimulation, while CD8+ T-cells from the same source produced only detectable levels of TNF. This is important as TNF is a well-known pleiotropic cytokine with both pro-inflammatory and anti-inflammatory capabilities (58). These findings may indicate the identification of a more anti-inflammatory CD8+ T-cell subset at the enthesis, alongside a more pro-inflammatory CD4+ T-cell subset.

Lymphocytes continually egress from peripheral tissues and lymph nodes and return to the peripheral blood, known as intravascular circulation, in a unidirectional manner via the lymphatic system. This underpins the immune surveillance concept. A large proportion of immune cells egress from both lymphoid and non-lymphoid tissues (LT and NLT respectively) into the thoracic duct. This daily lymphocyte migration via the thoracic duct is sufficient to replace the entire lymphocyte cohort within peripheral blood 48 times per day in humans

(59). However, the identification of TRM cells highlights that not all T-cells recirculate via lymphoid or non-lymphoid tissues, but remain resident.

In non-lymphoid tissues, TRM cells constitute the predominant subset of memory CD8+ T-cells. A recent investigation conducted by Buggert et al. in 2020 (60) revealed that the primary immune cell types present in thoracic duct lymph (TDL) were T and B cells. This study also noted a lower prevalence of innate lymphoid cells (ILCs) and a higher occurrence of granulocytes, monocytes, dendritic cells (DCs), and hematopoietic stem cells (HSCs) in the bloodstream compared to TDL. Furthermore, T effector memory (TEM) and T effector memory CD45RA+ (TEMRA) cells were found to be the dominant populations in the blood, while naive T-cells and T central memory (TCM) cells were primarily located in the TDL. Following mechanistic studies, it was demonstrated that TEM populations are mainly found in peripheral tissues, whereas TCM populations were mainly found in secondary lymphoid organs, where they are more proliferative than their TEM counterparts due to their higher production of IL-2, whereas T memory stem cells (TSCM) show further proliferative and survival capabilities that exceed both the TEM and TCM counterparts suggesting that TSCMs could serve as a future therapeutic target (61).

Compared to naïve cells of the same antigen-specificity, memory CD8 T-cells persist in greater numbers; can populate peripheral organs; are poised to immediately proliferate, execute cytotoxic functions, and secrete effector cytokines upon Ag re-encounter (62); and exist in different metabolic, transcriptional, and epigenetic states (63). Extensive flow staining panels found TDL-derived CD8+ memory T-cells expressed more CD103, CCR5, CXCR3, CXCR5, CD27, and CD127 than matched blood. Whereas blood-derived CD8+ memory T-cells expressed late differentiation markers such as CD57 and KLRG-1 (Killer cell lectin-like receptor G1), when compared to TDL-based CD8+ memory T-cells. Several cannulation studies showed that CD4+ T-cells enter and recirculate through lymph nodes faster than the CD8+ T-cell counterpart (64).

Principal Component Analysis (PCA) and t-distributed Stochastic Neighbor Embedding (tSNE) analysis identified distinct CD8+ memory T-cell clusters, each with unique phenotypic characteristics dependent on tissue location where CCR7- memory CD8+ T-cells in peripheral blood lacked CD27 and CD127 expression, favouring markers associated with late differentiation, whereas the same cells derived from TDL mostly expressed CD27 and CD127.

CD127 also known as IL-7Rα promotes survival in CD8+ memory T-cells without antigen stimulation via IL-7 mediated self-renewal, however, CD127 and IL-7 signalling is not sufficient for CD8+ T-cell memory formation, as identified in a study that demonstrated that CD127 expression did not improve survival of KLRG1^{hi} cells into memory (65), where KLRG1 belongs to the killer cell lectin-like receptor (KLR) family which is a group of transmembrane proteins mainly expressed in NK cells that exhibit a memory phenotype. Where KLRG1 plays an inhibitory role in NK and T-cell function by binding to non-MHC ligands (66).

Complete T-cell activation requires co-ligation of the TCR with the co-stimulatory molecule CD28 whilst downregulating IL-7RA, switching cytokine dependency from IL-7 to IL-2, where IL-2 works in an autocrine manner to maintain proliferation in effector T-cells. However, IL-7R expression is renewed as effector T-cells differentiate into memory T-cells.

When studying T-cell lymphocyte populations a large factor to consider is T-cell plasticity. It has been well documented in previous studies that there is a remarkable level of plasticity between the Th cell subsets, one such example is the stable Th1/Th2 hybrid cell population that is capable of producing both key cytokines (IFNγ and IL-4) from their respected Th subset. Furthermore, reports observe Th1 cytokine expression in Th17 cells and Tregs in human disease (67) and activated Th1, Th17, and Tregs can class switch towards a Th2 phenotype in helminth infections (68). Moreover, in rheumatoid arthritis patients there are cases of Tregs switching to inflammatory Th17 cells (69). From the results section 1.2, with regards to transcriptional profiling, there was an upregulation in Th1 master transcription factor T-Bet, which is abundantly expressed by subsets of circulating T-cells (70) which supports the findings as this was only present in peripheral blood with no statistical significance between the CD4+ and CD8+ populations which begs the question of whether T-Bet has a role in Th1 polarisation. The analysis of the relative expression of the Treg master transcription factor FOXP3, as presented in results section 1.4, reveals that while a population of CD4+ CD25+ FOXP3+ Tregs is identifiable in the blood, such a population is not apparent at the enthesis. This observation may imply a possible transition from the immunomodulatory Treg phenotype towards a more pro-inflammatory Th17 phenotype at the enthesis.

The imbalance of Th17 and Treg cells is considered to be a pivotal cause of autoimmune diseases, including the spondyloarthropathies. Before birth, approximately 10%–30% of all CD4+ T-cells in the blood, lymphoid tissue, and mucosal sites are Treg cells, whereas less than 5% are Treg cells in adults. Tregs have a higher turnover rate (measured by Ki67 expression) which may provide evidence for reduced Treg numbers as humans age. The $CD4^{+}$ $CD25^{+}$ $CD127^{lo}$ $FOXP3^{+}$ Tregs are crucial in inhibiting exaggerated T effector cell responses and aid in suppressing autoimmune disease development, whereas $CD4^{+}$ IL-17^{+} Th17 cells are known drivers of pathogenesis in many autoimmune diseases. The master regulators of these cell types are transcription factors FOXP3 (forkhead box P3) and RORγt (Retinoic acid receptor γt) respectively (71). Differentiated T-cells can co-express master regulators within the Th subsets, this produces a plastic phenotype; one example of this is Th17-like Tregs that express both RORyt and FOXP3, where this population is enriched in the synovium of rheumatoid arthritis (RA) patients (72).

The most well-characterised Tregs are those that are naturally occurring in the thymus (nTregs) and inducible Tregs in the periphery following stimulation (iTregs). Both nTregs and iTregs express FOXP3 however they exhibit different functional properties and cis control elements that are distinct between the populations, where nTregs are primarily involved with promoting self-tolerance and autoimmunity, in contrast, iTregs are instrumental in facilitating peripheral immune tolerance and aid in dampening inflammation. Tregs constitute approximately 10% of CD4+ T-cells expressing at CD45RA+ CCR7+ naïve T-cell phenotype in blood and lymphoid tissue and CD45RO+ in mucosal sites. Tregs constitutively express CD25 (IL-2R) and CD28 via IL-2 STAT5 signalling, this is essential for maintaining high levels of FOXP3 expression, where TCR stimulation is required for Treg suppressive function. Treg cells also suppress effector T-cell responses by consuming IL-2, limiting access to this important effector CD4 T-cell growth factor. Interestingly the results, section 1.2 showed an upregulation in IL-10, the anti-inflammatory, immunosuppressive cytokine produced by Tregs, and TGFβ1 which can promote either Th17 or Treg differentiation dependent on concentration, at low concentrations TGFβ synergizes with IL-6 and IL-21 to promote IL-23R expression, favouring Th17 differentiation, at high concentrations TGFβ represses IL-23R and favours Foxp3+ iTregs (inducible Tregs), which in turn inhibits RORγt function (73); in entheseal tissue compared to peripheral blood.

Calcium (Ca2+) plays a crucial role in the activation, proliferation and expression of T-cells, this second messenger is controlled by maintaining calcium equilibrium through CRAC channels and calcium influx channels, cAMP (Cyclic adenosine monophosphate) is an important second messenger associated with cell signalling and homeostasis. Adenosine, which is produced via ATP dephosphorylation, has a strong anti-inflammatory influence on immune cells and allows for the generation of intracellular cAMP (74). This reduces T effector cell activity whilst improving Treg immunomodulation. cAMP is regulated via phosphodiesterase (PDE) enzymes where the PDE4 isoenzyme PDE is largely expressed by immune cells, however, the isoform expression may vary between T-cell phenotypes and in association with disease pathogenesis (75). In T-cells, PDE4 plays a role in signal transduction, due to its association with the co-stimulatory molecule CD28, and cytokine release, where TNFα, IL-2, and IL-4 all depend on PDE4 signalling (76).

In T lymphocytes PDE4i's elevate cAMP which in turn modulates inflammatory pathways including the NFκβ signalling pathway, it also promotes T effector phenotypes including Th2, Treg and Th17 (77). cAMP regulates many physiological processes via the activation of protein kinase A (PKA). However, it is noteworthy that, despite its anti-inflammatory effects, cAMP is known to enhance the production of Th17-associated cytokines, including IL-1β, IL-6 and IL-23 by APCs. The PDE4i, such as apremilast, has been shown to clinically reduce enthesitis in PsA patients (78), while another PDE4i, Rolipram, is also effective in IL-17-driven autoimmune murine models (79). Surprisingly, Apremilast failed to reach clinical outcome for AS. In the results, section 1.5, PDE4i was able to attenuate TNF and IL-17 secretion in CD4+ T-cells and TNF from CD8+ T-cells. Mechanistically this finding is in line with previous observations showing PDE4i attenuating IL-17 and TNF from T-cells (80).

The surface marker CD39 serves as a marker for Tregs, where it converts ATP to AMP. This conversion is linked to the activity of CD73, which subsequently transforms AMP into adenosine, where adenosine produced via CD73 is known to downregulate NFκB signalling in effector T-cells. One significant mechanism by which Tregs influence the induction of immune responses is through adenosine-mediated interactions with dendritic cells, this is significant given that ~90% of FOXP3+ Tregs in humans are CD39+. This may highlight a surface marker that, in association with immune regulation, has not been fully explored, where CD39+ Tregs in humans have been described as regulatory effector/memory-like T-cells, and express higher levels of FOXP3, CD25, activation markers, co-inhibitory molecules, and suppressive cytokines but lower levels of CD127 compared with CD39− Tregs (81).

It is widely recognized that metabolic pathways play a significant role in determining the fate of CD4+ T-cells. Elevated glycolytic metabolism is associated with decreased expression of FOXP3, thereby facilitating the differentiation of Th17 cells. Additionally, robust glycolytic signalling diminishes the stability of nTregs, leading to the emergence of ex-Tregs that produce IFNγ and IL-17A. Furthermore, fatty acid synthesis is essential for the development of Th17 cells, while concurrently inhibiting Treg differentiation, highlighting another factor associated with the Th17-Treg equilibrium.

Interestingly, inflammatory Th17 and immunosuppressive Tregs are reciprocally induced from naïve CD4+ cells, subject to the presence of either IL-6 or IL-2, respectively. T-cells can diversify into several effector-type lineages, these are distinguished via cytokine signature and functional capabilities. Due to T-cell plasticity, lineages can switch phenotype from inflammatory to immunomodulatory and vice-versa dependent on specific transcription factors and cytokine milieu. It is well established that the gut microbiome can also alter T cell lineage, where the bacterially produced ligand-activated transcription factor AhR (Aryl hydrocarbon receptor) is associated with regulating a plethora of T cell populations including Th17, Treg, and γδ T-cells (82). Looking at the results with regards to transcriptional profiling, results section 1.2, there was an increased expression of AhR in entheseal tissue compared to matched blood, which supports the theory that AhR promotes the retention of tissue resident memory (TRM) cells (83), which may suggest the entheseal cells from the cohort are in fact TRM in nature. Furthermore, the other transcription factor upregulated in results section 1.2 was NR4A1 (Nuclear Receptor Subfamily 4 Group A Member 1), which has been shown in the context of influenza infection, to be of importance with regards to TRM maintenance (84). Both of these findings further solidifies the idea that the entheseal cells are in fact TRM cells.

During homeostasis, CD4+ Treg cells also play a key role in TRM maintenance, where they reduce the IL-2 supply for CD8+ T-cells via competitive consumption, furthermore, the constitutive expression of CTLA4 (cytotoxic lymphocyte antigen 4) which shares the same ligands as the CD28 costimulatory molecule, further diminishes T-cell activation. When this is coupled with low levels of pro-inflammatory signals this allows CD8+ T-cells to continue maturation into a TRM phenotype (85). These findings confirm what has been discovered in several studies from other tissues where an intimate relationship between $CD4^+$ and $CD8^+$ T-cells is emerging (86). The observed downregulation of KLF2, which is the transcription factor for Sphingosine-1-Phosphate Receptor 1 (S1PR1), as detailed in results section 1.2, highlights the potential of entheseal cells in maintaining their tissue retention capabilities and TRM phenotype. Unlike other target tissues in SpA such as the gut and skin, the basis for such populations in the normal enthesis in health is poorly understood and may be related to tissue repair and integrity.

Human Th1 cells originating from the phenotype shift of Th17 to Th1 cells were defined as non-classic Th1, to distinguish them from classic Th1 cells that were generated directly from the polarization of naïve cells. The transcription factor EOMES (Eomesodermin) is expressed by human non-classic Th1 cells and it is involved in their phenotype development from Th17 cells. Due to their plastic nature, non-classic Th1 cells can be more susceptible to phenotypic redirection under polarisation conditions (such as IL-1β, IL-6, TGFβ for Th17 cells). According to recent epigenetic studies, it has been established that the Th17 signature genes RORC and IL-17 possess repressive histone modifications (H3K27me3) in classic Th1 cells. This observation implies that it is difficult for terminally differentiated Th1 cells to transition to a Th17-like phenotype. This challenge may be attributed to the role of IFNγ, which is primarily secreted by Th1 cells and acts to repress Th17 development through the STAT1 signalling pathway. In contrast, non-classic Th1 cells exhibit distinct pathogenic characteristics, such as elevated cytokine production, enhanced proliferation, and a marked resistance to the suppressive influence of Treg cells (87).

4.2 MAIT Cells

In humans, mucosal-associated invariant T cells (MAITs) accumulate in the intestinal lamina propria and the bloodstream, accounting for roughly 1-8% of the total T cell compartment. These cells develop in the thymus shortly after birth and are positively selected by MR1+ (MHC-class Ib-related protein 1, also known as CD154) double-positive cortical thymocytes. This selection process leads to oligoclonal expansion, resulting in MAITs becoming the largest single specificity αβ T cell population in human blood (88). Utilising the transcription factor STAT3 for differentiation, most MAIT cells are classified as CD8+, with a smaller fraction identified as CD4–/CD8– double-negative (DN) cells, and a minor CD4+ population. Research indicates that stimulated DN MAIT cells produce greater amounts of IL-17 while secreting reduced levels of IFNγ and TNF in comparison to stimulated CD8+ MAIT cells (89).

TCR-dependent activation of MAIT cells plays a crucial role in initiating early immune responses to infections. These cells are capable of recognizing non-peptide antigens that are presented by MR1, which exhibits a 90% sequence similarity between murine and human models, where MR1 is also associated with β_2M like NKT cells. Upon stimulation through MR1, MAIT cells secrete a range of cytokines, including TNFα, IFNγ, IL-2, IL-17, and IL-22, thereby adopting a Th1/Th17-like phenotype characterised by the expression of T-bet and RORγt transcription factors. It is currently understood that the production of IL-17A by MAIT cells is 10-fold higher than that of conventional Th17 cells (90). MR1 is predominantly localised within the endoplasmic reticulum during steady-state conditions, with its expression on the plasma membrane occurring in response to 5-(2-oxopropylideneamino)-6-D-ribitylaminouracil (5-OP-RU), Microbe-Associated Molecular Patterns (MAMPs), or type I and II interferons (91). The administration of the MAIT cell agonist 5-OP-RU resulted in a decrease in MAIT cell populations within the thymus, indicating that MAIT cells may be vulnerable to negative selection (92). MAIT cells are known to exhibit responses to a range of pathogens, including both Gram-positive and Gram-negative bacteria, as well as yeasts. The antigens recognized by MAIT cells, specifically 5-OP-RU and 5-OE-RU (5-(2-oxoethylideneamino)-6-D-ribitylaminouracil), are produced through the condensation of 5-A-RU (5-amino-6-D-ribitylaminouracil). While there is considerable combinatorial diversity resulting from the use of TRAV and TRAJ segments, the interaction with 5-OP-RU is consistently mediated by the evolutionarily conserved Tyrosine 95 present in the CDR3 region of the TCR-α chain (93). Furthermore, the presence of 5-OP-RU is essential for the full development of MAIT cells, as it must reach the thymus. It is here that MAIT cells undergo a unique process of intra-thymic differentiation, distinct from that of conventional T-cells. As a result of this differentiation, MAIT cells gain immediate effector functions associated with their phenotype (94) and migrate to non-lymphoid tissues. This positioning enables MAIT cells to respond swiftly upon encountering antigens, thereby facilitating immune cell regulation and underscoring their critical role in immunopathology, which bridges the gap between innate and adaptive responses. The effector memory phenotype observed in MAIT cells is modulated by the Promyelocytic leukemia zinc finger protein (PLZF), whose expression increases as these cells mature. Previous studies have indicated that PLZF is associated with a heightened apoptotic rate in both MAIT and invariant natural killer T (iNKT) cells. Furthermore, the development of MAIT cells is dependent on TCF-1 and TCF-7, with the absence of TCF-7 resulting in a complete depletion of MAIT cells, thereby underscoring its importance in the initial phases of MAIT cell development (95).

Patients suffering from AS demonstrate a diminished frequency of MAIT cells in their peripheral blood, which likely signifies their recruitment to regions of active inflammation. Conversely, a higher frequency of MAIT cells is observed in the synovial fluid (SF) of these patients compared to healthy controls. Furthermore, MAIT cells originating from SF of AS patients have an exaggerated IL-17 phenotype which can be further enhanced upon stimulation with IL-7. However, research conducted by Gracey *et al.* in 2016(96), revealed that the upregulation of IL-17+ MAIT cells was predominantly observed in male AS patients. This sexual dimorphism in IL-17 frequency has also been recently noted in Th17 cells as well (97). Such findings may lend support to the concept of an IL-17 promoting axis in AS, as other investigations into unconventional T-cells have reported increased frequencies of IL-17+ cells, including ILC3s and γδ T cells (98).

4.3 RNA Seq

The generation of T cell receptor (TCR) diversity occurs through VDJ recombination, complemented by junctional diversity that is mediated by Terminal deoxynucleotidyl Transferase (TdT). This mechanism ultimately results in a diverse TCR antigen repertoire within a MHC-restricted repertoire (99).

The process of VDJ rearrangement occurs as a result of DNA double-stranded breaks on either side of the gene of interest. In adaptive immune cells, this mechanism is orchestrated by the RAG1/RAG2 enzyme, associated with the recombinase activating gene. The regions where splicing takes place are identified by recombination signal sequences (RSS). This splicing is inherently imprecise, allowing for the deletion and insertion of nucleotides at the cleavage site. Such imprecision leads to additional VDJ variation, further influenced by the enzyme TdT (Terminal deoxynucleotidyl transferase). This mechanism gives rise to extensive junctional diversity, which is crucial for the generation of a wide array of variable regions in both heavy and light chains, which aids in the generation of $\sim 10^{18}$ unique T cell antigen receptors. The significance of TdT in the generation of diversity has been emphasised in several mouse models. Research indicates that TdT knockout mice exhibit a tenfold decrease in TCR diversity (100). While TdT can add all 4 naturally occurring nucleotides there is a definitive propensity for the incorporation of dGMP and dCMP versus dAMP or dTMP observed *in vivo,* this may provide an explanation for the high GC content of the Ig and TCR N regions. Furthermore, secondary T-cell responses demonstrate a less diverse repertoire compared to primary responses, which can be attributed to the preferential selection and expansion of T-cells that possess the highest affinity TCRs.

Unlike MHC-independent TCR cells, MHC-specific TCRs are selected by both or Complement Determining Region 3 (CDR3) length and amino acid content. For TCR antigen specificity, CDR1 and CDR2 are necessary to conserve the ability of the TCR to recognize MHC, while CDR3 undergoes somatic hypermutation to allow for the formation of 'Collier-de-Perles' patterns, which is the higher-order structure required for antigen specificity, furthermore the CDR3 lacks the diversity set of genes in the light chain loci, unlike other CDRs, in summary this allows

CDR3 to arguably be the most diverse CDR which is essential for its role in antigen specificity.

MHC-restriction disfavours TCR's with CDR3 longer than 13 amino acids, this in turn limits positively charged and hydrophobic amino acids in CDR3β, and clonally deletes TCRs with cysteines in their CDR3 peptide-binding regions. Together, these MHC-imposed structural constraints form the basis to shape VDJ recombination sequences into MHC-restricted repertoires. (101) The CDR3 is highly diverse in composition and thus, correlations can be drawn between T- cell diversity and CDR3's broad variability. From the literature CDR3 length classically follows a Gaussian distribution with skewed amino acid profiles being indicative of lymphocyte selection and arguably clonal expansion (102). On a whole, amino acids forming the majority of the CDR3 region tend to be neutral or with slight tendencies towards hydrophilicity (103).

CDR3 plays a crucial role in determining the specific antigen recognition of individual cells. Computational models of antibodies indicate that even minor variations in the length of CDR3 can significantly influence the charge, hydrophobicity, and shape of the antigen binding site (104). Consequently, analysing variations in CDR3 length may provide valuable insights into the structure-function relationships across different classes of immune receptors. However, as observed in results section 2.1, there appears to be minimal variation in CDR3 length among CD4+, CD8+, PEB, and ST respectively.

Looking at TCR repertoire across all ages, in a range of recent studies (105, 106), there is a reduction in diversity in the TCRβ chain in naïve T-cells in older patients. However, it is still diverse suggesting that humans are capable of responding to novel antigens even in the later stages of life. The examination of TCR repertoires in naïve, lymphoid, and memory T-cells demonstrated that CD4+ and CD8+ naïve T cells are more diverse and exhibit lower clonality than their memory counterparts found in the spleen and multiple lymph nodes, suggesting that naïve T-cells retain the capacity to respond to diverse antigens.

Clonality functions as a relative abundance metric that measures clonal expansion by determining the likelihood of identifying the same sequence in two different replicates, where an elevated clonality score signifies a greater extent of clonal expansion. This increase in clonal representation may be due to growth within the memory compartment, resulting from an uneven homeostatic proliferation of the naïve T-cell repertoire, or it may indicate the presence of a T-cell tumour. Given the sheer volume of inferences that can be ascertained by looking at clonality in RNA-Seq, many studies have looked into this to deduce disease pathogenesis in cancers and the spondyloarthropathies to name a few.

The examination of Bulk RNA-Seq data focusing on TCRs indicated that, in the assessment of clones targeting viral infections, Cytomegalovirus (CMV) and Influenza A Virus (IAV) were identified as the most common, as outlined in results section 2.2. This is a critical finding, as studies have indicated that CMV-specific T cells can vary in their distribution among individuals, typically found in the blood, bone marrow, lymph nodes, and spleen. In the case of RA, there is a positive correlation between CMV positivity and an increased presence of CD8+ CD28- T -cells; however, it remains to be determined whether this correlation is also observed in patients with spondyloarthritis (107).

Chapter 5

Conclusion

This work identified healthy human entheseal CD4+ and CD8+ T-cells which exhibited regulatory characteristics including high TGFβ1 transcripts, but low pro-inflammatory cytokine transcript levels and protein production. Furthermore, the entheseal-derived T-cells are predicted to exhibit antiviral reactivity with CD8+ T-cells expressing higher levels of transcripts suggestive of tissue residency. Inducible IL-17A and TNF production can be robustly inhibited *in vitro* following CD3/CD28 stimulation, without the use of other exogenous cytokines such as IL-23.

A recent study by Jacobse *et al.* (108), highlighted that colonic derived Tregs highly express IL23R. In murine models lacking IL23R in colonic Tregs, there was an observed increase in their frequency and a competitive advantage during inflammatory conditions. The researchers sought to ascertain whether these findings were applicable to human studies. Upon administering an IL23 blocker, they noted a restoration of Treg cells and an increase in pro-apoptotic TNFRSF9 expression. Following these results, they propose that IL23R signalling plays a role in modulating colonic Tregs through increased cellular turnover and antagonistic suppression, suggesting that IL23 may have a negative regulatory effect on colonic Tregs, which could lead to chronic inflammation in IBD patients.

The T memory subsets are crucial for maintaining immunological memory and include TCM (T Central Memory CCR7+ and CD45RA-), TEM (T Effector Memory, CCR7- and CD45RA-), TEMRA (T Effector Memory CD45RA+, CCR7- and CD45RA), TRM (Tissue Resident Memory cells, CD69+CD45RA- and CD103+ in CD8+ subpopulations) and TSCM a subset of TCM cells (T Memory Stem Cells, CCR7+CD62L+CD45RA+) which show enhanced self-renewal capabilities (109). The results within this work, section 1.2, support, but do not prove, a TRM phenotype in PEB and EST in contrast to the circulating memory (CD45RA+CD69-) peripheral blood phenotype.

Whereby immunofluorescence and cytometry suggested that entheseal CD4+ and CD8+ T-cells displayed a resident memory phenotype (CD69+/CD45RA-) supported by tissue residency gene transcripts (higher NR4A1/AhR and lower

KLF2/T-bet transcripts) as shown in results section 1.2. Both CD4+ and CD8+ T-cells showed increased expression of immunomodulatory genes including IL-10 and TGF-β compared with peripheral blood T-cells with entheseal CD8+ T-cells having higher CD103, CD49a and lower SIPR1 transcript that matched CD4+ T-cells following bulk RNAseq analysis, as shown in results section 2.2. However, recent studies have demonstrated the presence of TRM T-cells in different tissues including synovial fluid and gut in SpA patients (110) (111), and therefore whether these cells recirculate between these different sites awaits elucidation.

The downregulation of KLF2, an important transcription factor for S1PR1 expression, highlights the potential of entheseal cells in maintaining their tissue retention capabilities and TRM phenotype. Interestingly, the transcription factor Hobit (Homolog of Blimp-1 in T cells, also known as ZNF683), which directs a tissue-resident programme and prevents egress of immune cells (112), was downregulated in both CD4+ and CD8+ entheseal T-cells, respectively, compared with peripheral blood, as revealed in results section 1.2. This result contradicts previous findings in mice where Hobit is known to be upregulated, highlighting a difference between human and murine models and the signature TRM-associated genes (113). Unlike other target tissues in SpA such as the gut and skin, where direct interfacing with potential microbial pathogens occurs, the basis for such populations in the normal enthesis in health is poorly understood and may be related to tissue repair and integrity.

Following stimulation, CD4+ T cells produced more TNF than CD8+ T-cells and IL-17A was produced exclusively by CD4+ T-cells, as shown in results section 1.3. TNF and IL-17A production from CD4+ T-cells was effectively inhibited by PDE4i, while RORγti only reduced IL-17A secretion, as shown in results section 1.5. It is well known that RORγt is a transcription factor and is regarded as the master regulator of IL-17A (114). RORγt antagonists have been investigated in numerous murine models of inflammation and autoimmunity, yielding promising results (115)(116). In human studies, RORγt inhibition was recently shown to inhibit IL-17A from synovial T-cells from both PsA and AS patients and also blood-derived T-cells (117)(118). This ‘*in-vitro* enthesitis model’ may provide a robust model for testing the impact of therapeutic agents on the adaptive immune system in preclinical work in SpA but clear differences between activated peripheral blood cells undergoing drug antagonism were not apparent.

This work also confirmed that MAIT cells were present in the spinal entheses of healthy controls, as seen in results section 3.1, where they were mainly of the resident memory cell phenotype with inducible IL-17A protein production. It is well documented that human MAIT cells undergoing TCR-dependent activation are drivers of early responses to infection. MAITs recognise non-peptide antigens presented by the MHC-class Ib-related protein 1 (MR1 also known as CD154) with 90% sequence similarity between mice and humans, where MR1 is also associated with β2 Microglobulin (β2M) like NKT cells. Once stimulated via MR1 they produce TNFα, IFNγ, IL-2 and IL-17, IL-22 creating a Th1/Th17-like phenotype producing T-bet and RORyt transcription factors. It is currently considered that IL-17A production by MAIT cells is 10-fold higher than by conventional Th17 cells (119). Furthermore, it has been reported that co-stimulation with IL-18 significantly increases the production of pro-inflammatory IL-17A beyond the levels achieved by MR1 alone (120). Therefore, I wanted to confirm if IL-18 was present in entheseal-derived MAITS, which did confirm basal IL-18 protein expression, as shown in results section 3.2. This illustrates the vital importance of IL-18 with regards to MAIT cell regulation, where IL-18 has been demonstrated to work in conjunction with IL-12 to stimulate IL-17A/IL-17F production by MAIT cells, independent of IL-23 (121).

The investigation into transcriptional profiling of MAIT cells revealed that entheseal-derived MAITs showed elevated levels of *CXCR3* and *CCR6* compared to those derived from blood, as seen in results section 3.3. This observation suggests that entheseal-derived MAITs may be more proficient in mediating pro-inflammatory signals and promoting tissue migration. This is supported by elevated expression of VEGFA, a growth factor known to promote cell migration, and immunomodulatory IL-10 in entheseal-derived MAITs in comparison to matched peripheral blood–derived MAITs. Following stimulation, with PMA and ionomycin, MAIT cells demonstrated a production capacity for IL-17A that was comparable to that of CD4+ T-cells, as shown in results section 3.3. Collectively, these results significantly bolster the evidence linking innate-like lymphocytes to the pathogenesis of axial SpA.

Central to the T-cell antigen response is the CDR3 (Complementarity determining region 3) which provides both antigen specificity and affinity. The bulk RNAseq data looking for CDR3 showed a more diverse repertoire in PEB than EST, as seen in results section 2.2, arguably this could be due to the haematopoietic marrow that PEB contains. Bulk RNAseq predicted clonotype reactivity to both cytomegalovirus and influenza a virus in entheseal resident T-cells, in particular CD8+ T-cells. Bulk RNAseq highlights the presence of clonal populations in both CD4+ and CD8+ T-cell populations with the latter scoring higher on model-based scoring matrices (PAM-30). Overall, these results showing high diversity and limited clonality in PEB and vice versa in the EST suggest that the conventional T cells in each of these compartments are distinct.

In conclusion, this work shows that the normal human enthesis harbours both conventional T-cells and MAIT cells each with inducible production of IL-17 and TNF. The CD8+ T-cells at the enthesis displayed markers suggestive of tissue residency, but further single-cell RNAseq work is required to fully define this. The results also support the idea that IL-17 production may be independent of IL-23, where the *in vitro* enthesitis model allows for TCR engagement via CD3/CD28 crosslinking. These findings provide a base for future studies to define the role of adaptive immune cells in the pathogenesis of enthesitis in active early SpA. Further studies are needed to extend these findings into diseased tissue in SpA.

Future works

The presence of CD4+ and CD8 T-cells in the normal enthesis provides the first direct immunological evidence for adaptive immunity at the enthesis. This provides a basis for studies to explore T-cells in the pathology of axial inflammation in spondyloarthropathy-related disorders. Furthermore, additional studies are needed to confirm if these same cells are present in the enthesis of AS patients.

References

1. Sepriano A, Landewé R, van der Heijde D, Sieper J, Akkoc N, Brandt J, *et al.*, 2016, Predictive validity of the ASAS classification criteria for axial and peripheral spondyloarthritis after follow-up in the ASAS cohort: a final analysis. Ann Rheum Dis, Volume 75
2. Ostrowska. M, Maslinski. W, Prochorec-Sobieszek. M, Nieciecki. M, Sudol-Szopinska. I, 2018, Cartilage and bone damage in rheumatoid arthritis. Reumatologia, Volume 56, (2):111–120
3. Wang. R, Ward. M.M, 2018, Epidemiology of axial spondyloarthritis: an update. Curr Opin Rheumatol, Volume 30:137-43.
4. Bohn. R, Cooney. M, Deodhar. A, Curtis. J.R, Golembesky. A, 2018, Incidence and prevalence of axial spondyloarthritis: methodologic challenges and gaps in the literature. Clin Exp Rheumatol, Volume 36:263-74.
5. Poddubnyy. D and Sieper. J, 2020, Treatment of axial spondyloarthritis: what does the future hold?, Current Rheumatology Reports, Volume 22, 1-8.
6. Cortes. A, Hadler. J, et al., 2013, Identification of multiple risk variants for ankylosing spondylitis through high-density genotyping of immune-related loci, Nature genetics, Volume 45, Issue 7
7. Rahman. M. A, Thomas. R, 2017, The SKG model of spondyloarthritis, Best Practice & Clinical Rheumatology, Volume 31, Issue 6
8. McGonagle, D., Aydin, S. Z., et al., 2015, 'MHC-I-opathy'-unified concept for spondyloarthritis and Behcet disease, Nature Review Rheumatology, Volume 11, Issue 12
9. Costello. M.E., Ciccia. F., et al., 2015, Brief Report: Intestinal Dysbiosis in Ankylosing Spondylitis, Arthritis and Rheumatology, 2015, Volume 67, Issue 3
10. Li. Z, Haynes. K, et al., 2017, Epigenetic and gene expression analysis of ankylosing spondylitis-associated loci implicate immune cells and the gut in the disease pathogenesis, Genes and Immunity, Volume 18, Issue 3

11. Garcia-Montoya. L, Gul. H, Emery. P, 2018, Recent advances in ankylosing spondylitis: understanding the disease and management, F1000Res, Volume 7
12. Watad. A, Rowe. H, Russell. T, Zhou. Q, Anderson. L.K, Khan. A, et al., 2020, Normal human enthesis harbours conventional CD4+ and CD8+ T cells with regulatory features and inducible IL-17A and TNF expression, Ann Rheum Dis, Volume 79(8):1044–54
13. Julier. Z, Park. A. J, Briquez. P. S, & Martino. M. M, 2017, Promoting tissue regeneration by modulating the immune system. Acta biomaterialia, Volume 53, 13-28.
14. Walker. C, Essex. M. N, Li. C, & Park. P. W, 2016, Celecoxib versus diclofenac for the treatment of ankylosing spondylitis: 12-week randomized study in Norwegian patients. The Journal of international medical research, Volume 44, Issue 3, 483–495.
15. Sadoughi, A., Mansouri, R., Nazeri, S., & Mirshafiey, A. (2021). Evaluation of the oral administration of α-l-guluronic acid on COX-1 and COX-2 gene expression profile in ankylosing spondylitis patients. Drug Development Research, 82(2)
16. Sieper. J, Poddubnyy. D, Miossec. P, 2019, The IL-23-IL-17 pathway as a therapeutic target in axial spondyloarthritis. Nat Rev Rheumatol, Volume 15:747-57
17. Stockinger. B, 2021, Lumpers and splitters: Birth of Th17 cells, J Exp Med, Volume 218, Issue 5
18. Reveille. J. D, Sims. A. M, Danoy. P, Evans. D. M, Leo. P, Pointon. J. J, *et al.*, 2010, Genome-wide association study of ankylosing spondylitis identifies non-MHC susceptibility loci. Nature genetics, Volume 42, Issue 2, 123–127
19. Sutton. C.E, Lalor. S.J, Sweeney. C.M, Brereton. C.F, Lavelle. E.C, Mills. K.H, 2009, Interleukin-1 and IL-23 induce innate IL-17 production from gammadelta T cells, amplifying Th17 responses and autoimmunity, Immunity, Volume 31:331-41.
20. Buus. T. B, Odum. N, Geisler. C, & Lauritsen. J. P. H, 2017, Three distinct developmental pathways for adaptive and two IFN- γ - producing γ δ T subsets in adult thymus. Nat. Commun, Volume 8, 1911

21. El-Zayadi. A. A, Jones. E. A, Churchman. S. M, Baboolal. T. G, Cuthbert. R. J *et al.*, 2017, Interleukin-22 drives the proliferation, migration and osteogenic differentiation of mesenchymal stem cells: a novel cytokine that could contribute to new bone formation in spondyloarthropathies, Rheumatology, Volume 56, Issue 3
22. Sherlock. J.P, Joyce-Shaikh. B, Turner. S.P, Chao. C.C, Sathe. M, Grein. J, *et al.,* 2012, IL-23 induces spondyloarthropathy by acting on ROR-gammat+ CD3+CD4-CD8- entheseal resident T cells. Nat Med, Volume 18, Issue 7
23. Virtanen. A.T, Haikarainen. T, *et al.,* 2019 Selective JAKinibs: Prospects in Inflammatory and Autoimmune Diseases, Biodrugs, Volume 33, Issue 1
24. Sieper. J, Poddubnyy. D, 2017, Axial spondyloarthritis. Lancet, Volume 390:73- 84.
25. Baeten. D, Østergaard. M, Wei. J.C, Sieper. J, *et al.*, 2018, Risankizumab, an IL-23 inhibitor, for ankylosing spondylitis: results of a randomised, double-blind, placebo-controlled, proof-of-concept, dose-finding phase 2 study. Ann Rheum Dis, Volume 77(9):1295-1302.
26. Deodhar. A, Gensler. L.S, Sieper. J, Clark. M, Calderon. C, Wang. Y, Zhou. Y, Leu. J.H, Campbell. K, Sweet. K, Harrison. D.D, Hsia. E.C, Van der Heijde. D, 2019 Three Multicenter, Randomized, Double-Blind, Placebo-Controlled Studies Evaluating the Efficacy and Safety of Ustekinumab in Axial Spondyloarthritis. Arthritis Rheumatol,71(2):258-270.
27. Ritchlin. C, Rahman. P, Kavanaugh. A, McInnes. I.B, Puig. L, Li. S, Wang. Y, Shen. Y.K, Doyle. M.K, Mendelsohn. A.M, Gottlieb. A.B; PSUMMIT 2 Study Group, 2014, Efficacy and safety of the anti-IL-12/23 p40 monoclonal antibody, ustekinumab, in patients with active psoriatic arthritis despite conventional non-biological and biological anti-tumour necrosis factor therapy: 6-month and 1-year results of the phase 3, multicentre, double-blind, placebo-controlled, randomised PSUMMIT 2 trial., Annals of Rheumatic Diseases, Volume 73, 990-999
28. McInnes. I.B, Kavanaugh. A, Gottlieb. A.B, Puig. L, Rahman. P, Ritchlin. C, Brodmerkel. C, Li. S, Wang. Y, Mendelsohn. A.M, Doyle. MK; PSUMMIT 1 Study Group., 2013, Efficacy and safety of ustekinumab in patients with active psoriatic arthritis: 1 year results of the phase 3,

multicentre, double-blind, placebo-controlled PSUMMIT 1 trial. Lancet, 382(9894):780-9.

29. Reinhardt. A, Yevsa. T, Worbs. T, Lienenklaus. S, Sandrock. I, Oberdörfer. L, Korn. T, Weiss. S, Förster. R, Prinz. I, 2016, Interleukin-23-Dependent γ/δ T Cells Produce Interleukin-17 and Accumulate in the Enthesis, Aortic Valve, and Ciliary Body in Mice. Arthritis Rheumatol, Volume 68, (10):2476-86.
30. Cuthbert. R.J, Watad. A, Fragkakis. E.M, Dunsmuir. R, Loughenbury. P, Khan. A, Millner. P.A, Davison. A, Marzo-Ortega. H, Newton. D, Bridgewood. C, McGonagle. D.G, 2019, Evidence that tissue resident human enthesis γδT-cells can produce IL-17A independently of IL-23R transcript expression. Ann Rheum Dis, Volume 78(11):1559-1565.
31. Gracey. E, Qaiyum. Z, Almaghlouth. I, Lawson. D, Karki. S, Avvaru. N, Zhang. Z, Yao. Y, Ranganathan. V, Baglaenko. Y, Inman. R.D, 2016, IL-7 primes IL-17 in mucosal-associated invariant T (MAIT) cells, which contribute to the Th17-axis in ankylosing spondylitis. Ann Rheum Dis, Volume 75(12):2124-2132.
32. Laidlaw, B., Craft, J. & Kaech, S., 2016, The multifaceted role of CD4+ T cells in CD8+ T cell memory, Nat Rev Immunol, Volume 16, 102–111
33. Hirahara. K, Poholek. A, et al., 2013, Mechanisms underlying helper T-cell plasticity: implications for immune-mediated disease, Journal of Clinical Immunology, Volume 131, Issue 5
34. Muranski. P, Restifo. N. P, 2013, Essentials of Th17 cell commitment and plasticity, Blood, Volume 101, Issue 13
35. Sonnenburg. E. D, & Sonnenburg. J. L, 2019, The ancestral and industrialized gut microbiota and implications for human health. Nat. Rev. Micro Volume 17, 383–390.
36. Zeng. M. Y, Inohara. N, & Núñez. G, 2016, Mechanisms of inflammation-driven bacterial dysbiosis in the gut. Mucosal Immunol, Volume 10, 18–26.
37. Atarashi. K, et al., 2017, Ectopic colonization of oral bacteria in the intestine drives TH1 cell induction and inflammation. Science (New York, NY) Volume 358, 359–365

38. Geddes, K. et al., 2011, Identification of an innate T helper type 17 response to intestinal bacterial pathogens. Nat. Med. Volume 17, 837–844.
39. Atarashi, K. et al., 2013, Treg induction by a rationally selected mixture of Clostridia strains from the human microbiota. Nature, Volume 500, 232–236.
40. Jeffery. V, Goldson. A.J, Dainty. J.R, Chieppa. M, Sobolewski. A, 2017, IL-6 signaling regulates small intestinal crypt homeostasis. Journal of immunology, Volume 199(1):304–11
41. Fachi. J.L, Pral. L.P, Dos Santos. J.A.C, et al., 2021, Hypoxia enhances ILC3 responses through HIF-1α-dependent mechanism. Mucosal Immunol
42. Gaffen, S. L., Jain, R., Garg, A. V., & Cua, D. J, 2014, The IL-23-IL-17 immune axis: from mechanisms to therapeutic testing. Nature reviews. Immunology, Volume 14, Issue 9, 585–600.
43. Shi. L. Z, et al., 2011, HIF1alpha-dependent glycolytic pathway orchestrates a metabolic checkpoint for the differentiation of TH17 and Treg cells. J. Exp. Med, Volume 208, 1367–1376.
44. Arias. C, Sepúlveda. P, Castillo. R. L, & Salazar. L. A, 2023, Relationship between Hypoxic and Immune Pathways Activation in the Progression of Neuroinflammation: Role of HIF-1α and Th17 Cells. International journal of molecular sciences, Volume 24, Issue 4
45. Donaldson, G. P. et al., 2018, Gut microbiota utilize immunoglobulin A for mucosal colonization. Science (New York, NY) Volume 360, 795–800
46. Fagarasan. S, Kawamoto. S, Kanagawa. O, & Suzuki. K, 2010, Adaptive immune regulation in the gut: T cell-dependent and T cell-independent IgA synthesis. Annual review of immunology, Volume 28, 243–273.
47. Fadlallah. J, El Kafsi. H, Sterlin. D, Juste. C, Parizot. C, et al., 2018, Microbial ecology perturbation in human IgA deficiency. Science translational medicine, Volume 10,(439)
48. Du. H, Bartleson. J.M, Butenko. S, et al., 2023, Tuning immunity through tissue mechanotransduction. Nat Rev Immunol, Volume 23, 174–188
49. Secio-Silva, A., Emrich, F., Evangelista-Silva, P.H., Prates, R.P., Hijo, A.H., Figueira-Costa, T.N, *et al.,* 2023, Which housekeeping gene is the

best choice for RT-qPCR analysis in mice fed with a high-fat diet? Studies in the liver, kidney, pancreas, and intestines. Gene Reports, Volume 31

50. Dean. J. W, Helm. E. Y, Fu. Z, Xiong. L, Sun. N, *et al*., 2023, The aryl hydrocarbon receptor cell intrinsically promotes resident memory CD8+ T cell differentiation and function. Cell reports, Volume 42, Issue 1
51. Odagiu, L., May, J., Boulet, S., Baldwin, T. A., & Labrecque, N. (2021). Role of the Orphan Nuclear Receptor NR4A Family in T-Cell Biology. Frontiers in endocrinology, 11,
52. Kumar. B. V, Ma. W, Miron. M, Granot. T, Guyer. R. S, Carpenter. D. J, Senda. T, *et al.,* 2017, Human Tissue-Resident Memory T Cells Are Defined by Core Transcriptional and Functional Signatures in Lymphoid and Mucosal Sites. Cell reports, Volume 20, Issue 12, 2921–2934
53. Pritchard. G. H, Kedl. R. M, & Hunter. C. A, 2019, The evolving role of T-bet in resistance to infection. Nature reviews, Immunology, Volume 19, Issue 6
54. Kyte, J., & Doolittle, R. F. (1982). A simple method for displaying the hydropathic character of a protein. Journal of molecular biology, 157(1), 105–132
55. Toussirot E, Saas P,2018, MAIT cells: potent major cellular players in the IL-17 pathway of spondyloarthritis?, RMD Open, Volume 4
56. Deodhar. A, Gensler. L.S, Sieper. J, Clark. M, Calderon. C, Wang. Y, *et al.*, 2019, Three Multicenter, Randomized, Double-Blind, Placebo-Controlled Studies Evaluating the Efficacy and Safety of Ustekinumab in Axial Spondyloarthritis. Arthritis Rheumatol, Volume 71:258–70.
57. Baeten. D, Ostergaard. M, Wei. J.C, Sieper. J, Jarvinen. P, Tam. L.S, *et al.*, 2018, Risankizumab, an IL-23 Inhibitor, for Ankylosing Spondylitis: Results of a Randomised, Double-Blind, Placebo-Controlled, Proof-of-Concept, Dose-Finding Phase 2 Study. Ann Rheum Dis, Volume 77:1295–302
58. Aggarwal. B.B, Gupta. S.C, Kim. J.H, 2012, Historical perspectives on tumor necrosis factor and its superfamily: 25 years later, a golden journey. Blood, Volume 119(3):651–65.
59. Schick. P, Trepel. F, *et al.,* 1975, Autotransufsion of 3H-cytidine-labelled blood lymphocytes in patients with Hodgkin's disease and non-Hodgkin

patients. I. Limitations of the method, Acta Haematologica, Volume 53, Issue 4, 193-205

60. Buggert. M, Vella. L. A, Nguyen. S, Wu. V. H, Chen. Z, *et al.,* 2020, The Identity of Human Tissue-Emigrant $CD8^+$ T Cells. Cell, 183(7), 1946–1961.e15.
61. Wherry. E.J, Teichgraber. V, Becker. T.C, *et al.* 2003, Lineage relationship and protective immunity of memory CD8 T cell subsets, Nature Immunology, Volume 4, Issue 3
62. DiSpirito. J.R, Shen. H, 2010, Quick to remember, slow to forget: rapid recall responses of memory CD8+ T cells. Cell Research, Volume 20, 13–23
63. Abdelsamed. H.A, Moustaki. A, Fan. Y, Dogra. P, Ghoneim. H..E, Zebley C.C, *et al.* 2017, Human memory CD8 T cell effector potential is epigenetically preserved during in vivo homeostasis. J Exp Med, Volume 214:1593–606
64. Mandl. J.N, Liou. R, Klauschen. F, Vrisekoop. N, Monteiro. J. P, Yates. A. J., Huang. A.Y, Germain. R. N, 2012, Quantification of lymph node transit times reveals differences in antigen surveillance strategies of naive CD4+ and CD8+ T cells. Proceedings of the National Academy of Sciences, Volume 109, Issue 44, 18036-18041.
65. Hand. T.W, Morre. M, Kaech. S.M, 2007, Expression of IL-7 receptor alpha is necessary but not sufficient for the formation of memory CD8 T cells during viral infection. Proc Natl Acad Sci USA. Volume 104:11730–5
66. Voehringer. D, Koschella. M, and Pircher. H, 2002, Lack of proliferative capacity of human effector and memory T cells expressing killer cell lectinlike receptor G1 (KLRG1). Blood, Volume 100:3698-3702.
67. Dominguez-Villar. M, Baecher-Allan. C. M, and Hafler. D. A, 2011, Identification of T helper type 1-like, Foxp3+ regulatory T cells in human autoimmune disease. Nature medicine, Volume 17, Issue 6, 673–675.
68. Panzer. M, Sitte. S, Wirth. S, Drexler. I, Sparwasser. T, and Voehringer. D, 2012, Rapid in vivo conversion of effector T cells into Th2 cells during helminth infection. Journal of immunology (Baltimore, Md.: 1950), Volume 188(2), 615–623.
69. Komatsu. N, Okamoto. K, Sawa. S, Nakashima. T, Oh-hora. M, Kodama. T, Tanaka. S, Bluestone. J. A, and Takayanagi. H, 2014, Pathogenic

conversion of Foxp3+ T cells into TH17 cells in autoimmune arthritis. Nature medicine, Volume 20(1), 62–68.

70. Mackay. L. K, Wynne-Jones. E, Freestone. D, Pellicci. D. G, Mielke. L. A, *et al.*, 2015, T-box Transcription Factors Combine with the Cytokines TGF-β and IL-15 to Control Tissue-Resident Memory T Cell Fate. Immunity, Volume 43, (6), 1101–1111.
71. Omnetti. S, Pizarro. T. T, 2015, The Treg/Th17 Axis: A Dynamic Balance Regulated by the Gut Microbiome, Frontiers in Immunology, Volume 6, article 639
72. Komatsu. N, *et al.*, 2014, Pathogenic conversion of Foxp3+ T cells into TH17 cells in autoimmune arthritis. Nat. Med, Volume 20, 62–68
73. Saravia. J, Chapman. N. M, 2019, Helper T cell differentiation, Cellular and Molecular Immunology, Volume 16, Issue 7
74. Ohta. A, Sitkovsky. M, 2014, Extracellular adenosine-mediated modulation of regulatory T cells, Frontiers in Immunology, Volume 5
75. Beltejar. M.G, Lau. H.T, *et al.*, 2017, Analyses of PDE-regulated phosphoproteomes reveal unique and specific cAMP-signaling modules in T cells. PNAS, Volume 114, Issue 30
76. Boniface. K., Bak-Jensen. K. S., *et al.* 2009, Prostaglandin E2 regulates Th17 cell differentiation and function through cyclic AMP and EP2/EP4 receptor signalling, Journal of Experimental Medicine, Volume 206, Issue 3
77. Yao. C, Sakata. D, *et al.* 2009 Prostaglandin E2-EP4 signaling promotes immune inflammation through Th1 cell differentiation and Th17 cell expansion, Nature Medicine, Volume 15
78. Gladman. D. D, Kavanaugh. A, Gomez-Reino. J. J, Wollenhaupt. J, *et al.,* 2018, Therapeutic benefit of apremilast on enthesitis and dactylitis in patients with psoriatic arthritis: a pooled analysis of the PALACE 1-3 studies, RMD Open Volume 4, Issue 1
79. Sommer. N, Martin. R, McFarland. H.F, Quigley. L, Cannella. B, Raine. C.S, *et al.,* 1997, Therapeutic potential of phosphodiesterase type 4 inhibition in chronic autoimmune demyelinating disease, Journal of Neuroimmunology, Volume 79, Issue 1

80. Schafer. P.H, Parton. A, Capone. L, Cedzik. D, Brady. H, *et al.,* 2014, Apremilast is a selective PDE4 inhibitor with regulatory effects on innate immunity, Cellular Signalling, Volume 26, Issue 9
81. Gu. J, Ni. X, Pan. X, Lu. H, Lu. Y, Zhao. J. *et al.*, 2017, Human CD39hi regulatory T cells present stronger stability and function under inflammatory conditions. Cell Mol Immunol, Volume 14(6):521-528.
82. Quintana. F.J and Sherr. D.H, 2013, Control of Adaptive Immunity by the AhR Pharmacological Reviews, Volume 65, Issue 4 1148-1161
83. J. Ye, J. Qiu, J. W. Bostick *et al.,* 2017, The aryl hydrocarbon receptor preferentially marks and promotes gut regulatory T cells, Cell Reports, Volume 21, no. 8, pp. 2277–2290
84. Boddupalli. C.S, Nair. S, Gray. S..M, Nowyhed. H.N, Verma. R, Gibson. J.A, *et al.*, 2016, ABC transporters and NR4A1 identify a quiescent subset of tissue-resident memory T cells. J Clin Invest, Volume 126:3905–16.
85. Laidlaw. B.J, Craft. J.E, Kaech. S. M, 2016, The multifaceted role of CD4+ T cells in CD8+ T cell memory. Nature Reviews Immunology, Volume 16, Issue 2
86. Shedlock. D. J, Shen. H, 2003, Requirement for CD4 T cell help in generating functional CD8 T cell memory, Science, Volume 300, Issue 1561
87. Basdeo. S. A, Cluxton. D, Sulaimani. J, *et al.*, 2017, Ex-Th17 (Nonclassical Th1) cells are functionally distinct from classical Th1 and Th17 cells and are not constrained by regulatory T cells. J Immunol, Volume 198:2249–59.
88. Koay H.F, Gherardin N.A, Enders. A, Loh. L, Mackay. L.K, *et al.*, 2016, A three-stage intrathymic development pathway for the mucosal-associated invariant T cell lineage, Nat. Immunol., Volume 17 pp. 1300-1311
89. Dias, J. *et al.* 2018, The CD4–CD8– MAIT cell subpopulation is a functionally distinct subset developmentally related to the main CD8+ MAIT cell pool. Proc. Natl Acad. Sci. USA, Volume 115, E11513–E11522 (2018)
90. Rahimpour. A, Koay. H.F, Enders. A, *et al.*, 2015, Identification of phenotypically and functionally heterogeneous mouse mucosal-associated invariant T cells using MR1 tetramers. J Exp Med Volume 212:1095

91. Lamichhane. R, Galvin. H, Hannaway. R.F, De La Harpe. S.M, Munro, F, *et al.*, 2020, Type I interferons are important co-stimulatory signals during T cell receptor mediated human MAIT cell activation. Eur. J. Immunol., Volume 50: 178-191
92. Legoux. F, *et al.*, 2019, Microbial metabolites control the thymic development of mucosal- associated invariant T cells. Science, Volume 366, 494–499
93. Reantragoon. R, Kjer-Nielsen. L, Patel. O, Chen. Z, Illing. P. T, *et al.*, 2012, Structural insight into MR1-mediated recognition of the mucosal associated invariant T cell receptor. The Journal of experimental medicine, Volume 209, Issue 4, 761–774.
94. Amini. A, Pang. D, Hackstein. C. P, & Klenerman. P, 2020, MAIT Cells in Barrier Tissues: Lessons from Immediate Neighbors. Frontiers in immunology, Volume 11
95. Mielke. L. A et *al.*, 2019, TCF-1 limits the formation of Tc17 cells via repression of the MAF–RORγ t axis. J. Exp. Med. 216, 1682–1699
96. Gracey. E, Qaiyum. Z, Almaghlouth. I, *et al.,* 2016, IL-7 primes IL-17 in mucosal-associated invariant T (MAIT) cells, which contribute to the Th17-axis in ankylosing spondylitis, Ann Rheum Dis, Volume 75:2124–2132.
97. Gracey. E, Yao. Y, Green. B, *et al.*, *2016,* Sexual Dimorphism in the Th17 Signature of Ankylosing Spondylitis, Arthritis Rheumatol, Volume 68:679–89.
98. Ciccia. F, Guggino. G, Rizzo. A, *et al.*, 2015, Type 3 innate lymphoid cells producing IL-17 and IL-22 are expanded in the gut, in the peripheral blood, synovial fluid and bone marrow of patients with ankylosing spondylitis, Ann Rheum Dis, Volume 74:1739–47.
99. Schatz. D.G, Ji. Y, 2011, Recombination centres and the orchestration of V(D)J recombination, Nature Reviews Immunology, Volume 11
100. Cabaniols, J. P. Fazilleau, N. *et al.* 2001, Most alpha/beta T cell receptor diversity is due to terminal deoxynucleotidyl transferase, Journal of Experimental Medicine, Volume 9, Issue 194
101. Lu. J, Van Laethem. F, Bhattacharya. A, *et al.,* 2019, Molecular constraints on CDR3 for thymic selection of MHC-restricted TCRs from a random pre-selection repertoire. Nat Commun, Volume 10, 1019

102. Soulillou. J. P, & Brouard. S, 2007, Statistical analysis of CDR3 length distributions for the assessment of T and B cell repertoire biases. Molecular immunology, Volume 44

103. Martin. D. A, Bradl. H, Collins. T. J, Roth. E, Jäck. H. M, & Wu. G. E, 2003, Selection of Ig mu heavy chains by complementarity-determining region 3 length and amino acid composition. Journal of immunology, Volume 171

104. Zemlin. M, Klinger. M, Link. J, Zemlin. C, Bauer. K, Engler. J.A, *et al.,* 2003, Expressed murine and human CDR-H3 intervals of equal length exhibit distinct repertoires that differ in their amino acid composition and predicted range of structures. J Mol Biol., Volume 334(4):733-49.

105. Sun, X., Nguyen, T., Achour, A., Ko, A., Cifello, J., Ling, C., Sharma, J., Hiroi, T., Zhang, Y., Chia, C. W., Wood, W., 3rd, Wu, W. W., Zukley, L., Phue, J. N., Becker, K. G., Shen, R. F., Ferrucci, L., & Weng, N. P. (2022). Longitudinal analysis reveals age-related changes in the T cell receptor repertoire of human T cell subsets. The Journal of clinical investigation, 132(17)

106. Thome. J.J, Grinshpun. B, Kumar. B.V, Kubota. M, *et al.*, 2016, Longterm maintenance of human naive T cells through in situ homeostasis in lymphoid tissue sites. Sci Immunol., Volume 1, Issue 6

107. Schirmer. M, Goldberger. C, Wurzner. R, 2002, Circulating cytotoxic CD8(+) CD28(-) T cells in ankylosing spondylitis, Arthritis Research, Volume 4, Issue 1

108. Jacobse. J, Brown. R. E, Li. J, Pilat. J. M, Pham. L, Short. S. P, Peek. C. T, *et al.* 2023, Interleukin-23 receptor signaling impairs the stability and function of colonic regulatory T cells. Cell reports, Volume 42, Issue 2

109. Gattinoni. L, Speiser. D.E, Lichterfeld. M, *et al.*, 2017, T memory stem cells in health and disease. Nat Med, Volume 23,18–27.

110. Qaiyum. Z, Gracey. E, Yao. Y *et al.,* 2019, Integrin and transcriptomic profiles identify a distinctive synovial CD8+ T cell subpopulation in spondyloarthritis. Ann Rheum Dis, Volume 78,1566–75.

111. Guggino, G., Rizzo, A., Mauro, D., Macaluso, F., & Ciccia, F, 2021, Gut-derived CD8+ tissue-resident memory T cells are expanded in the peripheral blood and synovia of SpA patients. Annals of the rheumatic diseases, Volume 80, 11

112. Mackay. L.K, Minnich. M, Kragten. N.A.M *et al.,* 2016, Hobit and Blimp1 instruct a universal transcriptional program of tissue residency in lymphocytes. Science, Volume 352, 459–63
113. Kok. L, Masopust. D, & Schumacher. T.N, 2022, The precursors of CD8+ tissue resident memory T cells: from lymphoid organs to infected tissues. Nat Rev Immunol, Volume 22, 283–293
114. Zhong C , Zhu J., 2017, Small-Molecule RORγt antagonists: one stone kills two birds. Trends Immunol, Volume 38, 229–31
115. Solt. L.A, Kumar. N, Nuhant. P et al., 2011, Suppression of Th17 differentiation and autoimmunity by a synthetic ROR ligand. Nature Volume 472, 491–4
116. McGeehan. G, Bukhtiyarov. Y, Zhao. Y , *et al.,* 2015, VTP-43742 is a potent and selective RORγt blocker that demonstrates oral efficacy in a mouse model of autoimmunity through suppression of IL-17A production, J Immunol, Volume 194:205–8.
117. de Wit. J, Al-Mossawi. M.H, Hühn. M.H, *et al.,* 2016, RORγt inhibitors suppress T(H)17 responses in inflammatory arthritis and inflammatory bowel disease. J Allergy Clin Immunol, Volume 137, 960–3
118. Venken. K, Jacques. P, Mortier. C, *et al.,* 2019, Rorγt inhibition selectively targets IL-17 producing iNKT and γδ-T cells enriched in spondyloarthritis patients. Nat Commun Volume 10, 9
119. Rahimpour. A, Koay. H.F, Enders. A, *et al.,* 2015, Identification of phenotypically and functionally heterogeneous mouse mucosal-associated invariant T cells using MR1 tetramers. J Exp Med, Volume 212, 1095–108
120. Hinks. T.S.C, & Zhang. X. W, 2020, MAIT Cell Activation and Functions. Frontiers in immunology, Volume 11, 1014
121. Navarro-Compán. V, Puig. L, Vidal. S, Ramírez. J, Llamas-Velasco. M, *et al.*, 2023, The paradigm of IL-23-independent production of IL-17F and IL-17A and their role in chronic inflammatory diseases. Frontiers in immunology, Volume 14